Development of a Design-Based Computational Model of Bioretention Systems

Jia Liu

Dissertation submitted to the faculty of the Virginia Polytechnic Institute and State University
in partial fulfillment of the requirements for the degree of

Doctor of Philosophy
In
Biological Systems Engineering

David J. Sample, Chair
Thomas J. Grizzard
Adil N. Godrej
Durelle T. Scott
Gregory K. Evanylo

October 30, 2013
Virginia Beach, Virginia

Keywords: bioretention, stormwater, frequency analysis, phosphorus, nitrogen, isotherm adsorption, mesocosm experiment, computational model, sensitivity analysis

ABSTRACT

Multiple problems caused by urban runoff have emerged as a consequence to the continuing development of urban areas in recent decades. The increase of impervious land areas can significantly alter watershed hydrology and water quality. Typical impacts to downstream hydrologic regimes include higher peak flows and runoff volumes, shorter concentration times, and reduced infiltration. Urban runoff increases the transport of pollutants and nutrients and thus degrades water bodies adjacent to urban areas. One of the most frequently used practices to restore the hydrology and water quality of urban watersheds is bioretention (also known as a rain garden). Despite its wide applicability, an understanding of its multiple physiochemical and biological treatment processes remains an active research area.

To provide a wide ability to evaluate the hydrologic input to bioretention systems, spatial and temporal distribution of storm events in Virginia were studied. Results generated from long-term frequency analysis of 60-year precipitation data demonstrate that the 90 percentile, or 10-year return period rainfall depth and dry duration in Virginia are between 22.9 – 35.6 mm and 15.3 – 25.8 days, respectively. Monte-Carlo simulations demonstrated that sampling programs applied in different regions would likely encounter more than 30% of precipitation events less than 2.54 mm, and 10% over 25.4 mm.

Further experimental research was conducted to evaluate bioretention recipes for retaining stormwater nitrogen (N) and phosphorus (P). A mesocosm experiment was performed to simulate bioretention facilities with 3 different bioretention blends as media layers with underdrain pipes for leachate collection. A control group with 3 duplicates for

each media was compared with a replicated vegetated group. Field measurement of dissolved oxygen (DO), oxidation-reduction potential (ORP), pH, and total dissolved solids (TDS) was combined with laboratory analyses of total suspended solids (TSS), nitrate (NO_3), ammonium (NH_4), phosphate (PO_4), total Kjeldahl nitrogen (TKN) and total phosphorus (TP) to evaluate the nutrient removal efficacies of these blends. Physicochemical measurements for property parameters were performed to determine characteristics of blends. Isotherm experiments to examine P adsorption were also conducted to provide supplementary data for evaluation of bioretention media blends. The results show that the blend with water treatment residuals (WTR) removed >90% P from influent, and its effluent had the least TDS / TSS. Another blend with mulch-free compost retained the most (50 – 75%) total nitrogen (TN), and had the smallest DO / ORP values, which appears to promote denitrification under anaerobic conditions. Increase of hydraulic retention time (HRT) to 6 h could influence DO, ORP, TKN, and TN positively. Plant health should also be considered as part of a compromise mix that sustains vegetation. Two-way analysis of variance (ANOVA) found that single and interaction effects of HRT and plants existed, and could affect water quality parameters of mesocosm leachate.

Based upon the understanding of the physiochemical and hydrologic conditions mentioned previously, a design model of a bioretention system became the next logical step. The computational model was developed within the Matlab® programming environment to describe the hydraulic performance and nutrient removal of a bioretention system. The model comprises a main function and multiple subroutines for hydraulics and treatment computations. Evapotranspiration (ET), inflow, infiltration, and outflow were calculated for

hydrologic quantitation. Biomass accumulation, nitrogen cycle and phosphorus fate within bioretention systems were also computed on basis of the hydrologic outputs. The model was calibrated with the observed flow and water quality data from a field-scale bioretention in Blacksburg, VA. The calibrated model is capable of providing quantitative estimates on flow pattern and nutrient removal that agree with the observed data. Sensitivity analyses determined the major factors affecting discharge were: watershed width and roughness for inflow; pipe head and diameter for outflow. Nutrient concentrations in inflow are very influential to outflow quality. A long-term simulation demonstrates that the model can be used to estimate bioretention performance and evaluate its impact on the surrounding environment.

This research advances the current understanding of bioretention systems in a systematic way, from hydrologic behavior, monitoring, design criteria, physiochemical performance, and computational modeling. The computational model, combined with the results from precipitation frequency analysis and evaluation of bioretention blends, can be used to improve the operation, maintenance, and design of bioretention facilities in practical applications.

Acknowledgements

The research and work in this dissertation cannot be realized without the wise advisory and knowledgeable guidance from my committee professors, so I would like to express my sincerest appreciation for their excellent suggestions to improve and advance all aspects of the work summarized here. My every step in progress is supported by Drs. David Sample, Thomas Grizzard, Adil Godrej, Durelle Scott, and Gregory Evanylo. It is their comments, critiques, and encouragement that make the research in this dissertation possible.

I would like to extend my appreciation to Dr. Haibo Zhang, who reviewed the draft of this dissertation thoroughly and provided numerous valuable comments. Especially, I am quite thankful for the laboratory analyses conducted by Dr. Jinling Li and Hsuan-Chih Yu. Their professional skills on analytical experiments helped me collect necessary data on media samples and mesocosm leachate. Their contributions to the mesocosm experiment and media evaluation cannot be underestimated.

My fellow friends offered necessary help when I was in confusion. I am grateful for collaborating with Chih-Yu Wang. It is my luck to know him for the entire time of my PhD program with his devoted attitude towards research inspiring me. I also learned much on academic research methods from Drs. Saurav Kumar and Francisco Cubas at Occoquan Watershed Monitoring Laboratory (OWML). I also thank Drs. Jim Owen and Laurie Fox at Hampton Roads Agricultural Research and Extension Center (HRAREC), who allowed me to use their labs, and gave me multitudinous advices to improve my experiment. I am particularly indebted to Thomas Wilchynski, Alfred Smith, and Adam Sleeper at HRAREC, who assisted me to operate engineering machineries to mix bioretention media and install

mesocosm barrels. The completion of this work was also due in part to all of my dear friends at Virginia Tech, OWML, and HRAREC, without whose moral support I would not go this far.

Finally, my special thanks should go to my father Cunzhong Liu and mother Guilan Bian. Their warm supports encouraged me to surmount countless difficulties in life and to conquer the tedious long march of academic research. No matter whom I am or where I go, their love is always with me in my heart, and accompanies me to face challenges in the future. Therefore I would like to dedicate this dissertation to them, my beloved parents.

Attributions

Dr. David Sample (Department of Biological Systems Engineering, Virginia Tech) is the research advisor and committee chair. Dr. Sample is the co-author of Chapters 2, 3, and 4. He directed my research and contributed to the experimental design, data analysis, and edited the dissertation. Some of the dissertation chapters have been edited and submitted to academic journals for consideration; Dr. Sample is a coauthor of these. Additionally, Dr. Sample provided much of the financial support for the work presented in this dissertation through multiple funds and grants.

Dr. Gregory Evanylo (Department of Crop and Soil Environmental Sciences, Virginia Tech) is on the author's academic committee. Dr. Evanylo is the co-author of a journal manuscript based upon Chapters 3 of this dissertation. He was the Principal Investigator of the project to evaluate bioretention recipes. He provided lab space and analytical devices for the work of Chapter 3 and gave many valuable advices on the experimental design.

Drs. Grizzard, Godrej, and Scott are all on the author's academic committee. They oversaw the progress and development of this research, and provided wise suggestions to improve the in-depth investigation of experimental designs and modeling endeavors.

Table of Contents

List of Figures

List of Tables

List of Abbreviations and Acronyms

Al ..... aluminum
As ..... arsenic
ANOVA ..... analysis of variance
BEAM ..... Bioretention Evaluation and Assessment Model
BMPs ..... Best Management Practices
BOD-5 ..... biochemical oxygen demand
Ca ..... calcium
Cd ..... cadmium
Cl ..... chloride
Cr ..... chromium
Cu ..... copper
CDF ..... cumulative distribution function
COD ..... chemical oxygen demand
DO ..... dissolved oxygen
E. coli ..... *Escherichia coli*
EMC ..... event mean concentration
EPIC ..... Erosion-Productivity Impact Calculator
ET ..... evapotranspiration
Fe ..... iron
FA ..... frequency analysis
FAO ..... Food and Agricultural Organization
FFMC ..... Fundamental Formulation of Monte-Carlo
Hg ..... mercury
HEC-HMS ..... Hydrologic Engineering Center-Hydrologic Modeling System
HRAREC ..... Hampton Roads Agricultural Research and Extension Center
HRT ..... hydraulic retention time
ICP ..... Inductively Coupled Plasma
IDF ..... intensity-duration-frequency
LAI ..... leaf area index
LID ..... Low Impact Development

LXPET ..... Lamoreux Potential Evapotranspiration

Mg ..... magnesium

Mn ..... manganese

MIT ..... minimum inter-event time

N ..... nitrogen

N_2 ..... nitrogen gas

Ni ..... nickel

NH_4 ..... ammonium

NO_3 ..... nitrate

ORP ..... oxidation-reduction potential

OWML ..... Occoquan Watershed Monitoring Laboratory

P ..... phosphorus

Pb ..... lead

PAHs ..... polycyclic aromatic hydrocarbons

PAR ..... photosynthetic active radiation

PET ..... potential evapotranspiration

PDF ..... probability distribution function

PSD ..... particle size distribution

PO_4 ..... phosphate

RUE ..... radiation-use efficiency

RWH ..... rainwater harvesting

SCMs ..... Stormwater Control Measures

SWMM ..... Storm Water Management Model

TDS ..... total dissolved solids

TKN ..... total Kjeldahl nitrogen

TMDL ..... Total Maximum Daily Load

TN ..... total nitrogen

TOC ..... total organic carbon

TP ..... total phosphorus

TSS ..... total suspended solids

US EPA ..... United States Environmental Protection Agency

USDA .....United States Department of Agriculture

USGS ..... United States Geological Survey

VADCR.....Virginia Department of Conservation and Recreation

WTR ..... water treatment residuals

Zn .....zinc

1 Introduction

1.1 Urban Stormwater Problems

The 20th century has witnessed the rapid transformation of rural lands to urban areas on a global scale. The physical growth of urban areas leads to a phenomenon known as urban sprawl with high residential density and mixed land uses arranged in a spiderlike pattern extending outward from cities. At the end of 2008, the United Nations projected that half of the world's population would live in urban areas [1]; by 2050, 64.1% and 85.9% of the developing and developed world will be urbanized [2].

With the rapid processes of rural migration and suburban concentration into cities, the impervious surfaces created by buildings and pavement significantly alters the way water flows from watersheds, and transports more pollutants into streams. Understanding and mitigating the consequences of urbanization on urban stormwater hydrology and quality is the key to solving these issues.

1.1.1 Altered hydraulic pattern

In urban areas, impervious surfaces include roads, sidewalks, driveways, parking lots and rooftops that are covered by impenetrable materials (asphalt, concrete, brick and stone). Additionally, urban soils themselves become compacted by development practices, and can be nearly impervious. With the soil surface sealed by the pavement materials, rainwater infiltration and natural groundwater recharge subsequently decrease, resulting in increased runoff rates and volumes, losses of infiltration and baseflow to urban streams. The creation of impervious areas and the simplification of the drainage network also cause much faster runoff response to rainfall, leading to shorter times of concentration and reduced recession times [3].

The rapid expansion of urban areas dramatically impact catchment hydrology. A study on long-term hydrologic impacts from an apartment in Miami, FL showed that the directly connected impervious area covering 44% of the catchment contributed 72% of the total runoff volume during 52 years [4]. Another survey indicated a 4047-m^2 (1-ac) paved parking lot could generate 16 times more runoff than a meadow of the same size [5]. The increased volumes and rates of urban runoff can increase the risk of flooding, accentuate downstream channel erosion, change the shape and dimension of river channels, and alter aquatic habitat [6].

The hydrologic pattern altered by urban development can be seen in Figure 1.1 with larger volume, higher peak, lower baseflow, and reduced concentration time.

1.1.2 Increased washoff and transport of sediments and pollutants

The imperviousness in urban areas also has adverse effects on the health of water bodies within and adjacent to cities. Pollutants from various sources accumulate over impervious surfaces during dry periods are washed off when rain occurs, and they are quickly discharged into the receiving waters [7]. Changes in rainfall- runoff behavior and the generation of pollutants by urban land surfaces and activities result in the degradation of water quality and associated aquatic life in receiving waters. In general, this degradation is the result of two primary mechanisms (i) increased generation of pollutants, through land use and human activity and (ii) increased mobilization and transport as a result of increased surface runoff and hydraulic efficiency of the stormwater conveyance network [3].

The rapid rise and increased volume of stormwater represents a net input of energy into watersheds and downstream receiving waters. The outlet for this increase in

energy is an increase in erosion of soils. Sediment and debris are conveyed and transported by stormwater flow into sewer systems as the runoff travels across urban landscapes. The increased energy in receiving waters causes stream bank erosion, as the steam morphology changes to accommodate it [8]. These sediment inputs increase turbidity of receiving waters. The turbid water decreases the rate of photosynthesis, impairing the health of aquatic ecosystems. The solids may also clog fish gills, and depress the immune systems of aquatic animals [9].

Runoff from drainage areas in the Piedmont region of North Carolina was monitored, showing the annual export of sediment was 95% greater for the developed area due to a 68% increase in runoff volume in comparison with an undeveloped area of the same size [10]. A study of stormwater suspended sediments in an urban catchment in Florida recorded suspended sediment with an event mean concentration (EMC) of 23.7 – 194.6 mg/L in untreated urban runoff [11]. Sediment flushing is more acute during first flush, or the initial phase of the runoff hydrograph [12]. A research on the contaminants in urban runoff entering Columbia River by United States Geological Survey (USGS) collected a suspended sediment sample with a concentration of 834 mg/L during the first flush phase of a rain in Fall 2009, indicating that a large amount of soil material was flushed into the downstream during the rising limb of the hydrograph [13].

Urban stormwater can contain numerous pollutants including suspended solids, nutrients, organic compounds, pathogenic bacteria, heavy metals, toxic pesticides or herbicides, trash, debris, and floatable materials [7]. Many pollutant constituents appear either in dissolved or particulate form.

A recent stormwater quality survey in several Virginia cities provides detailed information on the magnitude of constituents within urban runoff (Table 1.1). An intensive monitoring study of the sources of urban runoff pollution in the Twin Cities metropolitan area compiled a database of urban and suburban runoff EMCs [14]. The results are plotted as boxplots in Figure 1.2. From a microscopic aspect, a study that characterized asphalt parking lot runoff quality indicated that the mean EMCs (mg/L) of TN, TKN, NH_4, NO_{2-3}, and TP were 1.57, 1.19, 0.32, 0.36, and 0.19 respectively. Rainfall depth, catchment area, the percentage of asphalt and natural surrounding land use have been found to be adequate predictors of nutrient concentrations and loads [15]. Excessive nutrients such as N and P entering water bodies may stimulate the growth of plants and algae, inducing eutrophic aquatic conditions, consequently causing an algae bloom, DO depletion, and decreased biodiversity.

Other possible pollutants, such as heavy metals, pesticides, bacteria, hydrocarbons, and vehicle byproducts may also be conveyed by urban runoff from impervious surfaces to receiving waters, and cause a wide variety of adverse (toxic, pathogenic, and sanitary) environmental issues in urban receiving waters [16]. The scope of this work is to focus on the nutrients of N and P.

1.1.3 Other major impacts

Urban stormwater flooding and pollution result in a multitude of economic losses. Pollutants in runoff lead to financial losses for the commercial fishing industries. Recreational beaches contaminated by urban runoff suffer from losses in sales and services [9].

1.2 Ecological Engineering Constructions

Rapid urban development has led to degradation of many water bodies adjacent to urban areas, thus reinforcing the need for better management of urban runoff. Increasing imperviousness in cities sharply changes the hydrologic regime and cause negative impacts such as urban flooding, stream erosion, and pollution. Traditionally, stormwater control systems were designed to convey runoff from urban areas as quickly as possible. This method transfers a problem to other regions and ultimately degrades the health of receiving waters [17]. Ecological engineering practices have emerged as a means of increasing the sustainability of our urban designs, and increasing the health of aquatic ecosystems for their benefit and that of society [18]. The philosophy of ecological engineering can be combined with concepts from basic and applied sciences from engineering, ecology, economics, and natural science for the restoration and construction of aquatic and terrestrial ecosystems. Applications of ecological engineering practices and techniques in urban areas include a wide variety of examples which will be discussed in the following sections.

1.2.1 Best Management Practices (BMPs)

BMPs are control measures developed specifically to mitigate the quantity and quality of urban runoff caused by urban development. They are designed to reduce stormwater volume, peak flows, and / or nonpoint source pollution through ET, infiltration, detention, and filtration or biological and chemical processes [19].

Typical BMPs are structural, vegetative or managerial practices. Structural and vegetative practices are distinctly observable objects, and include extended detention ponds, porous pavement, water quality inlets, and underground storage tanks as structural

BMPs; grassed swales, vegetative buffer areas as vegetative BMPs. Managerial practices include pollution prevention (e.g. street sweeping), education, pet waste collection, etc. [20].

1.2.2 Low Impact Development (LID)

LID was pioneered by Prince George's County, Maryland in the early 1990's [21, 22] as a means to mitigate the impacts of urban development. LID is a land planning and engineering design approach that implements small-scale hydrologic controls with pollution prevention measures to compensate for land development impacts on hydrology and water quality [21]. The goal of LID is to maintain or replicate the predevelopment hydrologic regime using a variety of runoff treatment and removal processes to reduce off-site runoff and ensure adequate groundwater recharge [23].

Popularly used LID includes bioretention cells (also known as rain gardens) rain barrels, green roofs, porous pavement, and bioswales. One or multiple LID practices constructed for an individual site have numerous purposes, including: enhancing management of runoff, increasing surface water quality, improving groundwater recharge, providing animal habitats, and providing enhanced aesthetics to the community [24]. When implemented broadly, LID may mitigate urban heat island effects, save energy, reduce air pollution, and provide an enriched education experience [25].

1.2.3 Stormwater management by LID

Stormwater management is "anything associated with the planning, maintenance, and regulation of facilities which collect, store, or convey stormwater" [26]. Present stormwater management methods are based on small-scale, environmentally sound

technologies of LID that involve natural or constructed biological systems for stormwater treatment [27].

Examples of LID on stormwater management can be found across the U.S. The United States Environmental Protection Agency (US EPA) is demonstrating LID in a landscape renovation project at its Federal Triangle Headquarters in Washington, D.C. The project has multiple stormwater management practices including bioretention, permeable concrete, permeable pavers, cistern, and sustainable landscaping to demonstrate the feasibility of using innovative stormwater management techniques for retrofits of already developed urban areas [28]. A combination of LID practices were designed and constructed at the Science Museum of Virginia including construction of a bioretention, tree planters, porous pavement, a green roof, and a rainwater harvesting system [29]. The project resulted in the construction of several large LID practices at a highly visible site providing an educational showcase.

With the increasing demands on LID construction, national and state regulations have been published which require the use of LID to mitigate urban impacts. US EPA strongly recommends its use and provides numerous design guidance at its website [30]. Approximately 32 states have published stormwater BMPs or LID manuals to customize designs for local environments and climates [31].

1.3 Bioretention Overview

1.3.1 Definition and functions

As one of the most common and unique LID practices, bioretention is a water quality and water quantity control practice that uses chemical, biological, and physical properties of plants, microbes, and soils for removal of pollutants from urban runoff [32].

A bioretention system is a landscaped depression that receives runoff from upstream impervious surfaces. Bioretention systems closely mimic the natural hydrologic cycle, allowing soils and plants to filter pollutants from stormwater [25]. The systems can also generate aesthetic value, create wildlife habitats, minimize soil erosion, and recharge groundwater [33].

Bioretention normally consists of a media layer of between 0.7 – 1.0 m of sand / soil / organic mixture for treating runoff, a surface mulch layer, various forms of vegetation, a storage pool of between 15 – 30 cm of freeboard and associated hydraulic control appurtenances for inlet, outlet, and overflow [34]. Figure 1.3 shows a diagram of a typical bioretention system. An underdrain is an option preferred when underlying soils are low in permeability [35]. Runoff is filtered sequentially through each layer; however the main filtration action is performed in the media layer [36]. Debris, particles, sediments, and other pollutants from runoff are filtered and treated before draining into a stormwater conveyance system or directly into receiving waters. The vegetated surface layer and surface storage slows down the runoff velocity, attenuates peak runoff, and traps the sediment [37]. Pollutants are also converted to less bioavailable forms. The multiple processes within bioretention enable it to reduce peak flows, runoff volume, pollutant load, increase ET by vegetation, and increase lag time to peak runoff [34].

1.3.2 Hydraulic restoration

One key feature of bioretention is its ability to mimic the pre-development hydroperiod of an undeveloped watershed and thus help maintain a natural water cycle in urban areas. A comparison study was conducted between bioretention outflows from 4 bioretention cells in North Carolina compared with streamflow from 3 nonurban

watersheds [38]. The results indicated that there was no statistical difference between flow rates in streams draining undeveloped watersheds and bioretention outflow rates for the 2 days following the commencement of flow. This study confirmed that bioretention outflow can mimic nonurban watershed shallow interflow to streams, and thus help restore the natural hydroperiod.

Through targeted bioretention design, adjusting the dimensions, treatment volume, media composition, underdrain configuration, and vegetation type, proscribed hydrologic goals may be achieved [39]. Among the design factors above, media depth may be the primary parameter controlling hydrologic performance [40]. A long-term observation from 2004 to 2006 of a bioretention cell in Charlotte, NC demonstrated that the peak outflow for 16 storms with less than 42 mm of rainfall was at least 96.5% less than the peak inflow, with a mean peak flow reduction being 99% [41]. From this study, it can be concluded that in an urban environment, bioretention can effectively reduce peak runoff from small to midsize storm events, depending on site characteristics.

The use of bioretention facilities can also increase the time of concentration and reduce the corresponding peak discharge values [42]. A time of concentration value in the range of 5 – 10 min would normally be estimated for a parking lot 0.2 – 0.4 ha in size draining directly to a storm drain inlet. In contrast, the placement of a bioretention facility in front of the inlet will increase the time of concentration for the runoff to reach the inlet by several hours, depending on the flow rates through the treatment media [43]. For processes of exfiltration and ET, annual water budget analysis suggests that approximately 20 – 50% of runoff entering bioretention cells was lost through these means [40].

A critical concern that impacts bioretention functions negatively is surface and underdrain clogging caused by fine silts and sediments in urban runoff. Hydrologic performance of bioretention can be significantly degraded leading to less-than-adequate water storage volume and surface infiltration rates [44]. A study on urban particle capture in bioretention media showed clay-sized components of incoming TSS exerted a controlling effect on media clogging [45].

In this dissertation, the hydrologic and water quality benefits of bioretention was measured through mesocosm experiment (Chapter 3), and estimated by a computational model developed to support the design of bioretention systems (Chapter 4).

1.3.3 Pollutant treatment

Pollutant removal mechanisms within bioretention facilities include filtration, adsorption, chemical reaction, and biological treatment [34]. The water quality improvement by bioretention has been extensively observed and reported through field experiment or management.

A study examines water quality improvements on numerous pollutant parameters including total arsenic (As), total cadmium (Cd), chloride (Cl), total chromium (Cr), total and dissolved copper (Cu), *Escherichia coli* (*E. coli*), fecal coliform, lead (Pb), mercury (Hg), N species, oil & grease, P species, total organic carbon (TOC), TSS, and total zinc (Zn) via monitoring for a 15-month period at 2 bioretention cells in Maryland. The monitoring result showed both bioretention cells effectively removed suspended solids, Pb, and Zn from runoff through concentration reduction or treatment. The bioretention effluent EMCs met local water quality criterion [46]. Long-term (9 years) PO_4 removal in a field-scale stormwater bioretention was observed, showing the PO_4 concentration

decreased from 0.21 – 0.25 mg/L in the ponded water to 0.03 mg/L in the pore water at the bottom of the infiltration bed, and the removal performance did not decrease during 9 years of monitoring [47]. Field sampling and analysis on 3 bioretention sites confirmed high annual NO_3 mass removal rates varied between 13 – 75% [48]. A bioretention cell in an urban setting was examined in North Carolina from 2004 to 2006 with water quality samples were collected for 23 events and analyzed for TKN, NH_4, NO_{2-3}, TP, TSS, biochemical oxygen demand (BOD-5), Cu, Zn, and Pb. Grab samples were collected from 19 storms for fecal coliform and 14 events for *E. coli*. There were significant reductions in the concentrations of TN, TKN, NH_4, BOD-5, fecal coliform, *E. coli*, TSS, Cu, Zn, and Pb. NO_{2-3} concentrations were essentially unchanged. Efficiency ratios for TN, TKN, NH_4, TP, TSS, fecal coliform, *E. coli*, Zn, Cu, and Pb were 0.32, 0.44, 0.73, 0.31, 0.60, 0.69, 0.71, 0.77, 0.54, and 0.31, respectively [49]. These results indicated that in an urban environment, bioretention systems can reduce concentrations of most target pollutants, including pathogenic bacteria indicator species. For those it does not provide treatment, it can reduce mass loading because of runoff reduction through exfiltration.

Besides typical nutrients and pollutants, bioretention media can also capture heavy metals and polycyclic aromatic hydrocarbons (PAHs). A bioretention cell in the District of Columbia performed a high rate of capture with accumulation for Zn, Pb, and Cu as 532, 660, and 75 mg/kg in surface media layer, respectively [50]. A monitored bioretention cell in Maryland reduced the EMCs of PAHs ranged from 31 – 99%, with a mean discharge EMC of 0.22 μg/L, and an average PAHs mass load reduction of 87% to the watershed [51].

Selection of bioretention media is critical due to the possibility that the media can be a source for pollutant leaching. Comparison on 3 bioretention sites showed the media with high P content can release more P into outflow after treatment [48].

In Chapter 3, the pollutant removal effectiveness by 3 different bioretention blends will be evaluated and compared through a mesocosm experiment; In Chapter 4, a numerical model will be presented to estimate bioretention treatment of N and P based on physicochemical and biochemical relationships, attenuation through storage, and mass load removal through exfiltration.

1.3.4 Research aspects

The popularization of bioretention in urban areas for stormwater management calls for enhanced and advanced studies to direct existing design criteria and promote facility performance. Moreover, the mechanisms and maintenance of bioretention are still evolving, which will dictate long-term performance and life-cycle costs [34]. In the long run, bioretention application will continue to evolve as design guidance matures and research continues.

Major aspects of bioretention research focus upon hydrologic mitigation and water quality treatment as described in previous sections. A study of a field-scale bioretention demonstration was conducted to provide design factors that are important to meet certain hydrologic and water quality goals [40, 44, 47, 48]. Laboratory-scale columns studies and mesocosms under controlled conditions with comparable groups [36, 52-54] were conducted to identify and quantify key factors in media design. The latter part will be discussed in details in Chapter 3.

Recent studies have extended to the aspects of management and maintenance to enhance bioretention performance and decrease its environmental impact. In a recent study, two bioretention cells were repaired by excavating the top 75 mm of fill media, increasing the surface storage volume by nearly 90% and the infiltration rate by up to a factor of 10. Overflow volume decreased from 35 – 37% to 11 – 12% respectively. Nearly all effluent pollutant loads exiting the post-repair cells were lower than their pre-repair conditions [44]. This outcome showed that maintenance is also critical to improving bioretention performance. A case study on the life cycle assessment of a bioretention cell used metrics including carbon footprint, acidification potential, human life cycle economic costs and etc. to evaluate its benefits and impacts [55]. The assessment provided a powerful tool towards refined design and sustainable management of bioretention practices.

Among the newly developed fields of bioretention study, computational model development is an area of active research. Computational models can provide powerful assistance to decipher and depict the complex processes occurring within bioretention systems. The major physical, chemical, and biological processes can possibly represent the hydrologic and treatment mechanisms of bioretention. For now, performance under given conditions are mainly estimated using observed data.

Some effective computational tool for simulating urban runoff hydrology incorporate rainfall data to compare LID's runoff volumes, peak flows, and flow duration with continuous simulation [56]. Bosley modeled multiple bioretention cells within a watershed using US EPA's Storm Water Management Model (SWMM) to evaluate their hydraulic performance [57]. A computational model of a single bioretention cell in a

parking area was developed using the Hydrologic Engineering Center-Hydrologic Modeling System (HEC-HMS) with a Green-Ampt infiltration process [58]. The model was successful in predicting the water mass balance for the catchment and bioretention over long-term events. Lucas conducted a design of integrated bioretention urban retrofits with storm event simulation by HydroCAD and compared them with results achieved using a SWMM continuous simulation [35]. SWMM can also be adapted to evaluate the removal behaviors of bioretention cells with its LID Controls module [56, 59, 60]. However, the fact that the module basically uses soil parameters to estimate pollutant removals undermines the credibility of its outputs. Another computational model, DRAINMOD, originally developed for the purpose of simulating agricultural drain fields, was recently adapted to simulate bioretention. It was developed to simulate the hydrology of poorly drained, high water table soils on an hourly or daily basis for long periods of climatological record [61, 62], but excludes consideration of nutrient treatment. Generally, these popular models can be used for developing a conventional hydrograph, but they have multiple restrictions to meet user requirements due to the fact that they are not developed or retrofitted especially for bioretention modeling purposes [63]. Thus their outputs cannot reflect the entire mass flow of water and nutrients within bioretention systems exactly.

The descriptions and uses of some popular computational programs that can be employed for modeling bioretention hydraulics are summarized in Table 1.2.

Some researchers coded programs or enhance specificity to evaluate the hydrologic performance and treatment effectiveness of bioretention facilities, rain gardens, and infiltration basins. RECARGA, a bioretention design model, uses a

physically-based approach to simulate the water balance for runoff inputs, surface ponding, infiltration, ET, overflows, underdrain outflows, and groundwater recharge [64]. RECARGA was applied to the Sugar River watershed in Verona, WI to develop site-specific hydrologic criteria. These RECARGA simulations illustrate trade-offs in design; i.e., maintaining a predevelopment recharge rate while minimizing increases in stormwater runoff. RECARGA performs well on hydraulics simulation, but does not simulate nutrients or other water quality parameters. Roy-Poirier and *et al.* developed a numerical model to calculate unit processes inherent in bioretention that reduce P in both soluble and particulate forms [65]. The authors presented simplified reaction equations to describe the processes of precipitation, dilution, vegetative uptake, isotherm sorption, and settlement. However, the inconsideration of vegetation uptake and defoliation cannot complete the full cycle of P transformation within bioretention systems. A sophisticated model on nutrient flow was developed by Kadlec and Hammer to describe the dynamic changes of P, N, and Cl within wetlands [66]. N is modeled through the processes of mineralization, plant uptake, nitrification, denitrification, and volatilization using coupled differential equations [67]. Event-based simulations are typically used to define limits of nutrient retention under standard conditions for regulatory compliance, and can be informative in comparing performance of design alternatives. A review of similar models for nutrient simulation is provided by Langergraber and et al. [68]. Many of these models take vegetation as a factor into account, but assume vegetation biomass remains constant, i.e., no growth, and no seasonal defoliation. Thus, the nutrient cycles may have missing inputs and outputs not reflected in the model.

The development of a model of bioretention hydrology and treatment will be described in Chapter 4 in this dissertation. An endeavor will be performed to remedy the flaws of existing modeling tools for bioretention simulation.

1.4 Objectives

The previous sections summarize the hydrologic and pollution problems caused by urban impervious areas, and the role of LID in mitigating these impacts. The primary functions of bioretention and similar LID practices are to restore predevelopment hydrologic pattern and reduce the sources of pollutants in urban runoff. The objectives and behavior of observed bioretention was reviewed, with a summary of its benefits, design criteria and important factors. Current knowledge gaps in addressing hydrologic and water quality environmental issues were compiled. Developing a better understanding of bioretention physicochemical processes and generalizing its behavior in a computational model to assist design is critical to improving its performance. Specific research objectives in this work include:

1) Perform long-term frequency analysis on rainfall events and dry durations in Virginia to understand the effect of climatological pattern on bioretention performance.
2) Conduct isotherm and mesocosm experiments on bioretention blends to measure media property parameters and compare their capabilities for N and P retention with synthetic stormwater.
3) Develop a general computational model with numerical methods and analytical relationships to describe and estimate bioretention performance, i.e. runoff reduction and pollutants removal.

TABLES AND FIGURES

Table 1.1 Minimum, mean, and maximum of pollutant concentrations in urban runoff of several Virginia cities. [69]

Cities	Conc. (mg/L)	TSS	COD	TN	TKN	NH_4	NO_{2-3}	TP
Virginia Beach	Min	3	10	0.34	0.33	0.05	0.01	0.07
	Mean	60.1	69.3	2.21	1.75	0.474	0.459	0.321
	Max	823	348	15.5	13.0	4.09	2.48	1.76
Norfolk	Min	3	5	0.14	0.1	0.05	0.04	0.05
	Mean	82.6	112	2.68	2.03	0.586	0.651	0.536
	Max	374	360	12.8	9.53	4.73	3.31	6.72
Chesapeake Bay	Min	4	12	0.27	0.19	0.05	0.08	0.05
	Mean	54.3	48.1	1.59	1.09	0.322	0.495	0.268
	Max	629	200	5.96	3.35	0.97	2.61	0.95

Table 1.2 Descriptions and uses of major computational models to simulate bioretention hydraulics. [63, 70]

Model	Brief Description	Recommended Use
SWMM	Hydrologic, hydraulic and water quality model with optional continuous simulation	Detailed analysis of watershed with storage-focused LID
Hydro-CAD	Hydrologic model to calculate runoff and detention pond routing with exfiltration option	Analysis of storage and infiltration based LID within a watershed
HEC-HMS	Model to develop standard hydrograph based on precipitation input	Obtaining standard, non-adjusted hydrographs. Not recommended for modeling integrated practices
RECARGA	Hydraulic model for optional event and continuous simulation or design purpose	Detailed analysis for bioretention hydraulics and runoff retention
DRAINMOD	Hydrologic model on an hourly, daily basis for long periods of climatological record	Determine hydraulic capacity of wetland for drained sites or land treatment

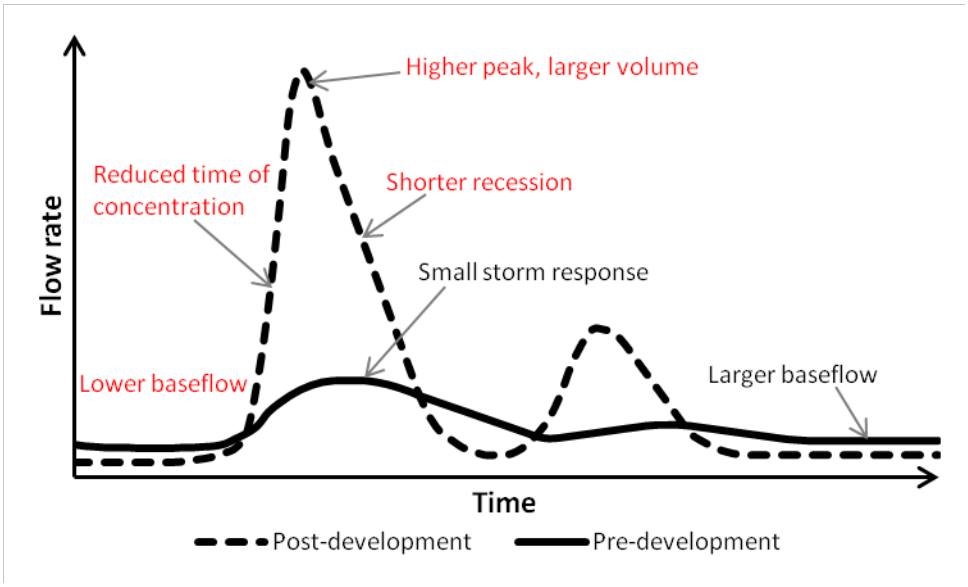

Figure 1.1 Schematic illustration of the pertinent impacts of urbanization on hydrology at the catchment scale (adapted from [3]).

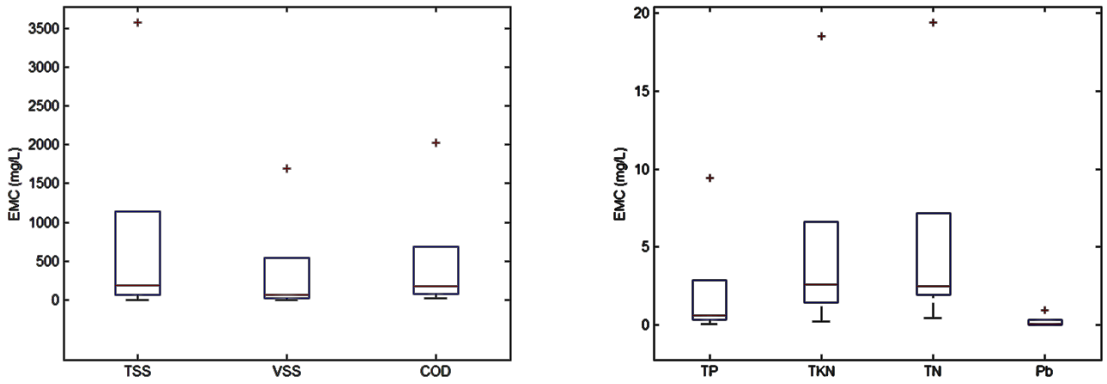

Figure 1.2 Pollutant EMCs in urban runoff of a metropolitan area in the United States (plotted from [14]).

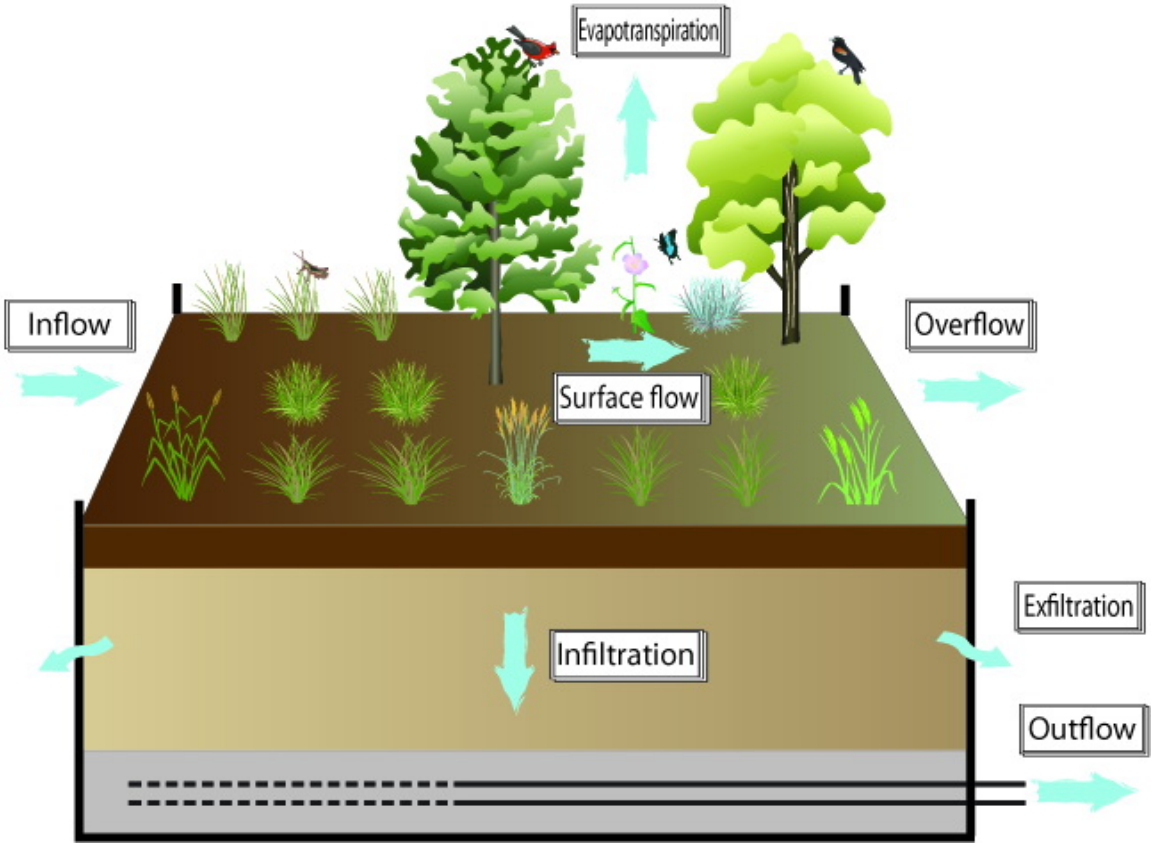

Figure 1.3 Schematic diagram of a bioretention facility and its hydraulic pattern.

References

1. UN News Centre. Half of global population will live in cities by end of this year, predicts UN. 2008; Available from: http://www.un.org/apps/news/story.asp?NewsID=25762.
2. The Economist. Open-air computers: cities are turning into vast data factories. 2012; Available from: http://www.economist.com/news/special-report/21564998-cities-are-turning-vast-data-factories-open-air-computers.
3. Fletcher, T.D., H. Andrieu, and P. Hamel, Understanding, management and modelling of urban hydrology and its consequences for receiving waters: a state of the art. *Advances in Water Resources*, 2013. **51**(0): p. 261-279.
4. Lee, J. and J. Heaney, Estimation of urban imperviousness and its impacts on storm water systems. *Journal of Water Resources Planning and Management*, 2003. **129**(5): p. 419-426.
5. Schueler, T.R., *Site planning for urban stream protection*, 1995, Metropolitan Washington Council of Governments: Washington, D.C.
6. Oregon's Stormwater Solutions Team, *Stormwater solutions: turning Oregon's rain back into a resource*, 2007, Oregon Environmental Council: Portland, OR.
7. Osman, A., *Urban stormwater hydrology: a guide to engineering calculations*. 1993, Lancaster, PA: Technomic Pub. Co.
8. Nelson, E.J. and D.B. Booth, Sediment sources in an urbanizing, mixed land-use watershed. *Journal of Hydrology*, 2002. **264**(1–4): p. 51-68.
9. Waterkeeper Alliance, *All stormwater is local: a manual for reading, understanding, and advocating for effective municipal stormwater permits in the United States*, 2009: Irvington, NY.
10. Line, D.E. and N.M. White, Effects of development on runoff and pollutant export. *Water Environment Research*, 2007. **79**(2): p. 185-190.
11. Arias, M., M. Brown, and J. Sansalone, Characterization of storm water–suspended sediments and phosphorus in an urban catchment in Florida. *Journal of Environmental Engineering*, 2013. **139**(2): p. 277-288.
12. Gupta, K. and A.J. Saul, Specific relationships for the first flush load in combined sewer flows. *Water Research*, 1996. **30**(5): p. 1244-1252.
13. Morace, J.L., *Reconnaissance of contaminants in selected wastewater-treatment-plant effluent and stormwater runoff entering the Columbia River, Columbia River Basin, Washington and Oregon, 2008-10*, 2012, US Geological Survey: Reston, VA.
14. Brezonik, P.L. and T.H. Stadelmann, Analysis and predictive models of stormwater runoff volumes, loads, and pollutant concentrations from watersheds in the Twin Cities metropolitan area, Minnesota, USA. *Water Research*, 2002. **36**(7): p. 1743-1757.
15. Passeport, E. and W. Hunt, Asphalt parking lot runoff nutrient characterization for eight sites in North Carolina, USA. *Journal of Hydrologic Engineering*, 2009. **14**(4): p. 352-361.
16. Makepeace, D.K., D.W. Smith, and S.J. Stanley, Urban stormwater quality: summary of contaminant data. *Critical Reviews in Environmental Science and Technology*, 1995. **25**(2): p. 93-139.

17. Davis, A.P. and R.H. McCuen, *Stormwater management for smart growth*. 2005, New York, NY: Springer Science.
18. Mitsch, W.J. and J.S. Erik, *Ecological engineering: an introduction to ecotechnology*. 1989, New York, NY: Wiley.
19. Debo, T.N. and A.J. Reese, *Municipal stormwater management*. 2003, Boca Raton, FL: Lewis Publishers.
20. Northern Virginia Planning District Commission and Engineers and Surveyors Institute, *Northern Virginia BMP handbook: a guide to planning and designing best management practices in northern Virginia*. 1992, Annandale, VA.
21. Prince George's County, *Low-impact development: an integrated design approach*, 1999, Department of Environmental Resources: Largo, MD.
22. US Environmental Protection Agency, *Low impact development (LID): a literature review*, 2000, Office of Water: Washington, D.C.
23. Virginia Department of Conservation and Recreation, *Virginia stormwater management regulations*, 2001, Division of Soil and Water Conservation: Richmond, VA.
24. University of Arkansas, *Low impact development: a design manual for urban areas*. 2010, Fayetteville, AK.: University of Arkansas Press.
25. US Environmental Protection Agency, *Benefits of low impact development: how LID can protect your community's resources*, 2012, Office of Wetlands, Oceans, and Watersheds: Washington, D.C.
26. University of Virginia. *Stormwater management: definitions and abbreviations*. 2013; Available from: http://ehs.virginia.edu/ehs/ehs.stormwater/stormwater.definitions.html.
27. Niemczynowicz, J., *Urban hydrology and water management – present and future challenges. Urban Water*, 1999. **1**(1): p. 1-14.
28. US Environmental Protection Agency. *Stormwater management at EPA headquarters*. 2006; Available from: http://www.epa.gov/oaintrnt/stormwater/hq_lid.htm.
29. Greenway, M. and W.C. Lucas, *Advanced bioretention and panter-trench experiments: the Science Museum of Virginia*, in World Environmental and Water Resources Congress 2011: Palm Springs, CA. p. 3649-3658.
30. US Environmental Protection Agency. *Low impact development (LID)*. 2013; Available from: http://water.epa.gov/polwaste/green/.
31. US Environmental Protection Agency. *State storm water BMP manuals*. 2013; Available from: http://yosemite.epa.gov/R10/WATER.NSF/0/17090627a929f2a488256bdc007d8dee.
32. Prince George's County, *Bioretention manual*, 2007, Department of Environmental Resources: Upper Marlboro, MD.
33. US Department of Housing and Urban Development, *The practice of low impact development*, 2003, Office of Policy Development and Research: Washington, D.C.
34. Davis, A., et al., Bioretention technology: overview of current practice and future needs. *Journal of Environmental Engineering*, 2009. **135**(3): p. 109-117.

35. Lucas, W., Design of integrated bioinfiltration-detention urban retrofits with design storm and continuous simulation methods. *Journal of Hydrologic Engineering*, 2010. **15**(6): p. 486-498.
36. Davis, A.P., R.G. Traver, and W.F. Hunt, Improving urban stormwater quality: applying fundamental principles. *Journal of Contemporary Water Research & Education*, 2010. **146**(1): p. 3-10.
37. Winston, R., et al., Field evaluation of four level spreader–vegetative filter strips to improve urban storm-water quality. *Journal of Irrigation and Drainage Engineering*, 2011. **137**(3): p. 170-182.
38. DeBusk, K., W. Hunt, and D. Line, Bioretention outflow: does it mimic nonurban watershed shallow interflow? *Journal of Hydrologic Engineering*, 2011. **16**(3): p. 274-279.
39. Hunt, W., A. Davis, and R. Traver, Meeting hydrologic and water quality goals through targeted bioretention design. *Journal of Environmental Engineering*, 2012. **138**(6): p. 698-707.
40. Li, H., et al., Mitigation of impervious surface hydrology using bioretention in North Carolina and Maryland. *Journal of Hydrologic Engineering*, 2009. **14**(4): p. 407-415.
41. Hunt, W., et al., Pollutant removal and peak flow mitigation by a bioretention cell in urban Charlotte, N.C. *Journal of Environmental Engineering*, 2008. **134**(5): p. 403-408.
42. Davis, A., Field performance of bioretention: hydrology impacts. *Journal of Hydrologic Engineering*, 2008. **13**(2): p. 90-95.
43. Heasom, W., R.G. Traver, and A. Welker, Hydrologic modeling of a bioinfiltration best management practice. *Journal of the American Water Resources Association*, 2006. **42**(5): p. 1329-1347.
44. Brown, R.A. and W.F. Hunt, Improving bioretention/biofiltration performance with restorative maintenance. *Water Science & Technology*, 2012. **65**(2): p. 361-367.
45. Li, H. and A.P. Davis, Urban particle capture in bioretention media. I: laboratory and field studies. *Journal of Environmental Engineering*, 2008. **134**(6): p. 409-418.
46. Li, H. and A. Davis, Water quality improvement through reductions of pollutant loads using bioretention. *Journal of Environmental Engineering*, 2009. **135**(8): p. 567-576.
47. Komlos, J. and R. Traver, Long-term orthophosphate removal in a field-scale storm-water bioinfiltration rain garden. *Journal of Environmental Engineering*, 2012. **138**(10): p. 991-998.
48. Hunt, W., et al., Evaluating bioretention hydrology and nutrient removal at three field sites in North Carolina. *Journal of Irrigation and Drainage Engineering*, 2006. **132**(6): p. 600-608.
49. Hunt, W.F., *Pollutant removal evaluation and hydraulic characterization for bioretention stormwater treatment devices*, in Department of Agricultural and Biological Engineering 2003, The Pennsylvania State University: University Park, PA.

50. Li, H. and A.P. Davis, Heavy metal capture and accumulation in bioretention media. *Environmental Science & Technology*, 2008. **42**(14): p. 5247-5253.
51. DiBlasi, C.J., et al., Removal and fate of polycyclic aromatic hydrocarbon pollutants in an urban stormwater bioretention facility. *Environmental Science & Technology*, 2008. **43**(2): p. 494-502.
52. Hsieh, C.-h., A.P. Davis, and B.A. Needelman, Nitrogen removal from urban stormwater runoff through layered bioretention columns. *Water Environment Research*, 2007. **79**(12): p. 2404-2411.
53. Lucas, W.C. and M. Greenway, Nutrient retention in vegetated and nonvegetated bioretention mesocosms. *Journal of Irrigation and Drainage Engineering*, 2008. **134**(5): p. 613-623.
54. Lucas, W. and M. Greenway, Phosphorus retention by bioretention mesocosms using media formulated for phosphorus sorption: response to accelerated loads. *Journal of Irrigation and Drainage Engineering*, 2011. **137**(3): p. 144-153.
55. Flynn, K.M. and R.G. Traver, Green infrastructure life cycle assessment: a bio-infiltration case study. *Ecological Engineering*, 2013. **55**(0): p. 9-22.
56. Aad, M.P.A., M.T. Suidan, and W.D. Shuster, Modeling techniques of best management practices: rain barrels and rain gardens using EPA SWMM-5. *Journal of Hydrologic Engineering*, 2010. **15**(6): p. 434-443.
57. Bosley, E.K., *Hydrologic evaluation of low impact development using a continuous, spatially-distributed model*, in Civil Engineering 2008, Virginia Polytechnic Institute and State University: Blacksburg, VA.
58. Palhegyi, G.E., Modeling and sizing bioretention using flow duration control. *Journal of Hydrologic Engineering*, 2010. **15**(6): p. 417-425.
59. Stander, E. and M. Borst, Hydraulic test of a bioretention media carbon amendment. *Journal of Hydrologic Engineering*, 2010. **15**(6): p. 531-536.
60. Gironás, J., et al., A new applications manual for the Storm Water Management Model (SWMM). *Environmental Modelling & Software*, 2010. **25**(6): p. 813-814.
61. Skaggs, R.W., *DRAINMOD: a simulation model for shallow water table soils*, in *South Carolina Water Resources Conference*, 2008: Charleston, SC.
62. Brown, R.A., *Evaluation of bioretention hydrology and pollutant removal in the upper coastal plain of North Carolina with development of a bioretention modeling application in DRAINMOD*, in Biological and Agricultural Engineering 2011, North Carolina State University: Raleigh, NC.
63. White, K. and J. Walker, *Modeling techniques to incorporate low impact development features into detention analyses*, in World Environmental and Water Resources Congress: Great Rivers. 2009: Kansas City, MO. p. 1-10.
64. Atchison, D. and L. Severson, *Recarga user's manual, version 2.3*, 2004, University of Wisconsin - Madison: Madison, WI.
65. Roy-Poirier, A., P. Champagne, and Y. Filion, Bioretention processes for phosphorus pollution control. *Environmental Reviews*, 2010. **18**: p. 159-173.
66. Kadlec, R.H. and D.E. Hammer, Modeling nutrient behavior in wetlands. *Ecological Modelling*, 1988. **40**(1): p. 37-66.
67. Senzia, M.A., et al., Modelling nitrogen transformation and removal in primary facultative ponds. *Ecological Modelling*, 2002. **154**(3): p. 207-215.

68. Langergraber, G., et al., Recent developments in numerical modelling of subsurface flow constructed wetlands. *Science of The Total Environment*, 2009. **407**(13): p. 3931-3943.
69. Hirschman, D., K. Collins, and T. Schueler, *The runoff reduction method*, 2008, Center for Watershed Protection and Chesapeake Stormwater Network: Ellicott City, MD.
70. Montalto, F. and B. Lucas, *How are low impact stormwater control measures simulated by different computational models?*, in World Environmental and Water Resources Congress, 2011: Palm Springs, CA. p. 538-546.

2 Frequency Analysis for Precipitation Events and Dry Durations of Virginia[1]

Abstract

Stormwater Control Measures (SCMs) are widely used to control and treat stormwater runoff pollution. The first step in SCM design is to evaluate the precipitation patterns at a site. SCMs are normally designed using a storm with a specific return period. A robust design process that uses frequency distribution of precipitation and monitoring of performance could improve our understanding of the behavior and limitations of a particular design. This is not the current norm in design of SCMs. In this research, frequency analyses (FA) of precipitation events was conducted using hourly precipitation data from 1948 to 2010 for 8 sites representing the 4 major physiographic regions of Virginia. The available data were treated using an inverse distance method to eliminate missing gaps before processing into events determined by minimum inter-event times. FA was at each site to develop frequency plots of precipitation and dry duration. FA of the 8 locations indicates a range of rainfall depths from 22.9 mm in Bristol to 35.6 mm in Montebello, compared to the nominal "water quality storm" of 25.4 mm (i.e., 1 in.). Similarly, for dry duration, for a 10% exceedance probability, the range is from 16.8 days in Richmond and Norfolk to 19.5 days in Montebello. Dry duration provides guidance for vegetation selection, which is important for some SCMs. The degree of variability in both parameters argues for consideration of site specific information in design. FA was also used to provide guidance to improve monitoring programs. Monte-Carlo simulations

[1] An academic paper in press, allowed to reproduce in this dissertation. Liu, J., Sample, D., and Zhang, H. Frequency analysis for precipitation events and dry durations of Virginia. *Environmental Modeling & Assessment*, 2013. (DOI: 10.1007/s10666-013-9390-2)

demonstrated that performance monitoring programs applied in different regions would likely encounter more than 30% of precipitation events less than 6.35 mm, and 10% over 25.4 mm under various sampling regimes. The percentages of precipitation events encountered in Coastal Plain and Piedmont regions are not impacted by sampling regimes, however the Blue Ridge Mountains and Valley and Ridge regions are likely impacted. Anticipating event occurrences improves the chances of implementing a successful monitoring program. The use of these results could enhance the performance of SCMs with consideration of local conditions for both monitoring SCMs and their design basis.

Key words: stormwater control measures, frequency analysis, minimum inter-event time, depth-duration distribution, Monte-Carlo simulation

2.1 Introduction

Stormwater Control Measures (also known as BMPs) are often used at developing sites to mitigate the effects of urban development [1, 2]. One type of SCM is rainwater harvesting (RWH), which collects runoff for later reuse, and can achieve significant savings of non-potable water [3]. Other SCMs like bioretention or constructed wetlands are dependent on the influent runoff generated by precipitation. The design of RWH systems has a close relationship with the temporal / spatial variation and distribution of precipitation in its geographical region [4]. Determining frequency of precipitation patterns at a site is usually the first step in understanding local hydrological conditions, and determining the locations, sizes, and other design parameters of SCMs; an example of such is provided by Su et al. [5].

Intensity-duration-frequency (IDF) curves are traditionally used for risk-based design of SCMs [6]. However, IDF method is limited to a specific duration for a design storm and neglects inter-event dry periods [7]. A more robust method with simple but reliable results can be performed by frequency analysis (FA) for precipitation events and inter-event dry durations using long-term precipitation data [8]. The FA result of precipitation patterns can also provide information on more realistic events for design of SCMs, especially helpful for evaluating performance of SCMs by volume control estimation [9].

Some computational models have built-in capabilities for processing the long-term precipitation data, such as the SWMM [10], HEC-HMS [11], and others. A comparison of these models is provided by Montalto and Lucas [12].

One of the early uses of FA was for flood frequency to predict design floods for sites near rivers. A methodology was developed and published by USGS [13] that systemized flood FA in Guidelines for Determining Flood Flow Frequency (Bulletin 17B). Statistical techniques, such as log-Pearson Type III and log-normal fitting process, were introduced by Wurbs [14]. These methods can be applied to precipitation FA to investigate the likelihood of various precipitation events as a function of exceedance probability.

Numerous applications of FA in a variety of hydrologic conditions have been conducted [15]. Jou et al. [16] applied FA to monthly precipitation in Iran, using parametric methods (log-normal and log-Pearson distribution) and nonparametric method (Gaussian function). The authors compared the fit of both distributions and found the parametric methods to be better than nonparametric method. Sveinsson et al. [17] and

Norbiato et al. [18] applied regional FA of extreme precipitation based on index variable method and L-moments. The regional growth curves generated from Kappa distribution helped refine the design criteria for storm drainage in specific regions. With similar techniques of regional FA, Naghavi and Yu [19] identified the annual maximum series for precipitation durations from 1 – 24 h for 25 stations to the generalized extreme value distribution. The regional analysis procedure was tested by Monte-Carlo simulation. All results showed that the procedure could substantially reduce root-mean-square error and bias.

FA methods can also be applied on large-scale spatial and temporal features of precipitation. Englehart and Douglas [20] performed FA for mainland United States with the data sets from 1951 to 1980. A rainfall frequency atlas of the Midwest was constructed by FA methods too [21]. They defined the precipitation frequency as the number of days per month or season with total amounts >2.54 mm (0.10 in). The results suggest that FA is a more appropriate technique than total precipitation evaluation for climate studies. Long-term precipitation change was examined by Fowler and Kilsby [22] from regional frequency pooling of annual maxima for 1961 to 2000 in the United Kingdom. The generalized extreme value growth curves demonstrate few observable changes in precipitation extremes within these 40 years.

Some researchers have used FA to assess drought durations. Hershfield [23] chose precipitation data from 31 stations to establish an estimate for the frequency of dry periods in Maryland. Extreme-value and seasonal variation analysis indicated that dry periods of at least 10 days for the 2.54 mm threshold can be expected about only 5 times

a year. Dickerson and Dethier [24] provided a study on the drought patterns in the northeastern United States, estimating drought frequency probability and return period.

The design and maintenance of SCMs depend on the understanding of spatial and seasonal rainfall distributions at local locations. Previous studies of precipitation FA are majorly to discuss climatological pattern without considering SCMs. This paper is to apply a comprehensive analysis on the long-term rain-dry frequency pattern across Virginia to provide directions on SCMs criteria. This research also identified expected precipitation events through exploratory Monte-Carlo simulation with random process. The summarized results are to assist decision makers to manage / maintain SCMs and assess their performance through optimal sampling programs.

2.2 Methods

A description of the theoretical basis for the development of the model and the analysis of reliability curves are provided in the following section.

2.2.1 Database and data availability

Precipitation data are available at the online database of National Climate Data Center (http://www.ncdc.noaa.gov/oa/climate/stationlocator.html). The database of weather observation station records can provide long-term documented precipitation data of a certain site nationwide. Data of 8 stations were selected from the archive of NCDC for the range from 1948 to 2010.

2.2.2 Selection of stations and regions in Virginia

The weather observation stations were selected and then grouped according to the spatial location relative to the physiography of Virginia. Virginia can be divided into 5 regions from east to west: Coastal Plain, Piedmont, Blue Ridge Mountains, Valley and

Ridge, and Appalachian Plateau. Due to the sparseness of stations in or near Virginia with hourly precipitation data, only the 4 largest regions except Appalachian Plateau were considered. For each regional area, 2 weather stations with sufficient hourly data were selected as representative examples for frequency and Monte-Carlo approaches. Table 2.1 presents the features of the 4 selected regions and 8 weather observation stations with their locations in Virginia.

A weather station at the border of Virginia and Tennessee (BRISTOL AP) was selected because it was the only available station with long-term hourly precipitation data for the regional group of the Valley and Ridge region in Southern Virginia. The Richmond station was classified as being located in the Piedmont region, which is true of the city; however, the airport is actually located just inside the coastal physiographic region.

The physiographical regions and selected weather stations in Virginia are shown in Figure 2.1, which demonstrates the distribution of the 8 investigated weather stations across the Commonwealth of Virginia.

2.2.3 Raw data screening and processing

To perform further analysis, the raw data from the NCDC database was arranged on a spreadsheet. The smallest precipitation data not more than 2.54 mm was converted to 0. This process is intended to screen the smallest precipitation events to concentrate the analysis of significant precipitation events without adversely affecting the dry duration analysis.

Effective data processing work is necessary to eliminate false annual maxima associated with a variety of data measurement, reporting and transcription errors [25].

There are basically 2 kinds of erroneous data to be eliminated: missing gaps and cumulative data. Missing observations occur due to interruption of measurements, extreme natural phenomena, artificial mishandling of data or accidental loss of recorded files [26]. A cumulative datum is a combination of several original observations of previous hourly precipitation records.

A robust data analysis stands on reasonable and scrutinized treatment to eliminate data gaps. Some researchers applied complicated methods of regression trees plus artificial neural networks to reconstruct missing weather data for a large watershed with a network of data sources [27]. For this study on a limited number of weather stations, the missing data were treated by a relatively simple but effective method of inverse distance to patch the gaps with the precipitation data from 2 neighboring stations as well as the distances between the investigated and those neighboring stations. A general formula can be represented as [28, 29].

$$P_x = \frac{\sum_{i=1}^{N_S} \frac{1}{d_i{}^2} p_i}{\sum_{i=1}^{N_S} \frac{1}{d_i{}^2}} \tag{2-1}$$

Where P_x = estimate of missing precipitations for the investigated station (mm)

p_i = precipitations from neighboring stations at the same time of missing period (mm)

d_i = distance from each neighboring station to the investigated station (m)

N_s = number of neighboring stations involved into calculation (dimensionless)

The cumulative data were screened out and distributed evenly by the number of previous observation hours included in the cumulative period, assuming that the precipitation has an equivalent event in each related hour. In the case that the distributed precipitation values are no more than 2.54 mm, the values are converted to 0, or the events recorded as cumulative data were omitted.

The amounts of missing and cumulative data were counted and summarized in Table 2.2. The summarization shows that MONTEBELLO FISH HTCHY and STAR TANNERY have by far the largest data gaps, at 11.7% and 13.1% of the total available period, respectively.

2.2.4 Determination of minimum inter-event time

The inter-event time is usually referred as the dry duration without precipitation between 2 consecutive events. The minimum inter-event time (MIT) is used to categorize precipitation data into continuous events by a minimum period of time without precipitation between 2 consecutive events [30]. To distinguish 2 consecutive precipitation events, a proper MIT can be estimated as the minimum dry period separating these events.

A popular and intuitive method to define the MIT is through examination of the relationship between the average annual precipitation event number and different inter-event time [30]. The inter-event time was varied from 1 to 12 h and the average annual precipitation event was estimated for each case. Results of event numbers are plotted versus corresponding inter-event time. As shown in Figure 2.2, the Event-Time curves of the 8 stations have monotonically decreasing trends, and the decline of event numbers is not significant after 6 h of inter-event time. The observed change of slopes indicates that

after the threshold of 6 h, the increase of inter-event time has diminished influence on the quantity of events, and 6 h is the “knee of the curve” for these Event-Time curves.

In practice, the MIT determination is also governed by its application. MIT has not been universally defined, but the order of 4 – 8 h has been widely accepted [31]. For the following analysis on precipitation data, MIT was set at 6 h.

With MIT determined, the hourly precipitation data were categorized into numerous rainfall events. The following frequency and random analyses were based on event examinations of previous processes.

2.2.5 Statistical fit and check on data processing

The calculated rainfall depth of each precipitation event can be developed into histogram with rainfall depth and probability density as independent and dependent variables to examine typical range of characteristic magnitudes. It is obvious from the shape of histogram that exponential, gamma, or log normal probability distribution function (PDF) can be employed to represent the depth data [32]. With Matlab’s Distribution Fitting Tool, these 3 PDFs were plotted and compared to check the appropriate statistical fit of depth probability density histogram. Figure 2.3 shows the 3 fitting curve with WASHINGTON REAGAN AP as example.

The Kolmogorov-Smirnov hypothesis test was used to statistically examine the goodness-of-fit of these 3 PDFs. The result shows the p-values of the 3 fits are smaller than the desired significance level as 0.05, which means the null hypothesis that these 3 PDFs can statistically fit the density histogram should be rejected. Therefore PDF fits were not used in the following FA approach.

It can be visually observed that the log normal PDF fits the density histogram better than exponential and gamma PDFs. The statistical check verified this conclusion that log normal PDF had greater log likelihood value than the other 2 PDFs, which means it is a better fit for the histogram. Exponential and gamma PDFs have similar log likelihood values that are a little smaller than log normal PDF. Since the exponential PDF is relatively simpler to express and easier to manipulate, it is likely to be used to roughly represent the histogram distribution of depth density.

To evaluate the acceptability of our missing data algorithm, it is necessary to examine the difference between the distribution of unprocessed and processed precipitation event data for statistical significance. If the difference between the distributions is small or negligible, the processes to eliminate missing and cumulative data can be considered not influential on original statistical distribution of precipitation data.

The 2 series of unprocessed and processed event data were compared with two-sample Kolmogorov-Smirnov goodness-of-fit hypothesis test to determine if independent random samples are drawn from the population with the same distribution pattern. The returned hypothesis parameter (h) is 0 for all cases, indicating the null hypothesis of same distribution at significance level of 0.05 cannot be rejected. As seen on the results of hypothesis test are in Table 2.3. The asymptotic p values are mostly near 1, which means the 2 distributions have nearly 100% possibility to be the same. The null hypothesis can be accepted since p-values are larger than the level of significance as 0.05. Thus, the difference between two samples distributions is not significant enough to say that they have different distribution. This analysis indicates the processes to eliminate missing gaps

and cumulative data did not alter the underlying distribution of precipitation. The processed data are thus acceptable for FA.

2.2.6 Depth-duration probability

Precipitation data are represented as depths. The probability of full-scale precipitation depths with different event durations was analyzed to identify the overall precipitation distribution and characteristics across the 4 regions in VA. The duration values and precipitation depths (including the smallest values no more than 2.54 mm) were imported to a Matlab® program for distribution calculation. The processes were applied on the 4 representative regions to investigate the statistical similarity and difference of local precipitation features.

2.2.7 Frequency analysis of precipitations

The FA approach follows the computing steps as follows to calculate the probabilities of exceedance [33].

1) Sort the long-term precipitation depths from the largest value to the smallest one, including a total of n values.

2) Assign each value a rank (M), starting from 1 (the largest value) to n (the smallest value).

3) Calculate exceedance probability (E) with the equation:

$$E = \frac{\mathrm{M}}{m+1} \times 100 \tag{2-2}$$

Where E = probability that a given precipitation event is equaled to or exceeded (dimensionless)

M = ranked position of the investigated precipitation events (dimensionless)

m = number of precipitation events during the recorded period (dimensionless)

With these steps, the original precipitation data were recomputed as exceedance probabilities and corresponding ranks of precipitation values. The exceedance probability is the occurrences frequency for a precipitation event to exceed a predetermined amount.

A Matlab® program was developed to assist in calculation and visualization. Processed precipitation data were used as input to the program to plot the frequency distribution of precipitation events.

2.2.8 Frequency analysis of dry durations

The prime cause of drought is the occurrence of precipitation at levels below normal. Meteorological droughts are deemed to occur when precipitation is below the range of values considered as normal [34]. In the following discussion, dry duration is defined as the inter-event periods between 2 consecutive events without measured precipitation records.

A similar methodology can be applied to assess the exceedance probabilities of dry duration after filtering out smallest ($\leq$2.54 mm) precipitation events. The sorted ranks are the time spans of dry duration between any 2 consecutive precipitation events. The exceedance probability represents the frequency of occurrences for a dry duration to exceed a certain period of time.

2.2.9 Monte-Carlo simulation

Monte-Carlo simulation is a computerized mathematical simulation technique that provides a distribution of possible outcomes using random sampling of the historical dataset [35]. Typical Monte-Carlo methods use probability concepts and random numbers

to obtain statistical parameters of random variables and simulate random processes to model phenomena with significant uncertainty. Monte-Carlo methods can be used to assess sampling strategies on a large dataset [36]. The Monte-Carlo method is an efficient means to provide a simulated estimate of expected precipitation depths during sampling regimes.

Monte-Carlo methods are based on the Fundamental Formulation of Monte-Carlo (FFMC), with which a generated random number can be related with the random variables under investigation [37].

$$\int_a^x p(x)dx = \int_0^{\varsigma} q(\varsigma)d\varsigma \tag{2-3}$$

If the generated random numbers are distributed uniformly, q(η) is 1 and (3) can be written as (4).

$$P(x) = \varsigma \tag{2-4}$$

Where a = the minimum of event precipitation data as random variable x (mm)

x = event precipitation data as random variable (mm)

$p(x)$ = PDF of event precipitation data as random variable x (dimensionless)

ς = random number (dimensionless)

$q(\varsigma)$ = function of random number (dimensionless)

$P(x)$ = cumulative distribution function (CDF) of event precipitation data as random variable x (dimensionless)

Since the function of event precipitation data is not continuous over time, the general functions to calculate PDF and CDF are given by the following 2 equations.

$$p(t) = \frac{f(t)}{\sum_0^{T_t} f(t)} \quad (2\text{-}5)$$

$$P(t_n) = \sum_{i=1}^{n} p(t_i) \quad (2\text{-}6)$$

Where t = time of recorded period (h)

T_t = total recorded time of the investigated period (h)

i = the i-th event precipitation data (mm)

With the concept of FFMC, a direct relationship between the random variable of event precipitation data and generated random numbers of η can be established.

$$min[P(t_n)] \geq \eta \quad (2\text{-}7)$$

These FFMC processes are to be programmed as Matlab® codes, and employed on historical precipitation events to perform an estimate on sampling scenarios.

2.3 Results and Discussion

2.3.1 Depth-duration probability

The results of regional depth-duration distributions are plotted as 3-D bar graphs in Figure 2.4.

It can be observed within each region that most of the precipitation events are of low-depth and short-duration. The overall probability distribution of precipitation depth-length in Virginia shows a peak at small precipitation depth (<2.54 mm) and short duration (0 – 2 h) events. This peak includes 70% of small events less than 2.54 mm. These trace events with short durations have little impacts on SCMs. The second peak represents events between 2.54 – 6.35 mm and 0 – 2 h. Compared with the events less than 2.54 mm, this portion of rainfall events may play a larger role dictating hydraulic conditions of SCMs. It can be observed that in all 4 regions of Virginia, the larger and

more infrequent events (>25.4 mm and >24 h) have low probabilities. The design of SCMs is typically driven by a moderately sized event of long duration (24 h) of a low probability of exceedance (usually 10%). By setting this design standard, it captures the behavior of the SCM during all events less than that value. In Virginia, this is known as the “water quality storm” and is set at a nominal value of 25.4 mm (1 in.).

2.3.2 Frequency analysis of precipitations

Precipitation FA provides insight on the characteristics of the pattern of precipitation over a long period of time. The calculation results from program were plotted as semi-log curves to represent the different precipitation features among the 4 regions of Virginia. The probabilities of exceedance on the x-axis were plotted on a linear scale, and the precipitation ranks on the y-axis are on a logarithmic scale. The curves are shown in Figure 2.5 to illustrate the percentage of time that precipitation is to equal or exceed some specific depth value.

Comparison of the curves of 4 Virginia regions demonstrates that Coastal Plain and Piedmont have better similarity than other cities of their respective regions, which might result from their similar geographical conditions of flat terrain. Three regions exhibit a trend of larger precipitation in northern cities than southern ones. However the Coastal Plain deviates from this trend, as the southern city Norfolk is very close to the Atlantic Ocean, and the northern city, Arlington, is at the border near Piedmont region. Norfolk has the SCS Type III rainfall distribution, whereas the rest of the stations are in Type II region categorized by United States Department of Agriculture (USDA) [38].

The smoothness of the curves representing MONTEBELLO FISH HTCHY and STAR TANNERY is relatively worse due to the fact they both have the most data gaps to

address. The replenishment of missing records and distribution of cumulative data generates many small and equivalent hourly values, which contribute roughness to the curve sections at higher probabilities, as seen in Figure 2.5.

The frequency curves in Figure 2.5 can be used to estimate the exceedance probability of a specific precipitation event. Each probability value is the reciprocal of a particular return period, or year design storm. Within the 4 regions, there is 20% probability (or 5-year return period) of precipitation to exceed 20 mm. For precipitation cases over 25.4 mm, the exceedance is slightly less than 10% (i.e., a 10-year return period), i.e., or conversely, 90% of the events are less than 25.4 mm. Other probabilities corresponding to different levels of precipitation can also be estimated from the frequency curves.

For precipitation events with exceedance probability higher than 10%, the curves maintain stable slopes decreasing in precipitation magnitude as probabilities increases. For precipitation events with exceedance probabilities less than 10%, the slopes of curves increase when probability is lower. As the inflection point of slope curves in Figure 2.5, a 10-year return period with 25.4 mm precipitation can be considered as a fundamental threshold for most SCMs in Virginia.

Depth-duration analysis shows 70% of the small rainfall events (<2.54 mm) have short periods (<2 h), which have small impacts on hydraulic conditions of SCMs. The events between 2.54 and 6.35 mm have high frequency probabilities and short return periods, but do not normally impact SCM design. The precipitation frequency results can support design of SCMs, or assist in estimating the storage needs of an RWH system. The size of the bioretention area is a function of the drainage area and the runoff generated

from the area. While the amount treated is a function of regulatory requirements, runoff is related to precipitation. Currently, the estimation of bioretention size is based on empirical or arbitrary precipitation data. However, the actual design storm criterion used in state, city or municipalities varies from one another, largely depending on the regulation requirements and availability of resources. For instance, sizing specifications in USEPA's [39] bioretention fact sheet are based on 13 – 18 mm (0.5 – 0.7 in) of precipitation; Virginia Department of Conservation and Recreation (VADCR) [40] uses 25.4 mm (1.0 in) of event precipitation depth in its bioretention design specification.

A reasonable design criterion for SCMs should be based on the return period for desired hydrologic conditions. If the treatment requirement is to fit rainfall events with 5-year return periods, the 20% exceedance probability of 20 mm of event depth can be applied to construct a more economic SCM with limited spending on materials and management. FA curves can support cost-effective decisions providing more flexible choices corresponding to local conditions. Typically, a 90^{th} percentile, or 10% probability of exceedance is of interest in design; both 50^{th} and 90^{th} percentiles are recommended, the former for average conditions, the latter as an indicator of hydraulic performance under stress.

2.3.3 Frequency analysis of dry durations

The FA of dry duration illustrates the distribution regime of arid periods in the 4 regions of Virginia using in a similar method to precipitation frequency curves. The output frequency curves are plotted in Figure 2.6, showing the exceedance probability of a specific dry duration.

The smoothness of dry frequency curves is better than the precipitation frequency curves. All 4 regions except Valley and Ridge have 2 closely overlapping curves, which demonstrate a common regime of dry duration in most Virginia areas. The discrepancy of 2 curves in the Valley and Ridge region might due to greater distance between STAR TANNERY and BRISTOL AP.

For the 4 investigated regions, the 50% probability (2-year return period) of dry duration is 5 – 6 days. For dry durations over 10 days, the corresponding probabilities are less than 30%, indicating that most (>70%) dry periods are less than 10-day duration in Virginia. For a 10% exceedance probability, the range is from 16.8 days in Richmond or Norfolk to 19.5 days in Montebello. Dry duration provides guidance for vegetation selection which is important for these new types of BMPs that depend upon vegetation for treatment. Plants should be able to withstand dry periods of between 16.8 to 19.5 days, or external irrigation should be supplied.

The frequency curves show the distribution of dry periods of a certain location over the 62-year period. The result can be helpful for the selection of SCMs vegetation that can withstand experienced climatology, and provide supportive information for irrigation management and plant maintenance of bioretention, greenroof or other SCMs. This is an essential and often overlooked consideration in SCM design.

2.3.4 Monte-Carlo simulation

The results of Monte-Carlo simulation for precipitation depth of the 4 regions of Virginia are demonstrated in Figure 2.7.

These histograms demonstrate the precipitation events to encounter with different sampling sizes in the 4 regimes. The simulated sampling events are nearly proportional to

the change of sampling sizes, e.g., if the sampling size is halved, the simulated event number is nearly halved as well.

Monte-Carlo simulation presents similar sampling patterns within the 4 regions, for all the 4 regions, precipitation depths less than 2.54 mm are mostly possible to be encountered for all sampling and regional cases. The Ridge and Valley region has fewer cases of large precipitation events with more than 12.7 mm possibly due to its greater distance from coastal influences.

The histograms from Monte-Carlo simulation provide an important consideration when designing a sampling program for measuring performance of an SCM. For instance, a 24-size sampling program in the Piedmont region for a period of time may encounter about 3 events more than 25.4 mm, 4 events between 12.7 and 25.4 mm, 4 events between 6.35 and 12.7 mm, 4 events between 2.54 and 6.35 mm, and 9 events less than 2.54 mm. This sampling distribution pattern provided by Monte-Carlo simulation can be expected to present a typically integral description for performance evaluation of an SCM. The expected sampling frequency was used in developing a statewide program to evaluate the performance of proprietary SCMs [41]. Anticipating event occurrences will improve the ability to implement the monitoring program.

2.4 Conclusions

An understanding of the long term behavior of trends in event precipitation and dry duration can assist the design, management and maintenance of SCMs by providing an assessment of local climatology. About 30% of precipitation events across Virginia are less than 6.53 mm. Investigation on the rest influential precipitation events indicates that the 90% percentile of precipitation depth and dry duration in Virginia can be

generally determined as 22.9 – 35.6 mm and 15.3 – 25.8 days respectively from the frequency curves. Virginia's current criterion of empirical precipitation (1.0 in) has 10% exceedance probability and 10-year return period, which is used as a threshold for SCMs design. FA of various locations across Virginia indicates the wide variability in this metric for the design rainfall event as 22.9 mm to 35.6 mm. Dry duration, like the design rainfall event varies by location across Virginia, from 15.3 to 25.8 days, and should be incorporated into any design that uses vegetation to accomplish its treatment goals, such as bioretention and green roofs.

Monte-Carlo simulation provides direction in terms of sampling regimes necessary for measuring performance effectiveness. For a random sampling regime, small-depth events less than 2.54 mm are more prevalent in Coastal Plain and Piedmont regions while events with precipitation depth between 2.54 – 6.35mm are more prevalent in Blue Ridge Mountains and Valley and Ridge regions. The probability of encountering high events decreases with the increase of precipitation depth. Compared to Coastal Plain and Piedmont regions, different sampling sizes show higher impact on precipitation event encountered in Blue Ridge Mountains and Valley and Ridge regions, especially for precipitation depth less than 6.35 mm.

The topographic form of Virginia induces high precipitation with long, dry intervals in the flat plain regions of Coastal Plain; high precipitation depths with short dry durations in the narrow plain – mountain transition the Blue Ridge Mountain region; and small precipitation events with short dry period in the mountainous Valley and Ridge region. The similarities and differences are determined by geomorphology, elevation, geological terrain, and distance from the sea. A possible further study on the influence of

topography to precipitation and dry period might be performed quantitatively with the helpful application of topographical data and GIS tools. Further evaluation of decadal trends on long-term precipitation data may reveal possible influences on the precipitation-drought pattern in Virginia by climate change.

Acknowledgments

The authors are thankful to Dr. Glenn E. Moglen of the Charles Edward Via Jr. Department of Civil and Environmental Engineering, Virginia Tech for providing with instructive and inspiring suggestions on precipitation FA. This project was partially funded by Project No. 135885, 19 Stormwater Management Research, Assessing Improvements in Design and Operation on Performance, 135885, U.S. Department of Agriculture, National Institute of Food and Agriculture Hatch Project. Opinions contained herein are exclusively those of the authors.

TABLES AND FIGURES

Table 2.1 Selected weather stations in four regions of Virginia for frequency analysis.

Region	Station	COOPID	County/City	Latitude/Longitude
Coastal Plain	WASHINGTON REAGAN AP	448906	Arlington	38.84833N/-77.03417W
	NORFOLK INTL AP	446139	Norfolk	36.90333N/-76.19222W
Piedmont	RICHMOND INTL AP	447201	Henrico	37.50500N/-77.32028W
	LYNCHBURG INTL AP	445120	Campbell	37.32083N/-79.20667W
Blue Ridge Mountains	MONTEBELLO FISH HTCHY	445690	Nelson	37.84611N/-79.12972W
	ROANOKE INTL AP	447285	Roanoke	37.31694N/-79.97417W
Valley and Ridge	STAR TANNERY	448046	Frederick	39.08583N/-78.44417W
	BRISTOL AP	401094	Sullivan	36.47306N/-82.40444W

Table 2.2 Available and Erroneous data of precipitation from NCDC records between 1948 and 2010.

Region	Station	Start Date	End Date	Total Days	Missing Hours	Cumulative Hours
Coastal Plain	WASHINGTON REAGAN AP	1948.05.01	2010.09.30	22798	159	0
	NORFOLK INTL AP	1948.08.05	2010.09.29	22701	13	4081
Piedmont	RICHMOND INTL AP	1948.08.04	2010.09.30	22703	2	4
	LYNCHBURG INTL AP	1948.08.02	2010.09.30	22705	61	232
Blue Ridge Mountains	MONTEBELLO FISH HTCHY	1948.11.01	2007.09.30	21518	59518	848
	ROANOKE INTL AP	1948.08.11	2010.09.30	22696	2880	29
Valley and Ridge	STAR TANNERY	1948.05.01	2009.09.28	22431	64750	6025
	BRISTOL AP	1948.09.01	2010.09.30	22675	106	254

Table 2.3 Kolmogorov-Smirnov statistical check of unprocessed and processed NCDC data of precipitation events.

Region	Station	α	h	p
Coastal Plain	WASHINGTON REAGAN AP	0.05	0	1
	NORFOLK INTL AP	0.05	0	0.9996
Piedmont	RICHMOND INTL AP	0.05	0	1
	LYNCHBURG INTL AP	0.05	0	1
Blue Ridge Mountains	MONTEBELLO FISH HTCHY	0.05	0	0.7129
	ROANOKE INTL AP	0.05	0	1
Valley and Ridge	STAR TANNERY	0.05	0	1.0000
	BRISTOL AP	0.05	0	1.0000

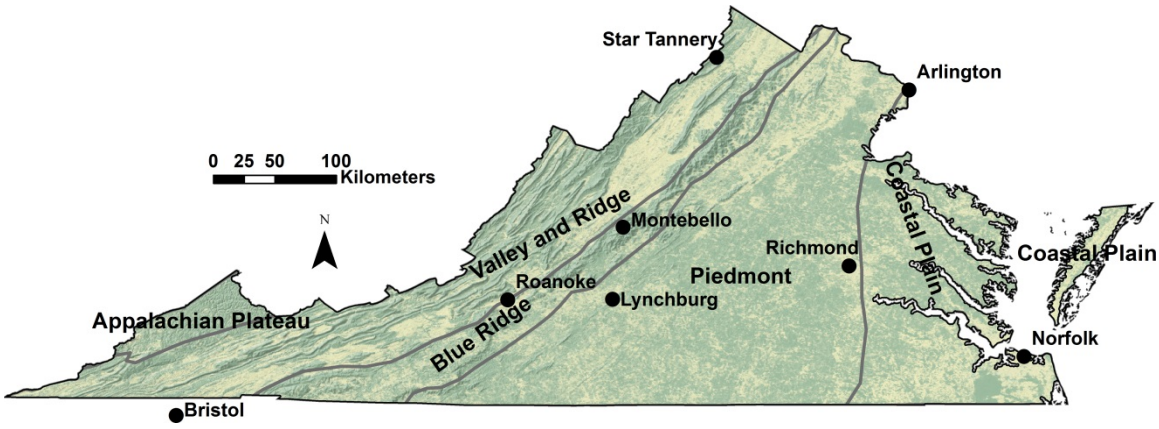

Figure 2.1 Virginia physiography and selected weather stations.

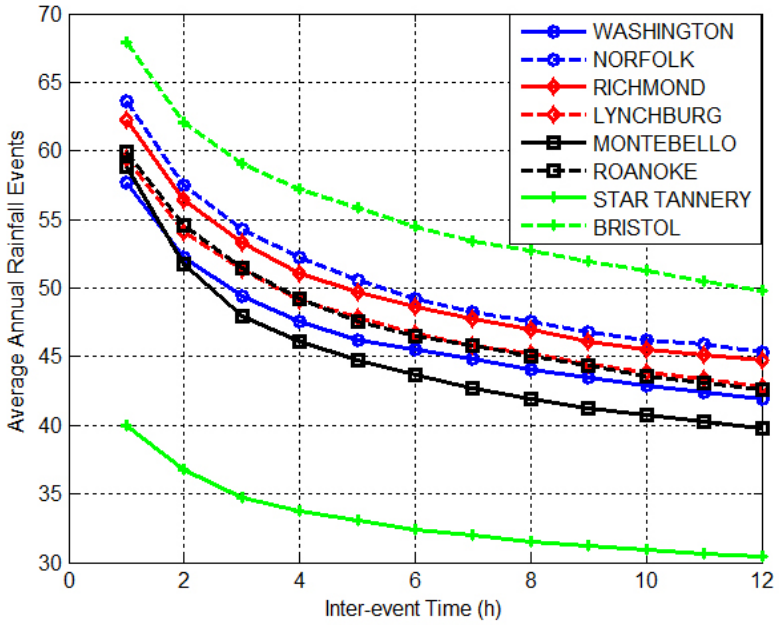

Figure 2.2 Event-Time curves from precipitation data for MIT determination.

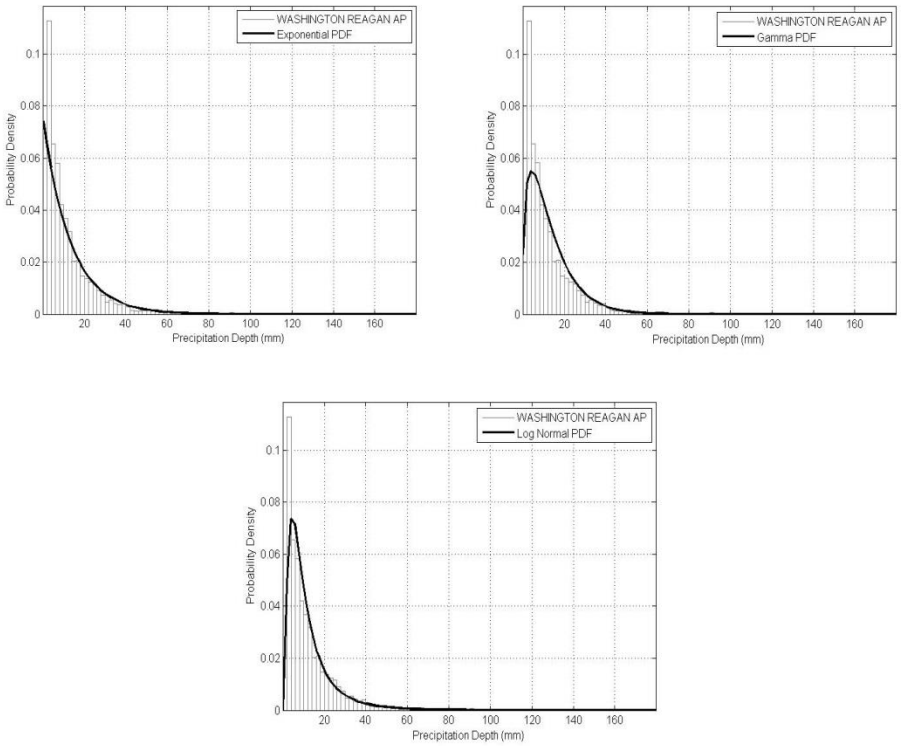

Figure 2.3 Statistical fits to histogram of rainfall depth at WASHINGTON REAGAN AP (a: exponential PDF; b: gamma PDF; c: log-normal PDF).

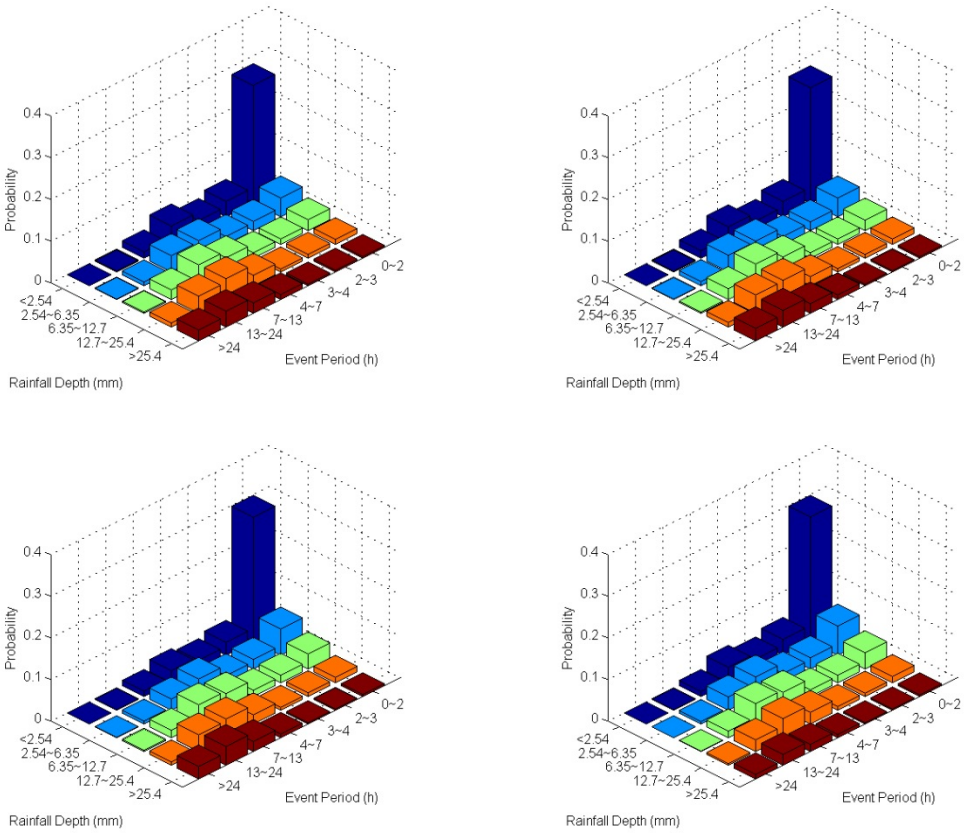

Figure 2.4 3-D bar figure of depth-duration distribution in Virginia (left top: Coastal Plain; right top: Piedmont; left bottom: Blue Ridge Mountains; right bottom: Valley and Ridge).

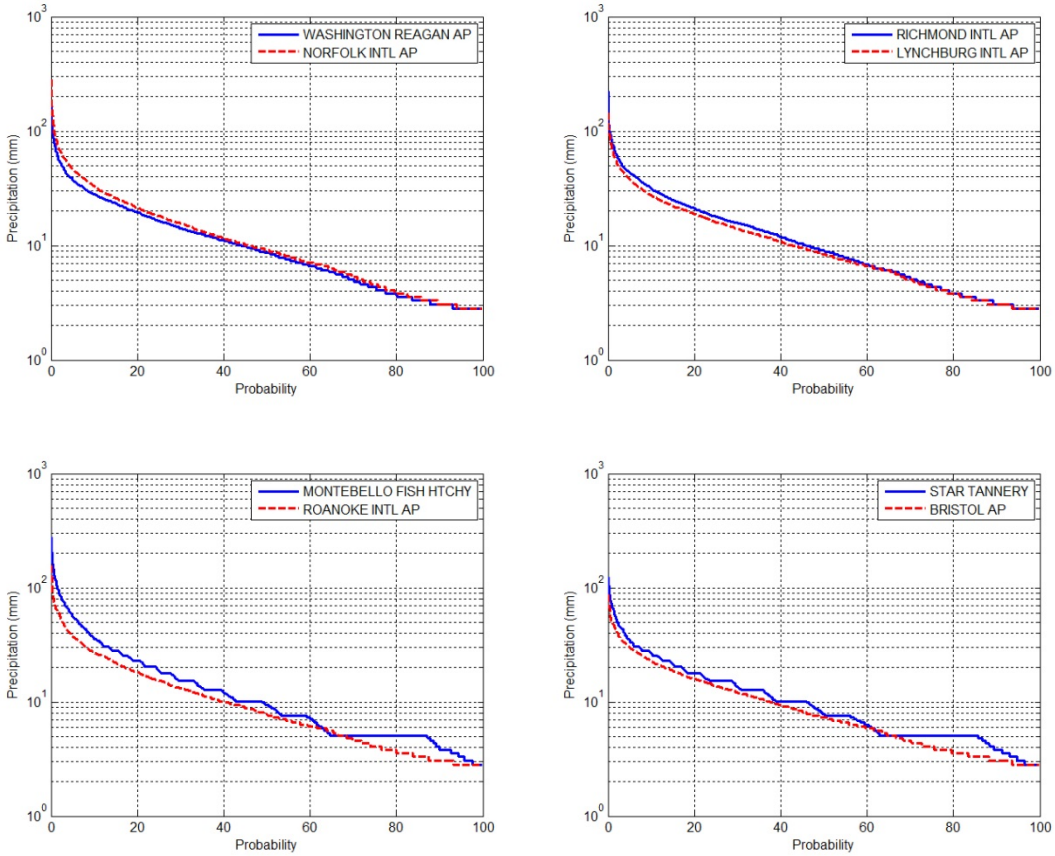

Figure 2.5 Frequency analysis curves of precipitations in Virginia (left top: Coastal Plain; right top: Piedmont; left bottom: Blue Ridge Mountains; right bottom: Valley and Ridge).

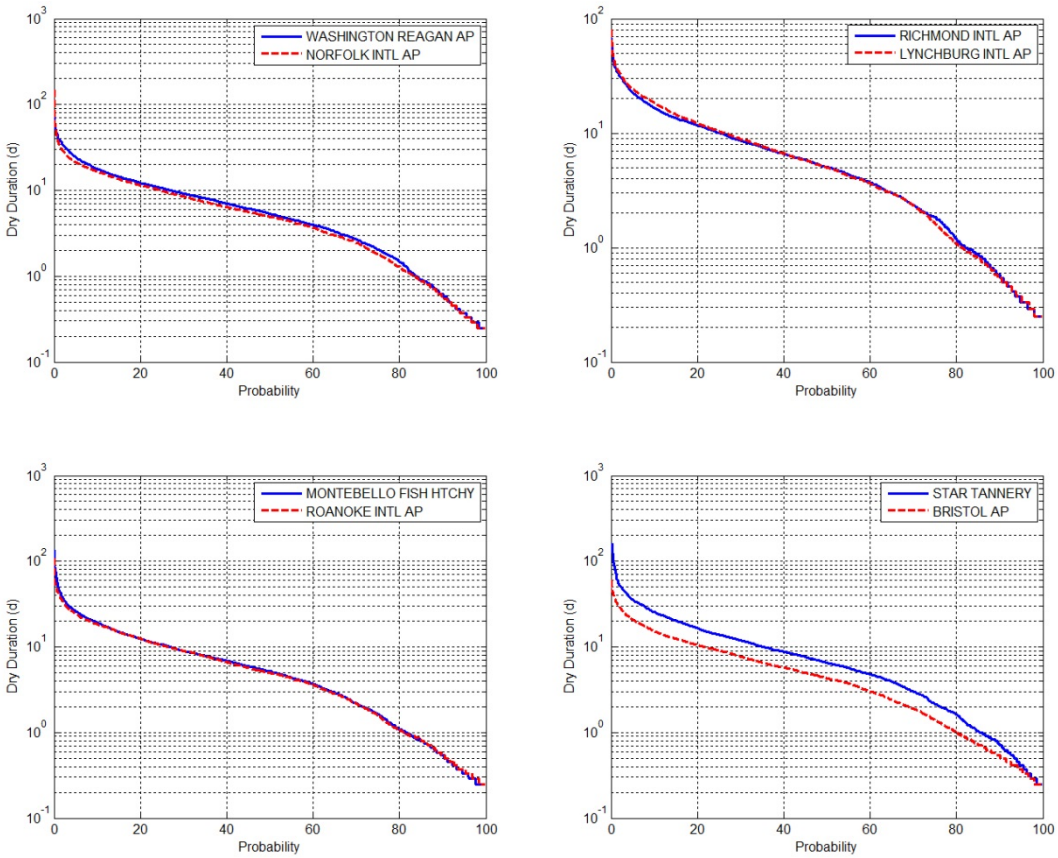

Figure 2.6 Frequency analysis curves of dry durations in Virginia (left top: Coastal Plain; right top: Piedmont; left bottom: Blue Ridge Mountains; right bottom: Valley and Ridge).

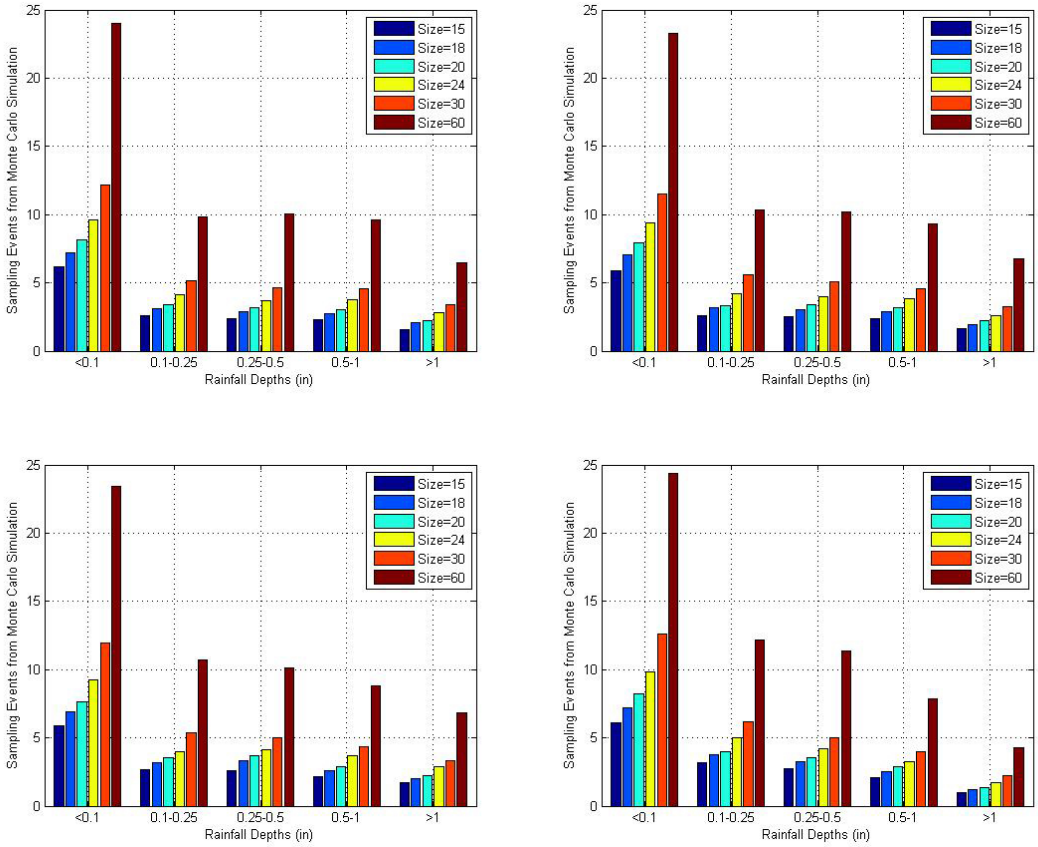

Figure 2.7 Monte-Carlo simulation of depth-duration distribution in Virginia (left top: Coastal Plain; right top: Piedmont; left bottom: Blue Ridge Mountains; right bottom: Ridge and Valley).

References

1. Missouri Department of Natural Resources, *Missouri guide to green infrastructure*, 2012: Jefferson City, MO.
2. Traver, R., et al., Special issue on urban storm-water management in the 21st century. *Journal of Irrigation and Drainage Engineering*, 2011. **137**(3): p. 113-113.
3. Miller, G.W., Integrated concepts in water reuse: managing global water needs. *Desalination*, 2006. **187**(1–3): p. 65-75.
4. Boers, T.M., *Rainwater harvesting in arid and semi-arid zones*, 1994, International Institute for Land Reclamation and Improvement: Wageningen, The Netherlands.
5. Su, M.-D., et al., A probabilistic approach to rainwater harvesting systems design and evaluation. *Resources, Conservation and Recycling*, 2009. **53**(7): p. 393-399.
6. Heneker, T.M., M.F. Lambert, and G. Kuczera, A point rainfall model for risk-based design. *Journal of Hydrology*, 2001. **247**(1-2): p. 54-71.
7. Hvitved-Jacobsen, T. and Y.A. Yousef, Analysis of rainfall series in the design of urban drainage control systems. *Water Research*, 1988. **22**(4): p. 491-496.
8. Lee, K.S., J. Sadeghipour, and J.A. Dracup, An approach for frequency analysis of multiyear drought durations. *Water Resources Research*, 1986. **22**(5): p. 655-662.
9. Lee, J.G., J.P. Heaney, and C.A. Pack, Frequency methodology for evaluating urban and highway storm-water quality control infiltration BMPs. *Journal of Water Resources Planning and Management*, 2010. **136**(2): p. 237-247.
10. Rossman, L.A., *Storm Water Management Model user's manual (version 5.0)*, 2004, U.S. Environmental Protection Agency: Washington D.C.
11. Scharffenberg, W.A. and M.J. Fleming, *Hydrologic Modeling System HEC-HMS, user's manual (version 3.5)*, 2010, US Army Corps of Engineers: Davis, CA.
12. Montalto, F. and B. Lucas, *How are low impact stormwater control measures simulated by different computational models?*, in World Environmental and Water Resources Congress, 2011: Palm Springs, CA. p. 538-546.
13. US Geological Survey, *Guidelines for determining flood flow frequency (Bulletin #17B of the Hydrology Subcommittee)*, 1982, Office of Water Data Coordination: Reston, VA.
14. Wurbs, R.A., State-frequency analyses for urban flood control reservoirs. *Journal of Hydrologic Engineering*, 2002. **7**(1): p. 35-42.
15. Hosking, J.R.M. and J.R. Wallis, *Regional frequency analysis : an approach based on L-moments*. 1997, New York, NY: Cambridge University Press.
16. Jou, P.H., et al., Parametric and nonparametric frequency analysis of monthly precipitation in Iran. *Journal of Applied Sciences*, 2008. **8**(18): p. 3242-3248.
17. Sveinsson, O.G.B., J.D. Salas, and D.C. Boes, Regional frequency analysis of extreme precipitation in northeastern Colorado and Fort Collins flood of 1997. *Journal of Hydrologic Engineering*, 2002. **7**(1): p. 49-63.
18. Norbiato, D., et al., Regional frequency analysis of extreme precipitation in the eastern Italian Alps and the August 29, 2003 flash flood. *Journal of Hydrology*, 2007. **345**(3-4): p. 149-166.

19. Naghavi, B. and F.X. Yu, Regional frequency analysis of extreme precipitation in Louisiana. *Journal of Hydraulic Engineering*, 1995. **121**(11): p. 819-827.
20. Englehart, P.J. and A.V. Douglas, A statistical analysis of precipitation frequency in the conterminous United States, including comparisons with precipitation totals. *Journal of Climate and Applied Meteorology*, 1985. **24**(4): p. 350-362.
21. Huff, F.A. and A.J. R., *Rainfall frequency atlas of the Midwest*. 1992, Champaign, IL: Illinois State Water Survey.
22. Fowler, H.J. and C.G. Kilsby, A regional frequency analysis of United Kingdom extreme rainfall from 1961 to 2000. *International Journal of Climatology*, 2003. **23**(11): p. 1313-1334.
23. Hershfield, D., The frequency of dry periods in Maryland. *Chesapeake Science*, 1971. **12**(2): p. 72-84.
24. Dickerson, W.H. and B.E. Dethier, *Drought frequency in the northeastern United States*, 1970, West Virginia University: Morgantown, WV.
25. Wallis, J.R., et al., Regional precipitation-frequency analysis and spatial mapping for 24-hour and 2-hour durations for Washington State. *Hydrology & Earth System Sciences*, 2007. **11**(1): p. 415-442.
26. Maidment, D.R., *Handbook of hydrology*. 1993, New York, NY: McGraw-Hill.
27. Kim, J.-W. and Y.A. Pachepsky, Reconstructing missing daily precipitation data using regression trees and artificial neural networks for SWAT streamflow simulation. *Journal of Hydrology*, 2010. **394**(3–4): p. 305-314.
28. Lo Presti, R., E. Barca, and G. Passarella, A methodology for treating missing data applied to daily rainfall data in the Candelaro River Basin (Italy). *Environmental Monitoring and Assessment*, 2010. **160**(1): p. 1-22.
29. Silva, R.P.D., N.D.K. Dayawansa, and M.D. Ratnasiri1, A comparison of methods used in estimating missing rainfall data. *The Journal of Agricultural Sciences*, 2007. **3**(2): p. 101-108.
30. Adams, B.J. and F. Papa, *Urban stormwater management planning with analytical probabilistic models*. 2000, New York: Wiley.
31. Dunkerley, D., Identifying individual rain events from pluviograph records: a review with analysis of data from an Australian dryland site. *Hydrological Processes*, 2008. **22**(26): p. 5024-5036.
32. Adams, B., et al., Meteorological data analysis for drainage system design. *Journal of Environmental Engineering*, 1986. **112**(5): p. 827-848.
33. Davis, A.P. and R.H. McCuen, *Stormwater management for smart growth*. 2005, New York, NY: Springer Science.
34. Panu, U.S. and T.C. Sharma, Challenges in drought research: some perspectives and future directions. *Hydrological Sciences Journal*, 2002. **47**(sup1): p. S19-S30.
35. Rahman, A., et al., Monte Carlo simulation of flood frequency curves from rainfall. *Journal of Hydrology*, 2002. **256**(3–4): p. 196-210.
36. Fishman, G.S., *Monte Carlo : concepts, algorithms, and applications*. 1996, New York, NY: Springer-Verlag.
37. Gentle, J.E., *Random number generation and Monte Carlo methods*. 1998, New York, NY: Springer.
38. US Department of Agriculture, *Urban hydrology for small watersheds (TR-55)*, 1986, Natural Resources Conservation Service: Washington D.C.

39. US Environmental Protection Agency, *Storm water technology fact sheet - Bioretention*, 1999, Office of Water: Washington D.C. .
40. VA Department of Conservation and Recreation, *Stormwater design specification No. 9 bioretention (version 1.9)*, 2011: Richmond, VA.
41. Sample, D.J., et al., Assessing performance of manufactured treatment devices for the removal of phosphorus from urban stormwater. *Journal of Environmental Management*, 2012. **113**(0): p. 279-291.

3 Assessment of Selected Bioretention Media Blends for Phosphorus and Nitrogen Retention Using Mesocosm Experiment[2]

Abstract

The purpose of this study is to compare the treatment effectiveness of 3 different bioretention blends (TerraSolve, LuckStone, and VT Mix) with respect to N and P retention from simulated urban runoff. TerraSolve has 10% coconut coir peat, 15% WTR, 15% compost, and 60% sand. LuckStone contains 25% mineland overburden, 20% compost and 55% sand. VT Mix consist of 3% alum sludge, 15% mineland overburden, 25% mulch-free compost, and 57% sand, all by volume. Adsorption isotherm experiments showed TerraSolve had greater P adsorption capacity than the other two media blends. A mesocosm experiment was performed to simulate field-scale bioretention systems and differential nutrient retention. Each of media blends was tested both with and without vegetation to determine the effect of plants on treatment performances. HRT was altered to examine the influence of retention time on treatment efficiency. Water quality data including pH, DO, ORP, TDS were measured *in situ* with a multi-parameter meter. TSS, TKN, TN and TP were analyzed with standard methods. TerraSolve removed the highest amount of P (>90%), likely due to the high quantity of WTR in the mix. VT Mix retained the most (50 – 75%) N. This may be due to the high amount of organic carbon from the compost in the mix promoted denitrification. Statistical analysis using two-way ANOVA that single and interaction effects of HRT and plants existed, and could affect water quality parameters of mesocosm leachate. WTR

[2] Prepared to be submitted to *Journal of Environmental Quality*, allowed to reproduce in this dissertation.

and mulch-free compost are recommended for P and N retention, respectively. Increasing retention time to 6 h or longer increased effluent water quality.

Key words: bioretention blends, mesocosm simulation, N and P retention, hydraulic retention time, isotherm adsorption, physicochemical characteristics, two-way ANOVA

3.1 Introduction

The quality of urban surface waters and contributing groundwater is influenced by pollutants that collect on impervious surfaces conveyed through urban runoff [1]. A national survey of urban stormwater quality verified that nutrient pollution of N and P has become a growing concern due to the accelerating process of urbanization [2, 3]. Removal of vegetation and creation of impervious surfaces due to urban development causes such as flooding [4]; stream bank erosion and stream downcutting declining water quality [5, 6] resulting in increased sediment, nutrients, and heavy metals [7, 8]; and a corresponding decline in aquatic biota [9]. The National Research Council suggests a paradigm shift in regulation of the impacts from storage and treatment to source control using a set of practices known as LID [10]. The goal of LID is to restore existing hydrology and water quality to natural states. In many jurisdictions, reductions in runoff loads of nutrients and sediment are also required to meet new effluent criteria or Total Maximum Daily Load (TMDL) requirements such as those of the US EPA's Chesapeake Bay Program [11].

Bioretention systems, also known as "rain gardens" are probably the most unique LID treatment practice. A bioretention cell typically consists of a depression in the landscape that includes a vegetated layer, a mulch layer, a layer of an engineered soil mix consisting of sand, soil, and organic matter (termed the filter media) and, often, an

underdrain and internal storage reservoir [12]. Figure 1.3 illustrates a typical hydrology of a conventional bioretention system. Runoff pollutants are treated by media, plants, and microorganisms by a variety of physical (filtration), chemical (sorption, fixation), and biological (denitrification, immobilization, assimilation, and decomposition) processes. The treatment processes occur during stormwater transport through and storage within bioretention media. Underdrains, which may be omitted in highly permeable soil, consist of perforated pipe in a gravel-filled trench installed along the bottom of the media filter bed. Elevating the outlet of the underdrain increases HRT and promotes periodic anaerobic conditions in the filter media, facilitating denitrification [13]. Vegetated filtration systems with an anaerobic internal storage have been shown to promote high level N removal through denitrification and / or immobilization. These factors interact with each other through multiple and complicated physical, chemical, and biological reactions, including soil filtering, adsorption, biotransformation, and other natural mechanisms to retain water flow as well as improve its quality [14]. Bioretention systems have been shown to reduce runoff volume, TSS and TP; however, others have found them less effective for N. Some factors of media properties including porosity, infiltration, particle size distribution, and available nutrient content are important to have impact on performance both in terms of water quantity and quality [15].

Accompanying the stormwater regulations in the Commonwealth of Virginia are design specifications for bioretention systems developed by VADCR [16]. Media mix design is a critical research need, and the specification may be premature and not protective of water quality [17]. Specific criticisms of media criteria within the current VADCR bioretention specifications are provided by W. L. Daniels [18]. Considering the

anticipated demand for bioretention systems, there is an urgent need to investigate bioretention media properties and provide improved guidance for media design.

To accomplish this objective, simulation experiments are performed in mesocosms, whose size enables field-scale environments to be duplicated under controlled conditions. Due to the complex physiochemical and biological processes that are active within a bioretention cell, it is nearly impossible to account for every factor affecting treatment performance. Mesocosm experiments circumvent this problem by simplifying a complex full scale system, and separating individual factors for evaluation through replication. A mesocosm is an experimental tool which facilitates investigation of a small part of the natural environment in controlled conditions [19]. By mimicking the common functions within a field scale bioretention cell with artificial conditions, key processes can be isolated for detailed investigation.

Mesocosm experiments have been conducted to evaluate bioretention performance and understand internal treatment processes. To evaluate important design parameters for pollutant removal by bioretention, Hsieh and Davis [20] performed two experiments with 18 bioretention mesocosms employing synthetic runoff. The experiment recommended 2 schematic profiles of bioretention media with suggested depth of 55 –75 cm for single filter media and 65 – 115 cm for dual filter media. Stander and Borst [21] conducted a bench-scale experiment to test bioretention media characteristics. Their results showed media with too much clay could clog and, at least, temporarily increase TSS. An evaluation of removal performance of bioretention practices was conducted with mesocosm chambers filled by compost enhanced media. The project showed that filter socks with compost could remove an average 34% of

soluble P, 54% of NH_4, and 11% of NO_3 from simulated runoff events [22]. The technique with compost filtration practice in bioretention can be used to reduce soluble pollutants from urban runoff. Another mesocosm study [23]examined the capabilities of a bioretention soil mixture of sand, compost, and aluminum-based WTR to reduce nutrients from storm runoff. Results showed a saturation zone could reduce NO_3 significantly in effluent (71%), and PO_4 removal could reach 80% without a saturation zone.

Some researchers have shown that nutrient removal from stormwater can be maximized by promoting plant growth and microbial activity in bioretention systems [24, 25]. Retention and removal of nutrients in vegetated and unvegetated bioretention mesocosms were investigated with 30 well-established 240-L bioretention mesocosms to evaluate the effects of plants by Lucas and Greenway [26]. The mesocosms contained different ratios of sandy loam, loamy sand and pea gravel so media mixes could be compared. A vegetated group with shrubs / grasses and a non-vegetated control group were also compared. The observation demonstrated the vegetated sandy loam mesocosms had higher nutrient retention. The increase in TN retention by vegetated systems also exceeded plants N uptake rates, suggesting that denitrification conditions were present in the media. A specific media using WTR as an admixture can provide effective initial TP retention >94% [27].

A similar mesocosm experiment also compared vegetated and non-vegetated groups [29]. Average effluent removal rates of TN, TSS and TP by vegetated systems were 56%, 90%, and 58%, respectively, compared to non-vegetated system with 26%, 87% and 36%. These results indicated that the bioretention system removed pollutants

through complex interactions involving among plants, fungi, microbes and media properties.

Dosing rate can be deliberately controlled in laboratory to simulate local typical rainfall conditions. In a bioretention mesocosm experiment to evaluate the removal of pathogens and TSS, Rusciano and Obropta [28] mimicked typical precipitation to set the influent at a stable rate similar to the approach used in previous study.

HRT is a measure of the average time that water, wastewater, or stormwater is retained in a reactor, unit process, storage basin, or any similar facility at a given hydraulic loading [29]. HRT has strong influence on nitrification activities and pollutant removal of a biological system. It was reported with decreased HRT from 30 to 5 h, the specific ammonium-oxidizing rates varied between 0.32 and 0.45 kg NH_4, and the specific nitrate-forming rates increased from 0.11 to 0.50 kg NO_3, showing that the decrease in HRT led to a significant increase in the NO_3 oxidation activity [30].

HRT should be a significant factor in runoff retention and nutrient removal, especially for the processes of nitrification and denitrification. An attempt to control HRT by underdrain configuration found that a bioretention with HRT less than 3 h removed some TN but not much TP. The opposite was true in another bioretention with 7-day HRT, which achieved good removal for both TN and TP [31]. Lucas and Greenway conducted a series of bioretention mesocosm experiment with planted vegetation to compare hydraulic response and N retention with free discharge and regulated outlets. The outlet regulated mesocosms provided retention over 8 times longer than the free-draining ones. The regulated treatment retained 68% $NO_{2\text{-}3}$ and 60% TN; while the corresponding free-draining treatment retained 25% $NO_{2\text{-}3}$ and 27% TN [13, 32].

Obviously, these outlets provide longer HRT management and improve both runoff capture and N retention. Despite this information, current federal or state design criteria or regulations do not have an explicit recommendation on HRT for bioretention operation [33, 34]. The spreading implementation of bioretention systems calls for more detailed study of HRT and its influence on bioretention performance.

While mesocosm experiments can simulate P removal under different conditions, determining the idealized maximum P adsorption capacity by media is best determined by an adsorption isotherm, which describes the equilibrium of the P adsorption at particle surface at a constant temperature in the media-mixed solution [35]. Adsorption isotherms often use empirical models such as Freundlich or Langmuir [36]. These empirical isotherms can be used to estimate the maximum P removal threshold by bioretention blends since P equilibrium concentration levels are relatively low in urban runoff [37].

The two major objectives of this research are to compare bioretention media blends with and without plants on the performance of N and P reduction to identify a combination of recipes that enhance nutrient treatment. In addition to evaluating vegetative effects, we will also assess the influence of HRT on nutrient removals in order to suggest an optimal HRT for bioretention operation. Ultimately, tests such as these are intended to influence design guidelines and eventual specification development. These objectives will be accomplished through replicating major functions of bioretention cells by mesocosm simulation and conducting isotherm adsorption experiment in a laboratory.

3.2 Materials and Methods

3.2.1 Simulated runoff

Stormwater is extremely difficult to collect under controlled conditions within a reasonable time. Simulated runoff was used in the mesocosm experiment due to the practical difficulties in collecting and storing stormwater. Synthetic runoff used for the isotherm and mesocosm experiments was prepared based on the formula of Hsieh [38] and Hunt [39]. Table 3.1 summarizes the chemicals selected to mix with local well water at Virginia Beach, VA for the preparation of artificial stormwater runoff. This makeup should produce artificial runoff with similar concentrations of representative nutrients to typical runoff from urban asphalt parking lots [40].

3.2.2 Media and characterization

Three bioretention mix recipes were evaluated in this research. The first recipe was provided by TerraSolve^{TM} LLC. (Hillsborough, NJ). The media developed from this recipe was previously used at the Science Museum of Virginia in Richmond, VA, which is a demonstration bioretention facility [41]. The TerraSolve media is comprised of approximately (by volume) 10% coconut coir peat, 15% WTR, 15% compost, and 60% sand. The second blend was a biofilter media donated by LuckStone^{TM} Company (Ruckersville, VA), which has been used extensively as a media blend in Virginia. It contains 25% mineland overburden, 20% compost and 55% sand, respectively (by volume). The third blend (VT mix) was mixed by the authors at Hampton Roads Agricultural Research and Extension Center, Virginia Tech. It consisted of 3% WTR in the form of spent alum sludge, 15% mineland overburden, 25% mulch-free compost, and

57% sand (by volume). The intent of the VT mix media recipe was to serve as a compromise between the other two blends.

Two layers were deposited into each mesocosm barrel. The top media layer is composed of one of the 3 blends described previously. The bottom layer is rice gravel obtained from Procon Pacific^{TM}, LLC. The rice gravel layer is 30 cm (12 in) in depth, with a 60-cm (24-in) media layer on its top. The media layer is the major factor infiltrating and retaining pollutants in simulated runoff; while the gravel layer facilitates drainage through a 1.3-cm (0.5-in) perforated PVC underdrain pipe.

Physicochemical parameters may be related with bioretention functions and performance. Density, porosity, and water content of these 3 blends were measured with standard methods for soil characteristics [42]. Particle size distribution (PSD) of media was determined by sieve analysis. Representative metal content of these blends were analyzed on digested and extracted soil solutions with Inductively Coupled Plasma (ICP) using US EPA 3050B method [43]; Plant available metal concentrations were obtained with the Mehlich 1 method [44]. Common N forms including NO_3 and NH_4, as well as total and plant available P were analyzed using KCl extraction and acid digestion method respectively [45] to understand the background nutrient contents in these investigated blends.

3.2.3 Mesocosm design

The mesocosm containers used in the experiment are food grade plastic storage drums bought from local distributors in Chesapeake, VA. The major parts of the barrels are cylindrically-shaped, with slightly tapered bottom and top. The internal diameter of the barrel is 56 cm (22 in), with a height as 92 cm (36 in). The volume used for

experimental media is 265 L (70 gallons). The internal walls of these mesocosm barrels were rubbed by abrasives to increase the friction for higher hydraulic resistance and to avoid short-circuiting along the rim.

Two experimental groups were set up in this study: an unvegetated *media* group and a vegetated *plant* group that was surface seeded. For each type of media in either group, 3 replicates were prepared to allow for statistical variability. Tall fescue (*Festuca arundinacea*) seed was planted in the mesocosm barrels of the plant group in March, 2013. This cold-season grass has a high tolerance to drought, heat and coldness, and is a fast growing turf germinating in early spring [46]. The planted grasses were irrigated regularly from March to July. During this period, some weeds including barnyard grass (*Echinochloa crus-galli*), crabgrass (*Digitaria sanguinalis*), and fall panicgrass (*Panicum dichotomiflorum*) also germinated. These annual weeds were trimmed to about 30.5 cm (1 ft) above the media surface with the existing tall fescue to maintain a diversified vegetated stand simulating a field-scale bioretention facility (Figure 3.1).

Two water-supply tanks were prepared to store and dose the simulated runoff into the 18 mesocosm barrels to perform the experiment. Each tank contained 1000-L runoff with 9 ECO132® submersible pumps. The pumps dosed runoff through vinyl tubing (1.3-cm, or 0.5-in diameter) into mesocosm barrels with a measured outflow between 230 to 250 L/h, with a standard deviation of 29 L/h.

3.2.4 Experiments

Isotherm experiments were conducted to determine the equilibrium amount of P on the media surface as a function of its concentration in aqueous phase at a constant temperature. The samples were prepared by mixing 1-g screened blends with 25-ml

simulated runoff in tubes. The tubes were shaken by an Eberbach® Mid-Range Reciprocal Shaker for 1.5 days at a constant temperature of 22°C (72°F) with a frequency of 60 oscillations/min to reach adsorption equilibrium. The suspension was then filtered before being analyzed by a Lachat® QuikChem 8500 Flow Injection Analysis System to determine the amount of P being adsorbed by media particles during the experimental period.

Two experimental rounds were conducted in April and July 2013 to evaluate treatment performance for each blend. Five dosing runs with different HRTs of 1 h, 6 h, 12 h, 24 h, and 48 h were experimented in sequence in the first round on media group. The 1-h HRT run was used to simulate the engineering bioretention with free drainage; other HRTs were arbitrarily selected to investigate the possible treatment improvement under longer retention periods. The second round was conducted on both media and plant groups when the vegetation was fully germinated with 3 dosing runs of 1 h, 6 h, and 24 h respectively.

For both rounds, all the dosing runs were conducted at regular intervals of every 3 or 4 days. For each run, the irrigation time was set at 12 min with approximately 50-L simulated runoff being dosed into each barrel. The irrigation pattern was selected to simulate a variety of local rainfall events with precipitation exceedance probability from 0.30 to 0.35, and dry duration probability between 0.80 and 0.85 (Figure 3.2) based on frequency analyses of long-term precipitations and dry durations of Virginia [47].

The leachate that infiltrated the media was collected by a 1.3-cm (0.5-in) diameter perforated PVC pipe buried at the height of 25 cm (10 in) within the gravel underdrain layer. The effluent flow was controlled by a PVC ball valve and collected into 19-L (5-

gallon) buckets for on-site measurement, including pH, DO, ORP, and TDS by YSI® Professional Plus portable meter. Leachate was then dumped into a separate mixing barrel to obtain composite samples for water quality analyses.

3.2.5 Water quality analyses

Half of each composite sample was filtered through Whatman™ 934-AH Glass Microfibre Filters to measure from the TSS amount with Standard Method 2540D [48]. The filtrate was filtered through Whatman™ NC 45 Membrane Filters for NO_3, NH_4, and PO_4 analyses. The remaining portion of the composite sample was not filtered and was subsequently used for TKN and TP analyses.

All filtered and unfiltered leachate samples of mesocosm experiment were stored in plastic bottles at -18°C before being transported to the laboratory of the Crop and Soil Environmental Sciences Department of Virginia Tech for water quality analyses. TKN, NO_3, NH_4, and TP were analyzed by a Lachat® QuikChem 8500 Flow Injection Analysis System. For the first round of mesocosm experiments on the media group, only TKN and TP were analyzed; for the second round on both media and plant groups, TKN, NO_3, NH_4, and TP were analyzed.

3.2.6 Analysis of variance (ANOVA)

ANOVA is a procedure in which the total variation in a measured response is partitioned into components that can be attributed to recognizable sources of variation, assuming the independence, normality and homogeneity of the variances [49]. For an experiment with a quantitative outcome and 2 categorical explanatory variables, two-way ANOVA was used to determine the main effect of contributions of each independent variable and identify significant interaction effect, if it exists, between the variables [50].

The *in situ* measured parameters of bioretention effluent were analyzed using two-way ANOVA to investigate the effect of media (TerraSolve, LuckStone and VT Mix), vegetation and their interaction on outflow data. Simple effects of these factors were utilized to further investigate significant interactions. Appropriate mean values of investigated parameters were separated using Tukey's honestly significant difference test.

3.3 Results and Discussion

3.3.1 Characteristics of bioretention blends

Physical properties of media blends can influence infiltration and redistribution of water within porous media. The properties of the 3 blends evaluated in this paper are tabulated in Table 3.2. The physical properties are determined by the media compositions. VT Mix has high content of compost, so its bulk density is the smallest, and porosity is the largest. In comparison, LuckStone has mineland overburden soil as its largest fraction, thus its density is the largest.

Particle-size distribution (PSD) can be defined as the average number or ratio of particles within a given size class of width for a unit volume of media [51]. It is important in affecting the reactivity of solids participating in chemical reactions, and the concentration of suspended solids in the outflow. Research was conducted to investigate how PSD affects the removal of suspended solids in storm runoff concluded that sedimentation rates are not affected by HRTs, but by outflow rates and PSD considerably [52]. PSD of these 3 different blends are tabulated in Table 3.3. Generally, each blend can all be categorized into the sand division of the Unified Soil Classification System [53]. TerraSolve is mostly composed of sand (94.7%), with little silt (2.2%) and clay (3.0%). LuckStone has higher contents of very coarse sand (26.3%) and coarse sand

(25.4%), but it also contains lesser amounts of medium sand (28.3%) and fine sand (8.7%) than the other 2 blends. VT Mix has a similar PSD to TerraSolve, but contains more clay-sized particles (4.5%) than the other blends.

Metal concentrations in bioretention blends can obviously affect P removal due to the strong affinity between the metal oxides and PO_4. In general, higher metal (esp., Al, Fe, and Ca) content in soil can result in better P removal. Some representative metals were analyzed to compare the metallic contents in the blends; these amounts are provided in Table 3.4. It can be seen that these 3 blends have proportions of metals: TerraSolve has mostly Al and Cu; LuckStone and VT Mix have more Ca, Fe, Mg, and Zn. All these 3 blends have similarly low contents of As, Cd, Mn, Ni, and Pb, which are important with respect to low potential toxicity. These results indicate that none of the blends have sufficiently high enough quantity of heavy metals to retard plant growth, and all appeared to have enough metal ions to retain P. Plant-available metals are metallic forms that can be uptaken by plant tissues from the terrestrial environment. The contents of plant available metals are listed in Table 3.5.

The contents of NO_3 and NH_4, with TP and plant-available P are summarized in Table 3.6. TOC and TN are expressed as percentages. The nutrient contents in media are important to govern vegetation growth within bioretention facilities; however, too much nutrient may decrease water quality of the filtrate upon leaching. Analytical results show that TerraSolve has the most TN and TP among the blends. Although VT Mix blend was mixed with a high ratio of mulch-free compost and its TOC is more than the others, this does not add much N or P content.

3.3.2 Isotherm experiment

The isotherm experiment on the 3 bioretention blends demonstrated their theoretical maximum capacity to retain P from stormwater through the process of adsorption. Two popular isotherm models, Freundlich and Langmuir, were selected to examine and describe the adsorption process.

The Freundlich model is a simple, empirical nonlinear expression representing the isothermal variation of solute adsorption by a unit mass of absorbent. The mathematical expression of Freundlich model can be written as

$$q = k_F c_t^{\gamma} \tag{3-1}$$

Where q = mass of adsorbate per unit mass of absorbent (mg/g)

c_t = equilibrium concentration of adsorbate (mg/L)

k_F, γ = heterogeneity parameters (dimensionless)

The Langmuir adsorption model is also commonly used to quantify the amount adsorbed on an absorbent material. It is assumed that the absorbent surface is homogeneous with equivalent probability of sites in their ability to adsorb 1 adsorbate molecule [54]. The Langmuir model can be mathematically expressed as the following formula.

$$q = \frac{q_m k_L c_t}{1 + k_L c_t} \tag{3-2}$$

Where q_m = the maximum adsorption per unit mass (mg/g)

k_L = a parameter related to the surface bonding energy (dimensionless)

The analyzed P concentrations were fit nonlinearly by the Curve Fitting Tool of Matlab®. The Freundlich and Langmuir equations with coefficients of determination are available from this fitting process (Table 3.7).

Both isotherm models can describe P adsorption by the blends with high coefficients of determination, but Freundlich equations have a better fit than Langmuir. The 3 Freundlich isotherm equations were plotted together in Figure 3.3 for comparison. The figure shows TerraSolve has the largest maximum adsorptive capability among these blends; while LuckStone and VT Mix perform within similarly lower ranges to adsorb P as their curves illustrate.

TerraSolve has best P adsorptive capability due to its unique constituent of WTR with the highest Al content, which are the residues resulting from coagulating dissolved organic acids and mineral colloids with either Al or Fe sulfate [27]. WTR have proved to be very effective in reducing the interstitial PO_4 concentrations in P-enriched soils [55].

3.3.3 Mesocosm experiment

The vegetation in the 3 blends exhibited different robustness of growth during the experimental period. Comparably, TerraSolve had the least plant coverage; while vegetation in LuckStone and VT Mix blends had much better growth conditions. The differences may be due to media characteristics. TerraSolve has the highest contents of sand-sized particles, making water infiltrate faster. Therefore little water could be retained at the top of media layers. LuckStone and VT Mix have more nutrient elements and less sand content, retaining moisture, and thus supporting robust vegetation growth.

The *in situ* measurement pH, DO, ORP, TDS with lab measured TSS were plotted in Figures 3.4 – 3.8, respectively. It was observed that all blends have some buffering capacity, i.e., they can adjust the slightly acidic influent to neutral conditions in the effluent. The pH values of effluent are close to the media pH in Table 3.2, indicating the outflow pH is strongly influenced by the pH of media. The difference between outflow

pH of media and plant groups is small, meaning the addition of vegetation does not add to the buffering capacity. DO data of TerraSolve are higher than others, and VT Mix has the lowest DO in effluent. This is due to the large quantity of compost in VT Mix; the decomposition reactions of organic matters consumed more oxygen in the water. The lower DO of the plant group may be due to organic compounds produced by vegetation. ORP demonstrated a similar pattern as DO. The lowest negative ORP of VT Mix and lower ORP of plant group results from the decomposition reactions of organic materials either in the compost or from physiological activities of vegetation. Low ORP values indicate that reducing conditions are dominant, and denitrification process can take place under this oxygen-depleted environment [56]. TerraSolve has the lowest TDS and TSS with cleaner leachate than the others because it is composed of larger, coarser particles which are difficult to transport by water flow. VT Mix has the highest levels of TDS and TSS, likely due to a soluble salts and particulate components in the compost, which may eventually be flushed out. Plant roots can loosen the media structure; therefore the TDS and TSS levels of the plant groups are higher than media group.

The mesocosm experiment evaluated the influence of HRTs on effluent quality in the 2 experimental rounds. With HRTs increasing, pH did not have significant change. DO and ORP decreased, indicating longer retention time of runoff leading to anaerobic conditions. TSS demonstrated clear trends to decrease with longer HRTs because more suspended solids precipitate as sediments. The penetration of interporosity flow through media can cause outflow with high TDS / TSS as shown by the peaks of the 12-h HRT in the first round.

The nutrient removals of TKN, TP, and TN were summarized in Table 3.8 with inflow concentrations of both experimental rounds. TKN, TP were analyzed in both rounds; while TN was only calculated from TKN and NO_3 data in the second round.

Generally, removal efficiencies of Round 2 were better than those of Round 1, showing the retention of nutrients can be improved with increased stabilization time. In the first experimental round, LuckStone had best TKN removal, and VT Mix showed high level TKN release. The extreme negative TKN removal at 12-h HRT is likely due to the low TKN concentration in inflow. In the second round, TerraSolve had better TKN removal, and VT Mix also showed lowest removal. TKN removal was highest at 6-h HRT. Plant group had lower TKN removal for LuckStone and VT Mix because robust vegetation generated more organics. The best TP removals of TerraSolve in isotherm experiment was confirmed by the mesocosm results, showing over 90% TP removals in both rounds. TP removal of VT Mix was better than LuckStone, which was due to the composition of alum sludge in it. Increasing HRT could improve TP removal, but the increase from 6-h HRT to 24-h HRT was not significant. Plant group had lower TP removals due to the physiological activities of plants. The highest TN removal (50% – 75%) was recorded from the data of VT Mix because the decomposition of mulch-free compost lowered DO and ORP, and maintained an anaerobic condition for nitrate treatment. 6-h HRT showed relatively higher retention for TN compared with other cases. The difference of removals between media and plant groups of TerraSolve was not as significant as that of LuckStone because vegetation was sparse in TerraSolve, but robust in LuckStone barrels. It can be seen that plant uptake can enhance TN removal in case the vegetation growth maintains a robust condition.

3.3.4 Two-way ANOVA

The outcomes of a two-way ANOVA which was used to evaluate the main effects of bioretention blends and vegetation on measured effluent parameters are tabulated in Table 3.9 and Table 3.10. The mean values are shown in these tables, and their significant differences are also displayed.

Results from two-way ANOVA demonstrate that these 3 blends had significantly different pH values, meaning pH values of effluent were determined by media type. TerraSolve had significantly higher DO data compared with LuckStone and VT Mix, which was likely due to the permeability of TerraSolve's sandy particles. Bioretention blends had different effects on ORP with various HRT. VT Mix was significantly different from TerraSolve and LuckStone when HRT was 6 h; three blends had different ORP values when HRT was increased to 24 h. The effect of the blends can be amplified with increased HRT.

From the statistical results of vegetation effects on effluent parameters, for all the events with HRT as 6 h and 24 h, vegetation showed significant influence on the measured effluent parameters, DO and ORP, at p-values less than 0.05. Adjustment of HRT is effective to alter DO and ORP. p-values of DO and ORP with 24-h HRT are higher than those with 6-h HRT, meaning that the longer retention time promotes the main effect of vegetation on DO and ORP.

3.4 Conclusions

Three different bioretention blends were compared and evaluated in this research. Physical properties and particle size distributions are determined for each blend composition and appeared to influence treatment performance. As the clay or silt-sized

particle fraction increases, bioretention outflow may contain more TDS or TSS. Metal and nutrient contents of blends are also important factors for water quality control. High content of Al in TerraSolve increases its P removal effectiveness. The nutrient contents of the blends are also factors for plant growth and effluent quality. An optimal choice is a blend that is not nutrient-rich, but contains enough nutrients for plant growth. Isotherm adsorption experiment showed that TerraSolve possessed the highest capacity to adsorb P than the other two blends. The mesocosm experiment compared the nutrient retention performance of these blends in a simulated environment. The results display that the composition of blend can apparently influence the water quality of effluent. The decomposition process of compost in VT Mix consumes oxygen and oxides, decreasing DO and ORP. The consequent anaerobic condition promotes the treatment of NO_3 and TN, making VT Mix the best blend for N removal with a ratio as high as 50 – 75%. WTR in TerraSolve contribute P removal effectively, so TerraSolve has good performance to remove over 90% P from influent. Two-way ANOVA evaluated the main effects of blends and vegetation on effluent parameters. The results showed that blends have significant influence on pH. TerraSolve had significantly higher DO values due to it had more sandy particles. VT Mix had significantly lower ORP because of the high level compost in it. The p-values from analysis of vegetation effects demonstrate plants can affect DO and ORP significantly. Higher HRT can increase the effect of vegetation on DO and ORP. The influence of vegetation to water quality data is related with the growth condition of plants. LuckStone and VT Mix have robust plants growth conditions, therefore vegetation adjusted effluent quality positively. Significant interactive effects of blends, HRT and vegetation were confirmed for nutrient concentrations of outflow,

which means a vegetated bioretention with a certain HRT may optimally maintain reducing conditions and enhance nutrient uptakes. From the experimental results, an HRT no less than 6 h is preferable for water quality improvement.

In general, a mix of TerraSolve and VT Mix, or WTR and compost, can be a good combination for nutrient retention with high retention of P and anaerobic condition for N removal. The recipe with both WTR and compost may also promote plant growth with enough nutrient supply and water retention to enhance vegetation effect on water quality improvement. Further study on the effect of plant uptake is recommended to quantitatively evaluate the nutrient consumed by vegetation through the analysis on plant tissues. Field-scale experiment on these blends is necessary to examine the treatment performance under natural environment. Advanced research on development of a numerical model with the analytical data and experimental results can describe the nutrient treatment within bioretention in a mathematical means, as an alternative to mesocosm or field-scale experiments. This can help determine an optimal recipe of bioretention blend to increase nutrient retention.

Acknowledgments

This study was funded by the Mid Atlantic Water Program as a research project: “Evaluation of Bioretention Recipes for Sequestering Stormwater Nitrogen and Phosphorus.” The authors are quite thankful for the assistance on media preparation by Thomas Wilchynski, vegetation identification by Dr. Jeffrey Derr, and laboratory supports by Dr. Jim Owen (Hampton Roads AREC, Virginia Tech). The authors are also grateful to these individuals and companies for their donation of media components: Jimmy Rodgers (LuckStone Co.); Jeff Weiner (TerraSolve LLC.); John Collett (Newport

News Compost Facility); Vicki Smith (Department of Public Utilities, City of Suffolk). Special thanks also go to Hsuan-Chih Yu and Kevin Bamber (Crop and Soil Environmental Sciences Department, Virginia Tech) for mesocosm leachate analyses.

TABLES AND FIGURES

Table 3.1 Concentrations of typical parking lot runoff and simulated urban runoff used for this study.

Parameter	Concentrations of parking lot runoff (mg/L)	Concentrations of simulated runoff (mg/L)	Chemicals
NH_4	0.12 - 9.6	0.10 - 0.50	NH_4Cl
NO_3	0.27 - 14	1.0 - 3.0	$NaNO_3$
PO_4	0.044 - 1.7	0.10 - 1.0	KH_2PO_4

Table 3.2 Physical properties of experimented bioretention blends.

Parameter / Media	Bulk density (g/cm^3)	Porosity	Water content (mg/g)	pH
#1 TerraSolve	1.22	0.359	59.6	6.58
#2 LuckStone	1.23	0.381	63.9	7.16
#3 VT Mix	1.08	0.420	58.6	6.92

Table 3.3 Particle size distribution of experimented bioretention blends.

Parameter / Media	Total Sand (%)					Total Silt (%)			Total Clay (mg/g)
	VCS (mg/g)	CS (mg/g)	MS (mg/g)	FS (mg/g)	VFS (mg/g)	CSI (mg/g)	MSI (mg/g)	FSI (mg/g)	
#1 TerraSolve	52	228	456	193	18	7	15	0	30
#2 LuckStone	263	254	283	87	24	12	29	12	36
#3 VT Mix	41	250	409	197	19	22	14	3	45

Table 3.4 Contents of total metals in experimented bioretention blends.

Parameter / Media	Al (mg/kg)	As (mg/kg)	Ca (mg/kg)	Cd (mg/kg)	Cu (mg/kg)	Fe (mg/kg)	Mg (mg/kg)	Mn (mg/kg)	Ni (mg/kg)	Pb (mg/kg)	Zn (mg/kg)
#1 TerraSolve	7541	1.3	622	0.29	6.3	1979	403	216	2.8	196	14.8
#2 LuckStone	4124	<1	695	0.23	5.7	10107	1227	219	5.5	179	30.6
#3 VT Mix	3367	<1	973	0.18	5.3	6613	798	163	3.2	138	22.8

Table 3.5 Contents of plant available metals in experimented bioretention blends.

Parameter / Media	B (mg/kg)	Ca (mg/kg)	Cu (mg/kg)	Fe (mg/kg)	K (mg/kg)	Mg (mg/kg)	Mn (mg/kg)	Zn (mg/kg)
#1 TerraSolve	0.6	569	0.9	39.9	66	72	24.1	2.6
#2 LuckStone	0.2	394	0.9	23.9	49	31	13.6	2.0
#3 VT Mix	1.2	809	0.6	16.5	114	112	25.8	3.4

Table 3.6 Contents of nutrients in experimented bioretention blends.

Parameter / Media	TOC (mg/g)	TN (mg/g)	NO_3 (mg/kg)	NH_4 (mg/kg)	TP (mg/kg)	P-plant (mg/kg)
#1 TerraSolve	7.27	5.17	4.71	4.85	196	20
#2 LuckStone	7.00	0.642	42.3	5.62	179	32
#3 VT Mix	12.9	0.624	0.119	2.46	138	27

Table 3.7 Nonlinear fit results of Freundlich and Langmuir isotherms to adsorption experimental data.

Blend	Freundlich nonlinear fit			Langmuir nonlinear fit		
#1 TerraSolve	k_F	n	R^2	Q	k_L	R^2
	7054	0.711	0.943	273	242	0.942
#2 LuckStone	k_F	n	R^2	Q	k_L	R^2
	29.8	0.300	0.999	40.6	4.51	0.947
#3 VT Mix	k_F	n	R^2	Q	k_L	R^2
	21.2	0.640	0.949	67.6	0.517	0.974

Table 3.8 Inflow concentrations and mean nutrient removals of mesocosm experiment.

Parameter	Round	HRT (h)	Inflow (mg/L)	TerraSolve Removal (%)		LuckStone Removal (%)		VT Mix Removal (%)	
				Media	Plant	Media	Plant	Media	Plant
TKN	1	1	0.217	-73.5	-	100	-	-1814	-
		6	0.325	-91.3	-	94.5	-	-896	-
		12	0.103	-665	-	-31.7	-	-1939	-
		24	0.848	86.5	-	87.9	-	-183	-
		48	0.896	51.5	-	83.0	-	-57.9	-
	2	1	0.747	-24.5	-1.45	-45.0	-114	-85.1	-85.5
		6	1.45	66.2	84.5	45.5	45.9	26.8	48.2
		24	0.504	-27.7	-13.3	-58.0	-19.2	-64.0	-134
TP	1	1	0.172	90.8	-	54.1	-	58.2	-
		6	0.225	90.7	-	76.0	-	78.5	-
		12	0.619	95.1	-	82.4	-	94.0	-
		24	0.805	97.9	-	93.7	-	97.9	-
		48	0.570	98.9	-	96.0	-	98.2	-
	2	1	1.02	96.8	92.5	80.2	45.3	91.3	71.7
		6	1.20	97.2	97.3	81.0	77.7	96.6	93.8
		24	1.14	94.4	97.5	84.4	80.6	93.3	93.3
TN	2	1	3.39	5.52	-10.4	-75.2	20.8	48.1	55.5
		6	3.79	10.9	5.22	-29.9	62.7	58.2	77.7
		24	2.23	-55.7	-75.6	-22.7	67.6	55.9	43.1

Table 3.9 Main effects of bioretention blends on measured effluent parameters of mesocosm experiment.

HRT (h)	Bioretention blends					
	TerraSolve		LuckStone		VT Mix	
	pH					
1	6.96	a*	6.29	b	6.63	c
6	6.96	a	6.23	b	6.56	c
24	6.93	a	6.21	b	6.55	c
	DO (mg/L)					
1	4.16	a	2.00	b	1.47	b
6	3.14	a	1.57	b	1.32	b
24	2.61	a	1.19	b	1.26	b
	ORP (mV)					
1	138	**	175	**	-44	**
6	128	a	152	a	-35	b
24	185	a	107	b	-39	c

*: means within a row with a different letter are significantly different at p = 0.05
**: means within a row were not analyzed due to significant interaction

Table 3.10 Main effects of vegetation on measured effluent parameters of mesocosm experiment.

HRT (h) / Groups	DO (mg/L)			ORP (mV)		
	1	6	24	1	6	24
Plant	2.39	1.78	1.41	55.4	57.1	49.9
Media	2.69	2.25	1.97	123.4	106	118
p-value	NS*	0.0137	0.0014	NA**	0.0086	0.0007

*: means within a column are not significantly different at p = 0.05
**: means within a column were not analyzed due to significant interaction

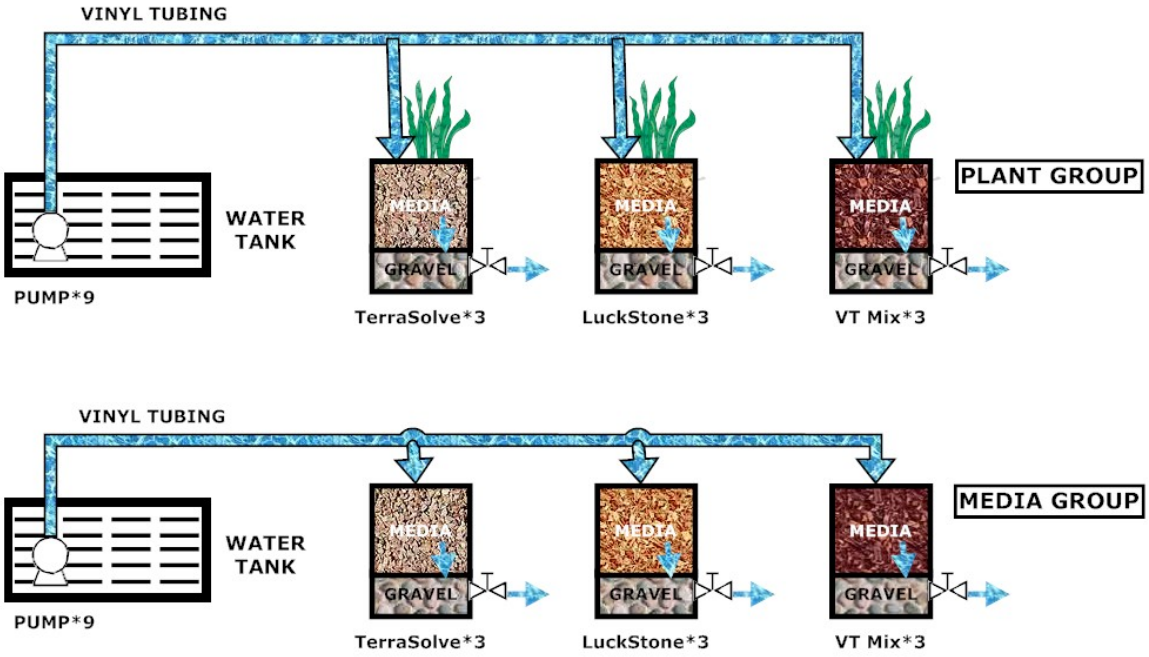

Figure 3.1 Irrigation systems for media and plant groups of mesocosm experiment.

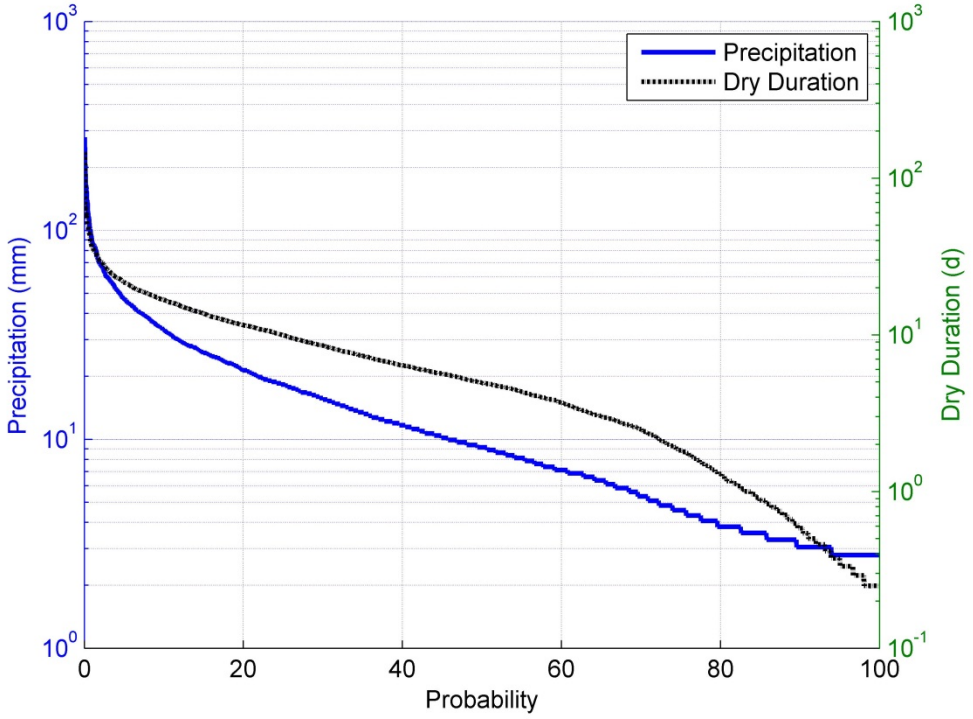

Figure 3.2 Frequency analyses on rainfall depth and dry duration at the experimental site in Virginia Beach, VA.

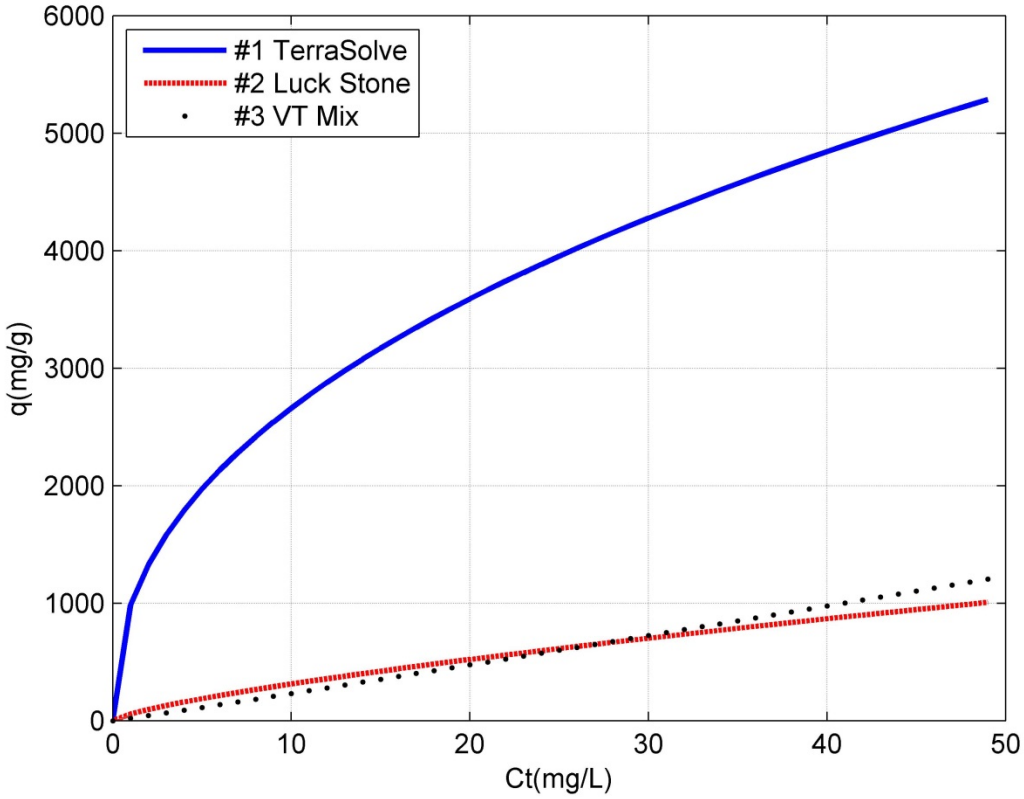

Figure 3.3 Freundlich isotherm adsorption curves of experimented blends.

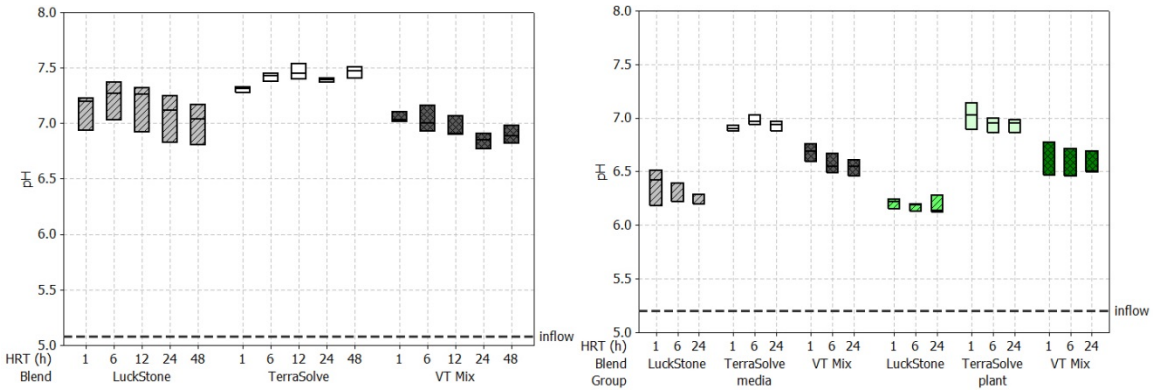

Figure 3.4 Inflow and outflow pH values of mesocosm experiment (left: Round 1; right: Round 2).

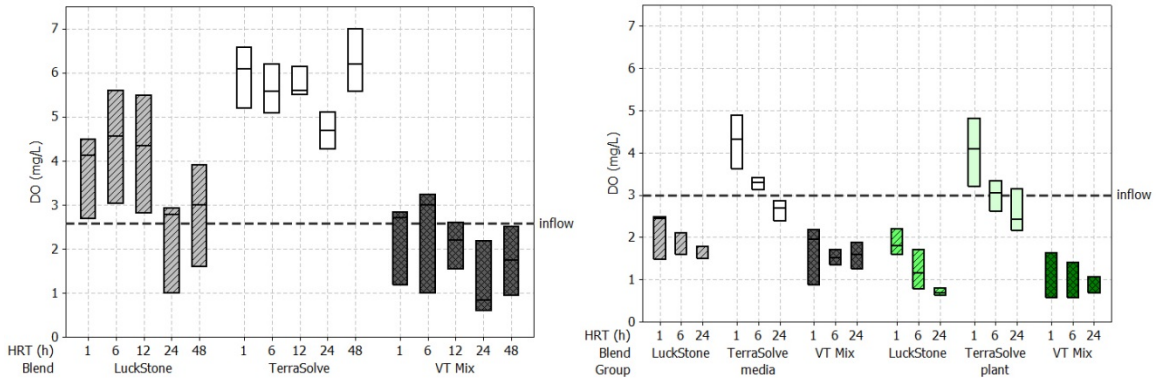

Figure 3.5 Inflow and outflow DO values of mesocosm experiment (left: Round 1; right: Round 2).

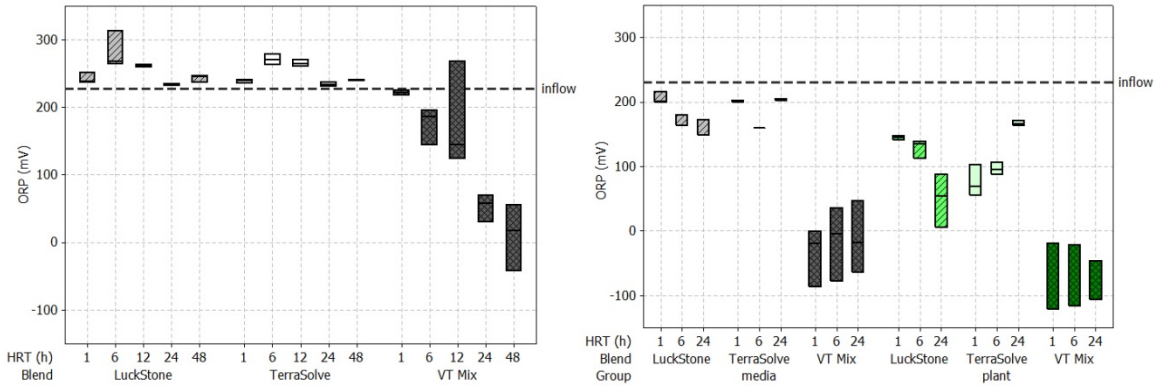

Figure 3.6 Inflow and outflow ORP values of mesocosm experiment (left: Round 1; right: Round 2).

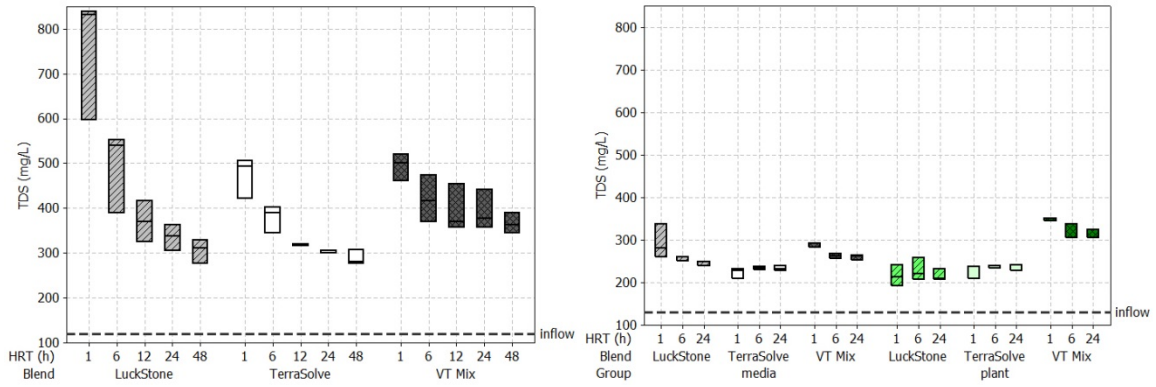

Figure 3.7 Inflow and outflow TDS values of mesocosm experiment (left: Round 1; right: Round 2).

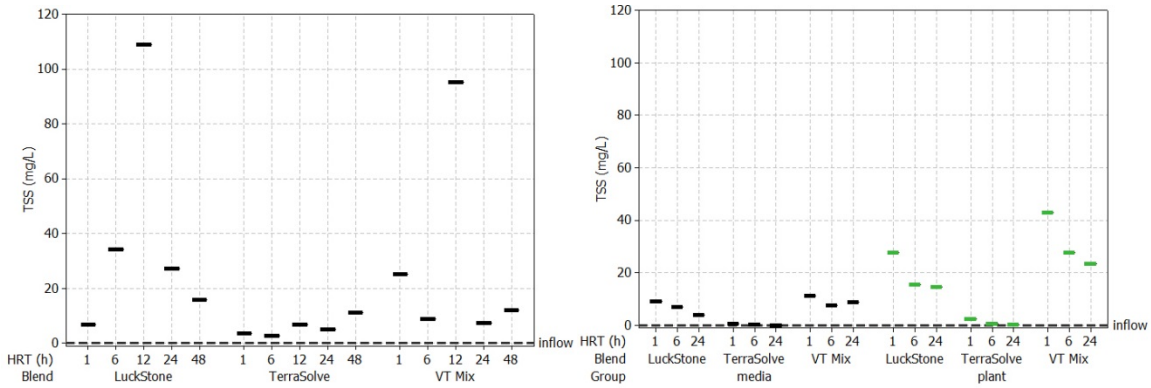

Figure 3.8 Inflow and outflow TSS values of mesocosm experiment (left: Round 1; right: Round 2).

References

1. Göbel, P., C. Dierkes, and W.G. Coldewey, Storm water runoff concentration matrix for urban areas. *Journal of Contaminant Hydrology*, 2007. **91**(1–2): p. 26-42.
2. US Environmental Protection Agency, *Results of the Nationwide Urban Runoff Program*. 1983, Washington, D.C.: Water Planning Division.
3. Pitt, R., A. Maestre, and R. Morquecho, *The national stormwater quality database (NSQD, version 1.1)*, 2004, University of Alabama: Tuscaloosa, AL.
4. Meierdiercks, K.L., et al., Heterogeneity of hydrologic response in urban watersheds. *Journal of the American Water Resources Association*, 2010. **46**(6): p. 1221-1237.
5. Cianfrani, C.M., W.C. Hession, and D.M. Rizzo, Watershed imperviousness impacts on stream channel condition in southeastern Pennsylvania. *Journal of the American Water Resources Association*, 2006. **42**(4): p. 941-956.
6. Nelson, E.J. and D.B. Booth, Sediment sources in an urbanizing, mixed land-use watershed. *Journal of Hydrology*, 2002. **264**(1–4): p. 51-68.
7. Carey, R.O., et al., Evaluating nutrient impacts in urban watersheds: challenges and research opportunities. *Environmental Pollution*, 2013. **173**: p. 138-149.
8. Hatt, B.E., et al., The influence of urban density and drainage infrastructure on the concentrations and loads of pollutants in small streams. *Environmental Management*, 2004. **34**(1): p. 112-124.
9. Alberti, M., et al., The impact of urban patterns on aquatic ecosystems: an empirical analysis in Puget lowland sub-basins. *Landscape and Urban Planning*, 2007. **80**(4): p. 345-361.
10. National Research Council, *Urban stormwater management in the United States*. 2009, Washington, D.C.: National Academies Press.
11. US Environmental Protection Agency, *Chesapeake Bay total maximum daily load for nitrogen, phosphorus and sediment*. 2010, Washington, D.C.: US EPA.
12. Davis, A.P., et al., Laboratory study of biological retention for urban stormwater management. *Water Environment Research*, 2001. **73**(1): p. 5-14.
13. Lucas, W.C. and M. Greenway, Hydraulic response and nitrogen retention in bioretention mesocosms with regulated outlets: Part II, nitrogen retention. *Water Environment Research*, 2011. **83**(8): p. 703-713.
14. Davis, A.P., et al., Water quality improvement through bioretention media: nitrogen and phosphorus removal. *Water Environment Research*, 2006. **78**(3): p. 284-293.
15. Carpenter, D. and L. Hallam, Influence of planting soil mix characteristics on bioretention cell design and performance. *Journal of Hydrologic Engineering*, 2010. **15**(6): p. 404-416.
16. Virginia Department of Conservation and Recreation, *VA DCR stormwater design specification No 9: bioretention (Version 1.9)*, 2011: Richmond, VA.
17. Davis, A., et al., Bioretention technology: overview of current practice and future needs. *Journal of Environmental Engineering*, 2009. **135**(3): p. 109-117.
18. Daniels, W.L. *Soil media designs for bioretention of nutrients and plant growth. Or: when is a spec not a spec?* 2012; Available from:

http://www.landrehab.org/userfiles/files/Stormwater%20Bioretention%20Media%203-23-12.pdf.
19. Pop, P.I., M. Dîrja, and A. Dumitraş, Outdoor experimental mesocosm construction for the evaluation of bioretention in Cluj-Napoca condition. *Bulletin of University of Agricultural Sciences and Veterinary Medicine Cluj-Napoca. Horticulture*, 2012. **69**(2): p. 529-530.
20. Hsieh, C.-h. and A.P. Davis, Evaluation and optimization of bioretention media for treatment of urban storm water runoff. *Journal of Environmental Engineering*, 2005. **131**(11): p. 1521-1531.
21. Stander, E. and M. Borst, Hydraulic test of a bioretention media carbon amendment. *Journal of Hydrologic Engineering*, 2010. **15**(6): p. 531-536.
22. Faucette, B., et al., Performance of compost filtration practice for green infrastructure stormwater applications. *Water Environment Research*, 2013. **85**(9): p. 806-814.
23. Palmer, E.T., et al., Nitrate and phosphate removal through enhanced bioretention media: mesocosm study. *Water Environment Research*, 2013. **85**(9): p. 823-832.
24. Henderson, C.F.K., *The chemical and biological mechanisms of nutrient removal from stormwater in bioretention systems*, in School of Engineering 2008, Griffith University: Nathan, Australia.
25. Blake, L., et al., Phosphorus content in soil, uptake by plants and balance in three European long-term field experiments. *Nutrient Cycling in Agroecosystems*, 2000. **56**(3): p. 263-275.
26. Lucas, W.C. and M. Greenway, Nutrient Retention in Vegetated and Nonvegetated Bioretention Mesocosms. *Journal of Irrigation and Drainage Engineering*, 2008. **134**(5): p. 613-623.
27. Lucas, W.C. and M. Greenway, Phosphorus retention by bioretention mesocosms using media formulated for phosphorus sorption: response to accelerated loads. *Journal of Irrigation and Drainage Engineering*, 2011. **137**(3): p. 144-153.
28. Rusciano, G.M. and C.C. Obropta, Bioretention column study: fecal coliform and total suspended solids reductions. *Transactions of the ASABE*, 2007. **50**(4): p. 1261-1269.
29. Adrien, N.G., *Computational hydraulics and hydrology : an illustrated dictionary*. 2004, Boca Raton, FL: CRC Press.
30. Li, H., et al., Effects of hydraulic retention time on nitrification activities and population dynamics of a conventional activated sludge system. *Frontiers of Environmental Science & Engineering*, 2013. **7**(1): p. 43-48.
31. Brown, R. and W. Hunt, Underdrain configuration to enhance bioretention exfiltration to reduce pollutant loads. *Journal of Environmental Engineering*, 2011. **137**(11): p. 1082-1091.
32. Lucas, W.C. and M. Greenway, Hydraulic response and nitrogen retention in bioretention mesocosms with regulated outlets: Part I, hydraulic response. *Water Environment Research*, 2011. **83**(8): p. 692-702.
33. US Environmental Protection Agency, *Low impact development (LID) a literature review*, 2000, Office of Water: Washington, D.C.
34. US Environmental Protection Agency. *State storm water BMP manuals*. 2013; Available from:

http://yosemite.epa.gov/R10/WATER.NSF/0/17090627a929f2a488256bdc007d8dee.
35. Atkins, P.W., *Physical chemistry*. 1978, San Francisco, CA: W.H. Freeman.
36. Goldberg, S., *Equations and models describing adsorption processes in soils*, in *Soil Science Society of America Book Series Number 8*. 2005, Soil Science Society of America Inc.: Madison, WI. p. 489-517.
37. Harter, R.D. and D.E. Baker, Applications and misapplications of the Langmuir Equation to soil adsorption phenomena. *Soil Science Society of America Journal*, 1977. **41**(6): p. 1077-1080.
38. Hsieh, C.-h., A.P. Davis, and B.A. Needelman, Nitrogen removal from urban stormwater runoff through layered bioretention columns. *Water Environment Research*, 2007. **79**(12): p. 2404-2411.
39. Hunt, W.F., *Pollutant removal evaluation and hydraulic characterization for bioretention stormwater treatment devices*, in Department of Agricultural and Biological Engineering 2003, The Pennsylvania State University: University Park, PA.
40. Passeport, E. and W. Hunt, Asphalt parking lot runoff nutrient characterization for eight sites in North Carolina, USA. *Journal of Hydrologic Engineering*, 2009. **14**(4): p. 352-361.
41. Greenway, M. and W.C. Lucas, *Advanced bioretention and panter-trench experiments: the Science Museum of Virginia*, in World Environmental and Water Resources Congress 2011: Palm Springs, CA. p. 3649-3658.
42. Dane, J.H., Topp G. Clarke, and Campbell Gaylon S., *Methods of soil analysis. Part 4, physical methods*. 2002, Madison, WI: Soil Science Society of America.
43. US Environmental Protection Agency, *Method 3050B: acid digestion of sediments, sludges, and soils*, in *Test methods for evaluating solid waste : physical/chemical methods*. 1996, Office of Solid Waste and Emergency Response: Washington D.C.
44. Bray, R.H. and L.T. Kurtz, Determination of total, organic, and available forms of phosphorus in soils. *Soil Science*, 1945. **59**: p. 39-45.
45. Sparks, D.L., Soil Science Society of America, and American Society of Agronomy, *Methods of soil analysis. Part 3, chemical methods*. 1996, Madison, WI: Soil Science Society of America.
46. Fairfax County Public Works and Environmental Services, *Recommended plant list for bioretention facilities - Fairfax County, Virginia*, 2007: Fairfax, VA.
47. Liu, J., D. Sample, and H. Zhang, Frequency analysis for precipitation events and dry durations of Virginia. *Environmental Modeling and Assessment*, 2013 DOI: 10.1007/s10666-013-9390-2 (in press).
48. Eaton A. D., American Public Health Association, and American Water Works Association, *Standard methods for the examination of water and wastewater*. 2005, Washington, D.C.: APHA-AWWA-WEF.
49. Milton, J.S. and J.C. Arnold, *Introduction to probability and statistics: principles and applications for engineering and the computing sciences*. 1995, New York, NY: McGraw-Hill.
50. Seltman, H.J., *Experimental design and analysis*. 2012, Pittsburgh, PA: Carnegie Mellon University.

51. Jillavenkatesa, A., Dapkunas S., and Lum Lin-Sien H., *Particle size characterization*. 2001, Washington, D.C.: National Institute of Standards and Technology.
52. Ferreira, M. and M.K. Stenstrom, The importance of particle characterization in stormwater runoff. *Water Environment Research*, 2013. **85**(9): p. 833-842.
53. ASTM Committee D-18 on Soil and Rock, *Standard practice for classification of soils for engineering purposes (unified soil classification system)*. 2011, Philadelphia, PA: ASTM International.
54. Hussain, A., et al., Application of the Langmuir and Freundlich equations for P adsorption phenomenon in saline-sodic soils. *Inernational Journal of Agriculture and Biology*, 2003. **5**(3): p. 349 - 356.
55. Bayley, R.M., et al., Water treatment residuals and biosolids coapplications affect semiarid rangeland phosphorus cycling. *Soil Science Society of America Journal*, 2008. **72**(3): p. 711-719.
56. Korom, S.F., Natural denitrification in the saturated zone: a review. *Water Resources Research*, 1992. **28**(6): p. 1657-1668.

4 A Computational Model to Simulate Hydraulic Function and Nutrient Fate for Assessment of Bioretention Performance[3]

Abstract

Bioretention is one of the most recognized LID practices emerging as an effective means to mitigate hydrologic impacts of urban development and improve water quality. The bioretention cell, filled with mulch, media, and plants, is the most unique of all LID practices. Bioretention cells attempt to replicate forested or grassland ecological systems through a variety of physical, chemical, and biological processes. While bioretention is being widely applied, its treatment processes are not well understood and predictive models are few. In this research, a computational model was developed to quantitatively describe a single bioretention cell with numerical algorithms in a computational model. The model is composed of multiple subroutines that depict water flow and nutrient fate. The hydraulic subroutines include precipitation, runoff, ET, infiltration, and outflow. An exfiltration parameter is set to achieve mass balance. Subroutines of N and P assess the transformation cycles of these nutrients within the bioretention cell. A biomass subroutine estimates the plant growth and decay rates and assists in computing nutrient mass flux between inorganic and organic forms. The model is then calibrated to a field-scale bioretention cell and used to estimate flows and nutrient removal. Sensitivity analyses determine the major factors to affect modeling outputs. A long-term simulation demonstrates that the model can be used to estimate bioretention performance and evaluate its impact on the surrounding environment.

[3] Prepared to be submitted to *Journal of Hydraulic Engineering*, allowed to reproduce in this dissertation.

Key words: computational model, numerical algorithm, bioretention, hydraulics, nutrient treatment, performance evaluation**,** sensitivity analysis, calibration and application

4.1 Introduction

Bioretention has emerged as a promising SCM, which is developed specifically to mitigate runoff quantity and reduce pollutants by multiple processes [1]. Bioretention cells are small depressions, which receive runoff from upland, normally impervious areas of a watershed. Within the cell are multiple media layers that provide water treatment through filtration prior to either exfiltration or draining to an outlet. A variety of vegetation is supported. Pollutants are removed through various physical, chemical, and biological processes by the plants, microbes, and soils [2]. Bioretention systems closely mimic the natural hydrologic cycle by retaining runoff to decrease flow rates and volumes. During this process, runoff is filtered through media particles, and nutrients are consumed by organisms. Other benefits may also include improved aesthetics, enhance wildlife habitat, minimize soil erosion, and recharge local groundwater [3].

Bioretention can be constructed in wide variety of urban environments. For example bioretention is likely the SCM of choice for median strips, parking lot islands, and swales [4]. Because of the widespread application of bioretention to manage and treat urban stormwater, the need for better understanding of their hydraulic functions and nutrient removal processes is acute. One means of addressing this need is a computational model based upon physical concepts and mathematical algorithms.

Generally, a *computational model* (as opposed to a physical or conceptual model) consists of *software code* which incorporates specific numerical algorithms, *inputs* or instructions for the model that tailor it to a specific situation, required *data* (such as

rainfall), and associated *calibration conditions* [5]. A computational model of bioretention can be a useful design tool by providing a means to generalize output metrics such as runoff peak, runoff volume and nutrient removal so that performance can be enhanced and maintenance timed appropriately.

The degree to which we can mimic the hydrology of bioretention systems is dependent upon how well we can predict their behavior with hydraulic processes, thus hydraulic simulation is normally primary. Many modeling applications of bioretention are based on the simulation of continuous long-term data. This is because single-event hydraulic modeling cannot accurately simulate dry periods between-storms and subsequent changes in soil moisture due to the lack of considerations of ET, infiltration, and initial moisture conditions [6].

The descriptions and uses of some popular computational programs that can be employed for modeling bioretention hydraulics are summarized in Table 1.2 in Chapter 1.

Most models for bioretention systems focus exclusively on hydraulics. Few models investigate nutrient cycles in bioretention based on physicochemical mechanisms. Those coded bioretention models for treatment simulations, as described in Chapter 1, neglect some functional processes for simplicity. Plant uptake and biomass variation are typically excluded in consideration, thus the computational calculation may not be comprehensive.

The increasing implementation of bioretention reinforces the demand for a comprehensive modeling tool to estimate the hydrologic performance and nutrient removal of bioretention. To accomplish this objective, we developed a computational model (Bioretention Evaluation and Assessment Model, or BEAM) based upon physical

concepts and mathematical algorithms to simulate a typical bioretention cell. The model is developed within Matlab® with one main function and multiple subroutines to perform simulation with hourly-scale on hydraulic pattern and event-scale on nutrient treatment. The main contribution of BEAM is the inclusion of computation on biomass change, plant uptake, and defoliation, which are important processes to calculate removal efficacies by completing the nutrient cycles and transformations within bioretention systems.

4.2 Methods

4.2.1 Model structure

The model BEAM was developed with Matlab® with a main function and numerous subroutines. The main function is the cardinal control panel of BEAM. The main function reads necessary data and parameters from MS EXCEL spreadsheets and outputs the simulation results in spreadsheets and graphs. The subroutines are called in sequence to perform model calculations. The subroutine for potential evapotranspiration (PET) computation is called first, followed by Inflow, Infiltration, Outflow, Biomass, N and P subroutines. Some results from previous subroutines are introduced into latter subroutines for computation.

Figure 4.1 illustrates the model structure of BEAM. A description of the analytical basis for the development of the subroutines is provided hereafter.

4.2.2 PET

Food and Agricultural Organization (FAO) of the United Nations released a dual crop coefficient method for estimating ET through reference ET [7-9], and a computer program was developed with the method's concepts [10]. Another temperature-based

method used by Thornthwaite [11] can avoid the difficulty to determine and use the representative crops and their coefficients by estimating ET from PET. PET is the amount of water that would be evaporated and transpired if there is sufficient water available. With Thornthwaite's equation, monthly PET can be calculated through the following equations [12].

$$PET_m = 16\left(\frac{L}{12}\right)\left(\frac{N}{30}\right)\left(\frac{10T_{eff}}{I}\right)^{\beta} \quad (4\text{-}1)$$

Where PET_m = monthly average potential evapotranspiration (m/month)

L = average day length of the calculated month (h)

N = total number of days in the calculated month (dimensionless)

T_{eff} = effective daily temperature (°C)

I = monthly heat index (dimensionless)

β = $(6.75\times10^{-7})I^3-(7.71\times10^{-5})I^2+(1.792\times10^{-2})I+0.49239$

To get the PET values in a daily time scale, an "effective temperature" parameter is required to be computed with daily maximum and minimum temperatures.

$$T_{eff} = \frac{k}{2}(3T_{max} - T_{min})\frac{L}{24-L} \quad (4\text{-}2)$$

Where k = 0.69 as the statistical value for estimating ET

T_{max} = daily maximum temperature (°C)

T_{min} = daily minimum temperature (°C)

Therefore monthly heat index can be defined with effective temperature.

$$I = \sum_{month} I_{daily} = \sum_{month}\left(0.2T_{eff}\right)^{1.514} \quad (4\text{-}3)$$

Average day length can be calculated with local geographical data.

$$L = \frac{24\omega_s}{\pi} = \frac{24}{\pi} arccos[-tan(\varphi)\,tan(\delta)] \quad (4\text{-}4)$$

Where ω_s = daily sunset hour angle (rad)

φ = latitude of experimental site (rad)

δ = solar declination (rad), $\delta = 0.409 \sin\left(\frac{2\pi}{365}J - 1.39\right)$

J = Julian day number in a year from 1 to 365 / 366 (dimensionless)

Then daily PET can be determined from above results.

$$PET_d = \begin{cases} 0 & T_{eff} < 0℃ \\ 16\left(\frac{L}{D_{yr}}\right)\left(\frac{10T_{eff}}{I}\right)^{\alpha} & T_{eff} > 0℃ \; and \; T_{eff} < 26℃ \\ \left(\frac{L}{D_{yr}}\right)\left(-415.85 + 32.24T_{eff} - 0.43{T_{eff}}^2\right) & T_{eff} \geq 26℃ \end{cases} \quad (4\text{-}5)$$

Where PET_d = daily potential evapotranspiration (m/h)

D_{yr} = total number of days in a year, 365 / 366 (dimensionless)

To convert daily PET to hourly values, a typical 24-h PET distribution in a day was employed. A program named LXPET (Lamoreux Potential Evapotranspiration) provides a general 24-h ET distribution in a day in the format of a reference matrix [13], this method was included in BEAM.

Hourly PET is then available from the daily PET and reference matrix.

$$PET = PET_d \times \frac{PETM_j}{\sum_{j=1}^{24} PETM} \quad (4\text{-}6)$$

Where PET = hourly potential evapotranspiration (m/h)

$PETM$ = reference matrix of 24-h daily PET, j = 1 – 24 h (dimensionless)

The calculation of ET is to be completed by the Infiltration subroutine with hourly PET data and media water content, which will be described in Section 4.3.4.

4.2.3 Inflow

Inflow into a bioretention cell is runoff from a known site, and is generated from precipitation. To calculate the hourly inflow entering a bioretention site, hourly precipitation data from the online database of NCDC were downloaded and organized in spreadsheets with other necessary parameters. A minimum inter-event time as 6 hours was used to separate consecutive hourly rainfall into different events.

With the hourly precipitation data, the inflow to be treated by bioretention systems can be estimated with the main algorithm of SWMM program [14] by a fourth-order Runge-Kutta numerical method.

$$\frac{\Delta d}{\Delta t} = i^* - \frac{W \cdot S^{1/2}}{A \cdot n}\left(d - d_p\right)^{5/3} \quad (4\text{-}7)$$

Where Δd = difference in rain depths between beginning and end of a time step (m)

Δt = time step (h)

d = rain depth in hourly time step (m)

d_p = depression storage (m)

A = watershed area (m^2)

W = watershed width (m)

n = Manning's n of watershed (dimensionless)

S = watershed slope (dimensionless)

i^* = effective rainfall (m/h)

The effective rainfall is calculated by the Rational Formula with a given runoff coefficient [15], and hourly PET data from PET subroutine.

$$i^* = C \times i - PET \quad (4\text{-}8)$$

Where C = runoff coefficient of watershed, for parking lot, C ≥ 0.95 (dimensionless)

i = hourly precipitation on watershed (m/h)

After getting hourly rain depths, another equation is to be solved to get the flow rate generated from precipitation.

$$Q_{in} = \frac{W}{n}\left(d - d_p\right)^{5/3} S^{1/2} \tag{4-9}$$

Where Q_{in} = inflow rate (m^3/h)

4.2.4 Infiltration

Infiltration is the movement of water from soil surface into soil [16]. To compute the infiltration rate of surface water into bioretention media, a 1-dimensional or 2-dimensional finite-volume model based on Richards equation can be developed [17, 18]. The integral form of Richards equation, however, is very complex, difficult to parameterize and can tend to increase computational times [19]. The Green-Ampt equation is a physically-based algebraic model that can be used to evaluate the losses of precipitation due to infiltration and is relatively easy to parameterize for solution [20]. The Green-Ampt model applies the principle of mass conservation in a finite-difference formulation to characterize the infiltration process [21]. This ordinary differential equation to be used in BEAM to simulate infiltration process through bioretention media is presented here.

$$f(t) = K_h\left[1 + \frac{|\psi_f|(\phi - \theta_0)}{F(t)}\right] \tag{4-10}$$

Where f = infiltration rate (m/h)

F = cumulative infiltration (m/h)

K_h = saturated hydraulic conductivity of soil (m/h)

ψ_f = characteristic suction head of soil (m)

ϕ = media porosity (dimensionless)

θ_0 = initial soil water content (dimensionless)

The Green-Ampt differential equation is solved by determining ponding time, which is the instant when the surface layer becomes saturated [22].

$$t_p = \frac{K_h|\psi_f|(\phi-\theta_0)}{w(w-K_h)} \tag{4-11}$$

Where t_p = ponding time (h)

w = water input rate as the sum of inflow and precipitation rates (m/h)

$$w = \frac{Q_{in}}{A_{brc}} + i \tag{4-12}$$

Where A_{brc} = bioretention area (m^2)

In case the ponding time is less than rainfall event length, a fourth-order Runge-Kutta numerical algorithm is applied to solve the Green-Ampt equation for infiltration rate and media water content, and the ponding water is regarded as overflow to discharge away from the bioretention.

ET is then calculable using the results of media water content and PET values [22, 23].

$$ET = \begin{cases} PET & \theta \geq \theta_{fc} \\ \frac{\theta-\theta_{pwp}}{\theta_{fc}-\theta_{pwp}} \times PET & \theta_{pwp} < \theta < \theta_{fc} \\ 0 & \theta \leq \theta_{pwp} \end{cases} \tag{4-13}$$

Where ET = hourly evapotranspiration (m/h)

θ = water content in media (dimensionless)

θ_{pwp} = permanent wilting point of media (dimensionless)

θ_{fc} = field capacity of media (dimensionless)

4.2.5 Outflow

Outflow is discharged through perforated pipes in bioretention systems. The flow rate of effluent is determined by the water table [24]. The Colebrook-White equation is applicable for solving fully-filled flow and partially-filled flow through the cross-sectional opening of pipes [25, 26].

In the modeling simulation of bioretention outflow, water table is computed with the inflow volume, media porosity, and bioretention area.

$$h = \frac{w(1-ex)}{\phi} \tag{4-14}$$

Where h = water table within the bioretention system (m/h)

ex = exfiltration factor (dimensionless)

Due to the fact that bioretention is not entirely separated from surrounding environment, the water table is adjusted by a coefficient of exfiltration factor, which is the ratio of the influent volume exfiltrating out of the bioretention system to the total influent volume.

With the water table known, outflow rate of bioretention can be calculated by Colebrook-White equation considering several scenarios either the pipes are emerged by water or not [27, 28].

$$Q_{out} = \begin{cases} 0 & h \le H_p - D_p/2 \\ \left(1 + \frac{logR_h}{log3.7\theta}\right) A_f R_h{}^{\frac{1}{2}} & h > H_p - D_p/2 \; and \; h < H_p + D_p/2 \\ -2\sqrt{2gD_pS_p}log\left(\frac{k_S}{3.7D_p} + \frac{2.51\nu}{D_p\sqrt{2gD_pS_p}}\right)A_p & h = H_p + D_p/2 \\ -2\sqrt{2gD_pS_p}log\left(\frac{k_S}{3.7D_p} + \frac{2.51\nu}{D_p\sqrt{2gD_pS_p}}\right)A_p + n_h c_h a_h\sqrt{2gH_h} & h > H_p + D_p/2 \end{cases} \tag{4-15}$$

Where Q_{out} = outflow rate (m^3/h)

R_h = hydraulic radius of perforated pipe (m)

A_f = area of partially filled flow in perforated pipe (m^2)

g = gravitational acceleration constant, 9.80665 (m/s^2)

H_p = pipe head, elevation from bioretention bottom to pipe center (m)

D_p = diameter of perforated pipe (m)

S_p = pipe slope, assume equals to hydraulic gradient (dimensionless)

k_S = pipe wall roughness index (m)

A_p = cross-sectional area of perforated pipe (m^2)

v = kinematic viscosity of water (m^2/s)

n_h = number of perforated holes (dimensionless)

c_h = orifice coefficient of perforated holes (dimensionless)

a_h = area of perforated holes (m^2)

H_h = height of water above pipe holes (m)

$$H_h = h - H_p - \frac{D_p}{2} \tag{4-16}$$

The following equations are used to solve hydraulic radius and partially filled flow area.

$$\alpha = 2\arccos\left(\frac{2|H_p - h|}{D_p}\right) \tag{4-17}$$

Where α = central angle of partially filled pipe (rad)

$$A_f = \begin{cases} \frac{{D_p}^2}{8}(\alpha - \sin\alpha) & h > H_p - D_p/2 \; and \; h < H_p \\ \frac{\pi {D_p}^2}{4} - \frac{{D_p}^2}{8}(\alpha - \sin\alpha) & h \geq H_p \; and \; h < H_p + D_p/2 \end{cases} \tag{4-18}$$

$$R_h = \begin{cases} \frac{2A_f}{D_p\alpha} & h > H_p - D_p/2 \; and \; h < H_p \\ \frac{2A_f}{2\pi D_p - D_p\alpha} & h \geq H_p \; and \; h < H_p + D_p/2 \end{cases} \quad (4\text{-}19)$$

In the partially filled equation, the parameter θ is available from pipe characteristics data.

$$\theta = \left(\frac{k_S}{D_p} + \frac{1}{3600 D_p {S_p}^{1/3}}\right)^{-1} \quad (4\text{-}20)$$

4.2.6 Biomass

Bioretention is regarded as a plant-based filtration device that removes pollutants through a variety of physical, chemical, and biological treatment processes. The vegetation plays an important role in the bioretention ecosystem to maintain a sustainable ecosystem. Bioretention plants uptake water [29], and add water storage by increasing hydraulic conductivity [30]. PET and Infiltration subroutines have been called to perform ET calculation to simulate the process of water uptake by plants.

Plants are also pivotal in the cycles of nutrients in bioretention. Defoliation of plants introduces organic nutrients into bioretention to decompose into inorganic compounds [31], which can be uptaken by plants for physiological activities after physicochemical reactions [32, 33]. However, as a dynamic biological system, the vegetation has time-variable changes on its biomass amount. The purpose of Biomass subroutine is to estimate the accumulation and decay processes of vegetation biomass within bioretention systems. The plant uptake of nutrients in BEAM will be modeled by N and P subroutines in the following sections.

The simulation of vegetation biomass in BEAM is based on the parameter of leaf area index (LAI) [34] and the concepts of the Erosion Productivity Impact Calculator

(EPIC) [35]. LAI is a dimensionless quantity that characterizes plant canopies. It is defined as the one-sided green leaf area per unit ground surface area in broadleaf canopies, and half of the total needle surface area per unit ground surface area in conifers [36].

LAI can be determined by taking a statistical sample of plant canopy by measuring leaf area and surface area [37]. In BEAM's development, typical monthly LAI data set of Mid-Atlantic region from academic literatures were cited as a matrix to represent this parameter [38]. The daily net radiation values were estimated with climatological data and following equations [39].

$$d_r = 1 + 0.033 \cos\left(\frac{2\pi}{365} J\right) \tag{4-21}$$

$$R_a = \frac{1440}{\pi} G_{sc} d_r [\omega_s \sin(\varphi) \sin(\delta) + \cos(\varphi) \cos(\delta) \sin(\omega_s)] \tag{4-22}$$

$$R_s = K_T R_a (T_{max} - T_{min})^{0.5} \tag{4-23}$$

Where d_r = inverse relative distance from Earth to sun (dimensionless)

G_{sc} = solar constant (0.0820 MJ/m^2-min)

R_a = daily extraterrestrial radiation (MJ/m^2-d)

R_s = daily total solar radiation (MJ/m^2-d)

K_T = 0.162 for interior, 0.19 for coastal regions (dimensionless)

Then photosynthetic active radiation (PAR) can be calculated. PAR designates the spectral wave band of solar radiation from 400 to 700 nanometers that are used by photosynthetic organisms in the process of photosynthesis [40]. PAR can be estimated with an equation derived from Beer's Law [41].

$$PAR = 0.5 R_s (1 - e^{-k_e \times LAI}) \tag{4-24}$$

Where PAR = photosynthetic active radiation (MJ/m^2-d)

k_e = light extinction coefficient (0.65, dimensionless)

Radiation-use efficiency (RUE) is also necessary for biomass simulation. The amount of biomass produced per unit of intercepted solar radiation season is defined as the crop RUE [34].

$$RUE = \frac{100(CO_2)}{(CO_2)+b_1\times e^{-b_2(CO_2)}} \tag{4-25}$$

Where RUE = radiation use efficiency (g/MJ)

(CO_2) = average atmospheric CO_2 concentration (391.57 ppm)

b_1 = coefficient (7784, dimensionless)

b_2 = coefficient (-0.00107, dimensionless)

Biomass is to be estimated by above results with the Monteith equation [42-44].

$$B = A_{brc} \times RUE \times PAR \tag{4-26}$$

Where B = daily biomass yields (g/d)

With the daily biomass amount calculated, the growth and decay rates of plants can be computed before passing them to N and P subroutines for simulation on nutrient processes. If vegetation biomass increases with time, then overall growth rate is positive and decay rate is 0 [45]; if biomass decreases with time, then overall growth rate is 0 and the absolute value of decay rate is positive [46].

$$gr_p = \frac{\ln(B_2)-\ln(B_1)}{t_2-t_1};\ \ de_p = 0 \qquad when\ B_2 \geq B_1 \tag{4-27}$$

$$de_p = \left|\frac{\ln(B_2)-\ln(B_1)}{t_2-t_1}\right|;\ \ gr_p = 0 \qquad when\ B_2 < B_1 \tag{4-28}$$

Where gr_p = relative growth rate of plants (d^{-1})

B_1 = biomass of plant at beginning of time step (g)

B_2 = biomass of plant at end of time step (g)

t_1 = beginning of time step (d)

t_2 = end of time step (d)

de_p = relative decay rate of plants (d^{-1})

4.2.7 Nitrogen

N is a key element controlling the species composition, diversity, dynamics, and functioning of many terrestrial, freshwater, and marine ecosystems [47]. In the natural environment, N exists in a number of chemical forms and undergoes transformations among these forms. In urban environment of stormwater runoff and soil particles, major N forms include organic N, NH_4, and NO_3. The transformations of these N forms in soil coexist in a dynamic system assisted by numerous biological or chemical reactions, mainly through the actions of microbes [48].

Figure 4.2 depicts the major mass flows of N forms to be modeled in a bioretention system. Among these mass flows, N is introduced into bioretention through the processes of inflow irrigation and vegetation defoliation. Organic N is converted to NH_4 through ammonification process. NH_4 can be uptaken by plants for physiological activities, or becomes NH_3 through volatilization, or be converted to NO_3 by nitrification microbes [49]. NO_3 can also be uptaken by vegetation, or released as N_2 under denitrification process [50].

The dynamic model of N is constructed upon a set of differential equations describing the numbered process in Figure 4.2. In the simulation, totally 4 N forms: organic N in media, NH_4 in media, NO_3 in media, and Organic N in plants are considered.

The differential equation group is a four-dimensional dynamic system to calculate the existence and transformation of these 4 N forms simultaneously within a bioretention cell.

$$\begin{cases} \dfrac{dx_1}{dt^*} = \dfrac{1}{HRT}(n_1 - x_1) - r_{am}x_1 + de_p x_4 \\ \dfrac{dx_2}{dt^*} = \dfrac{1}{HRT}(n_2 - x_2) + r_{am}x_1 - r_{ni}x_2 - r_{vo}x_2 - r_{p,a}x_4 \\ \dfrac{dx_3}{dt^*} = \dfrac{1}{HRT}(n_3 - x_3) + r_{ni}x_2 - r_{de}x_3 - r_{p,n}x_4 \\ \dfrac{dx_4}{dt^*} = r_{p,a}x_4 + r_{p,n}x_4 - de_p x_4 \end{cases} \quad (4\text{-}29)$$

Where x_1 = organic N content in media, expressed as concentration (mg/L)

x_2 = NH_4 content in media, expressed as concentration (mg/L)

x_3 = NO_3 content in media, expressed as concentration (mg/L)

x_4 = organic N content in plants, expressed as concentration (mg/L)

t^* = variable of time (d)

n_1 = organic N concentration in inflow (mg/L)

n_2 = NH_4 concentration in inflow (mg/L)

n_3 = NO_3 concentration in inflow (mg/L)

r_{am} = ammonification rate of organic N (d^{-1})

r_{ni} = nitrification rate of NH_4 (d^{-1})

r_{vo} = volatilization rate of NH_4 (d^{-1})

$r_{p,a/n}$ = plant uptake rate of NH_4 and NO_3 respectively (d^{-1})

r_{de} = denitrification rate of NO_3 (d^{-1})

Ammonification is the result of the breakdown of organic matter to NH_4 and related compounds accomplished by microorganisms [51]. The rate of ammonification is dependent on water temperature and concentration of organic N. The rate equation can be expressed in the following form [52].

$$r_{am} = \varepsilon T \tag{4-30}$$

Where ε = a correlation coefficient, ranges from 0.0005 to 0.143 (dimensionless)

Nitrification is a microbial process by which reduced N compounds (primarily NH_4) are sequentially oxidized to NO_2 and NO_3 [53]. The NH_4 conversion in nitrification process is carried out in 2 steps [54].

$$NH_4^+ + \frac{3}{2}O_2 \rightarrow NO_2^- + H_2O + 2H^+ \tag{4-31}$$

$$NO_2^- + \frac{1}{2}O_2 \rightarrow NO_3^- \tag{4-32}$$

As an intermediate product, nitrite is not considered in the modeling computation, thus the above 2 steps can be written into 1 single step from NH_4 to NO_3.

$$NH_4^+ + 2O_2 \rightarrow NO_3^- + H_2O + 2H^+ \tag{4-33}$$

The chemical reaction equation indicates nitrification process is influenced by DO, and pH. Microbial population (represented by *Nitrosomonas* bacteria) is the control agent of nitrification as an aerobic process; therefore the rate of nitrification can be expressed by the Monod-type equation [55].

$$r_{ni} = \frac{\mu_m}{Y}\left(\frac{1}{K_1 + x_2}\right)\left(\frac{DO}{K_2 + DO}\right) C_T C_{pH} \tag{4-34}$$

Where μ_m = maximum *Nitrosomonas* growth rate (d^{-1})

Y = yield coefficient for *Nitrosomonas* (mg VSS/mg N)

K_1 = ammonia *Nitrosomonas* half saturation rate constant (mg/L)

K_2 = oxygen *Nitrosomonas* half saturation rate constant (mg/L)

C_T = temperature dependence factor (dimensionless)

C_{pH} = *Nitrosomonas* growth limiting factor for pH (dimensionless)

Some variables in the N subroutine are given by the equations as follows.

$$K_1 = e^{0.051(T-1.58)} \tag{4-35}$$

$$C_T = e^{0.098(T-15)} \tag{4-36}$$

$$C_{pH} = \begin{cases} 1 - 0.833(7.2 - pH) & pH < 7.2 \\ 1 & pH \geq 7.2 \end{cases} \tag{4-37}$$

NH_4 volatilization is a physicochemical process determined by temperature and pH, and its rate can be described by the equation [52].

$$r_{vo} = \frac{1}{1+10^{10.068-0.033T-pH}} \tag{4-38}$$

As an important nutrient element for vegetation metabolism, N in soil is assimilated by plants through their root systems. Generally NH_4 and NO_3 are uptaken by plants and converted to organic N for vegetation physiological activities [56]. The N uptake rate is influenced by plant growth rate, and concentrations of inorganic N forms. These factors can be incorporated and expressed in the rate equation.

$$r_{p,a} = gr_p\left(\frac{x_2}{x_2+x_3}\right) \tag{4-39}$$

$$r_{p,n} = gr_p\left(\frac{x_3}{x_2+x_3}\right) \tag{4-40}$$

Denitrification is the process to convert NO_3 to gaseous N by microorganisms under anaerobic conditions. It is the only point in the N cycle at which fixed N reenters the atmosphere as N_2. The complete denitrification process can be expressed as a redox reaction [57].

$$2NO_3^- + 10e^- + 12H^+ \rightarrow N_2 + 6H_2O \tag{4-41}$$

Soil moisture (θ) and temperature are major factors to determine denitrification process rate by the equation [52].

$$r_{de} = e^{k_1 x_3 + k_2 \theta + k_3 T - k_4} \tag{4-42}$$

Where $k_{1\text{-}4}$ = adjustable coefficients (dimensionless)

4.2.8 Phosphorus

P is an essential nutrient for all life forms. It is required to form DNA and cell membranes, among other functions [58]. P is also a water pollutant as it promotes the productivity of most freshwater systems which can undergo eutrophication under high P inputs [59]. P forms in soil can be generally divided into 2 categories: soluble and particulate. The former section of P contains the forms that are soluble in soil-water system and can be assimilated by plants; the latter section includes most P that is adsorbed by soil particles and cannot be utilized by vegetation directly [60].

In the modeling development, 4 P forms will be considered including organic P in media, PO_4, inactive P, and organic P in plants. The soluble PO_4 represented as PO_4 is the most readily available form for vegetative uptake [61], while organic P and inactive P are considered as P pools to store and provide PO_4 for plant assimilation. The P cycle is shown in Figure 4.3**.** Similar to Nitrogen subroutine, P simulation in BEAM is also based upon a set of differential equations. With 4 P forms to simulate, the group is comprised by 4 differential equations to compute real-time concentrations of P forms.

$$\begin{gathered}
\frac{dy_1}{dt^*} = \frac{1}{HRT}(p_1 - y_1) - r_{mi} y_1 + de_p y_4 \\
\frac{dy_2}{dt^*} = \frac{1}{HRT}(p_2 - y_2) + r_{mi} y_1 - r_{pr} y_2 - \left[r_{ad}(p_2 - y_2) - r_{ad} q_e \frac{W_{brc}}{V_{brc}}\right] - r_p y_4 \\
\frac{dy_3}{dt^*} = \frac{1}{HRT}(p_3 - y_3) + r_{pr} y_2 + \left[r_{ad}(p_2 - y_2) - r_{ad} q_e \frac{W_{brc}}{V_{brc}}\right] \\
\frac{dy_4}{dt^*} = r_p y_4 - de_p y_4
\end{gathered} \tag{4-43}$$

Where y_1 = organic P content in media, expressed as concentration (mg/L)

y_2 = PO_4 content in media, expressed as concentration (mg/L)

y_3 = inactive P content in media, expressed as concentration (mg/L)

y_4 = organic P content in plants, expressed as concentration (mg/L)

p_1 = organic P concentration in inflow (mg/L)

p_2 = PO_4 concentration in inflow (mg/L)

p_3 = particulate P concentration in inflow (mg/L)

r_{mi} = mineralization rate of organic P (d^{-1})

r_{pr} = precipitation rate of PO_4 (d^{-1})

r_{ad} = adsorption rate of PO_4 (d^{-1})

q_e = amount of PO_4 adsorbed at equilibrium (d^{-1})

W_{brc} = weight of bioretention system (kg)

V_{brc} = volume of bioretention system (m^3)

r_p = plant uptake rate of PO_4 (d^{-1})

P mineralization is the conversion of organic P to inorganic forms [62]. The mineralization rate is determined by the decay rate of plants and the rate constant of the reaction from organic P to PO_4 [63].

$$r_{mi} = de_p\theta_p - k_{mi}y_1 \quad (4\text{-}44)$$

Where θ_p = P content ratio in plant biomass (dimensionless)

k_{mi} = P mineralization rate constant (μg P/kg soil-d)

The precipitation rate of P is mostly determined by the concentration of metal ions. As the metallic element with the highest content in the Earth's crust, Al ion is taken as the major factor in P precipitation process [64].

$$r_{pr} = \begin{cases} k_{pr}(Me - Me_m) & Me > Me_m \\ k_{pr} & Me \leq Me_m \end{cases} \quad (4\text{-}45)$$

Where k_{pr} = P precipitation rate constant (d^{-1})

Me = actual metal (Al) ion concentration (mg/L)

Me_m = equilibrium metal (Al) ion concentration at a given pH (mg/L)

Me_m is calculated with the inflow pH values and solubility product constant of $Al(OH)_3$ [65].

$$Me_m = \frac{10^{-pK_{sp}}}{(10^{pH-14})^3} \quad (4\text{-}46)$$

Where K_{sp} = solubility product constant of $Al(OH)_3$ (mg^4/L^4)

Adsorption is the main mechanism to retain P in natural treatment systems [66]. Typically, adsorption process is modeled using isotherm equations. However, with short time scales, equilibrium may not be reached [67]. In this case, kinetic rate models can be used to describe adsorption process [68]. The term of adsorption in P subroutine is derived from first-order kinetic adsorption equation with the conversion between P concentration and adsorption amount [69].

$$\frac{dq_t}{dt} = r_{ad}(q_e - q_t) \quad (4\text{-}47)$$

$$y_2 = c_2 - \frac{W_{brc}}{V_{brc}} q_t \quad (4\text{-}48)$$

Where q_t = amount of PO_4 adsorbed at time t (mg/g)

Then the adsorption term can be written as follows.

$$\left[\frac{dy_2}{dt}\right]_{ad} = -\frac{W_{brc}}{V_{brc}} r_{ad}(q_e - q_t) = r_{ad}(c_2 - y_2) - r_{ad} q_e \frac{W_{brc}}{V_{brc}} \quad (4\text{-}49)$$

Plants assimilate P as an important nutrient for metabolic and physiological activities [70]. The Michaelis-Menten kinetic equation defines the vegetative uptake rate of P as [71].

$$r_p = \frac{I_{max}(y_2 - y_{min})}{K_m + y_2 - y_{min}} \quad (4\text{-}50)$$

Where I_{max} = maximum P uptake rate (g/m^2-d)

y_{min} = minimum P concentration for uptake (mg/L)

K_m = P uptake rate (mg/L)

4.2.9 Sensitivity analysis

Sensitivity analysis is the study of how the uncertainty in the output of a mathematical model or system (numerical or otherwise) can be apportioned to different sources of uncertainty in its inputs [72]. To determine the major parameters that impact the performance of bioretention systems, sensitivity analysis is presented under a given set of assumptions on inflow / outflow rates and TN / TP concentrations in outflow. The sensitivity of BEAM's predictions to input parameters can be assessed with the equation [67].

$$\Delta S = \frac{R_i - R_0}{R_0} \times 100\% \quad (4\text{-}51)$$

Where ΔS = sensitivity of the modeling result to a parameter, or the difference caused by perturbation of the parameter (dimensionless)

R_i = a modeling result after perturbation of a parameter (unit of parameter)

R_0 = a modeling result with a set of original parameters (unit of parameter)

In the modeling simulation, the TN concentration was calculated as the sum of organic N, NH_4, and NO_3, and the TP concentration was the sum of organic P and PO_4 from BEAM computation. The process of sensitivity analysis is to adjust an input parameter with a certain percentage (-50%, -20%, -10%, -5%, 5%, 10%, 20%, 50%), and compute the relative difference of outputs with the equation above. The differences were then expressed as percentages and plotted with the percentage adjustments to show the sensitivity of the modeling outputs to adjusted parameters. For the sensitivity analyses on TN and TP, the percentage perturbation is conducted on all forms of nutrients in inflow simultaneously, i.e. 90% TN means the corresponding organic N, NO_3, and NH_4 are all 90% of their original data.

Besides the investigation on TN / TP, the influences of nutrient forms distribution are also involved. The TN / TP concentrations in inflow were kept same, but their components of organic N, NO_3, and NH_4 / organic P, PO_4, and particulate P were adjusted to extremes to determine the mainly influential processes or functions in the nutrient transformation cycles. The process is to change the distribution of each form from average (33%) to 100% with others as 0%, and calculate the relative difference between the results.

4.2.10 Calibration and application

Calibration is the adjustment of model parameters to improve the model's ability to reproduce the performance evaluation of bioretention systems [73]. Model calibration is performed after all the parameters of study site and bioretention cell were input to BEAM from spreadsheets. The modeling results from BEAM simulation were compared

with observed data with necessary adjustment on parameters to enhance the predictive ability of the model.

BEAM program was evaluated using observed data from a field-scale bioretention system located at 37°14'N, 80°24'W in Blacksburg, VA, which was designed to hold the storm runoff from a 1600-m^2 asphalt parking lot. The bioretention cell was filled with a mixture of 88% medium sand, 8% clay and silt fines, and 4% leaf compost. The experimental cell is 4.6 m in length, 7.6 m in width, and 1.8 m in depth, with a 30-cm drainage layer above the bottom. Two sets of perforated pipes with diameter as 10 cm were buried on top of the drainage layer to drain the leachate from bioretention as outflow [74]. Figure 4.4 illustrates the cross-section of the bioretention cell.

The bioretention facility was monitored in 2008 from January to March. For each rainfall event, inflow and outflow volumes and their TN / TP concentrations were recorded. Only 2 rainfall events in February and March were observed with outflow from bioretention [75]. These 2 months were selected to calibrate the BEAM program. The nutrient outputs of BEAM were compared with the observed data to evaluate its simulation accuracy.

By adjusting some parameters in the input spreadsheet, the modeling outputs can be altered. The priority parameters to be adjusted are determined from the sensitivity analysis. Those parameters that outputs are highly sensitive to are altered in the first place to match the modeling results with the observed data. After an iterative process modeling results were close enough to the observed data and thus generated a set of calibrated parameters.

The calibrated BEAM is then used with the precipitation and temperature data of Blacksburg, VA for the year of 2008 to estimate the annual load reduction for nutrients and other related environmental impacts of the bioretention cell. The model application used the mean values of monitored data as inflow concentrations of TN (2.7 mg/L) and TP (1 mg/L). The annual removal was calculated with the following formula.

$$\eta = \frac{\sum[Q_{in(e)} \times c_{in(e)}] - \sum[Q_{out(e)} c_{out(e)}]}{\sum[Q_{in(e)} \times c_{in(e)}]} \quad (4\text{-}52)$$

$$\eta' = \frac{\sum[Q_{in(e)} \times c_{in(e)}] - \sum\{[Q_{in(e)} - ET_{(e)} \times A_{brc}] c_{out(e)}\}}{\sum[Q_{in(e)} \times c_{in(e)}]} \quad (4\text{-}53)$$

$$\eta_Q = \frac{\sum[Q_{in(e)}] - \sum[Q_{out(e)}]}{\sum[Q_{in(e)}]} \quad (4\text{-}54)$$

Where η = annual nutrient load removal of outflow (dimensionless)

$Q_{in(e)}$ = inflow volume of each event (m^3)

$c_{in(e)}$ = inflow concentration of each event (mg/L)

$Q_{out(e)}$ = outflow volume of each event (m^3)

$c_{out(e)}$ = outflow concentration of each event (mg/L)

η' = annual nutrient load removal of pore water (dimensionless)

$ET_{(e)}$ = evapotranspiration of each event (m)

η_Q = annual volume reduction of runoff (dimensionless)

Equation (4-51) calculates removal from outflow volumes. However, the exfiltration process loses inflow water to the surrounding soil and causes few events with observed outflow. A more realistic estimate on the pollutant impacts to the natural

environment is computed by Equation (4-52) with an assumption that the outflow concentration is equal to the concentration of pore water, which is likely discharged, with some attenuation, to groundwater. This calculation preserves water mass balance, and estimate the role of bioretention in nutrient treatment on a macro scale. Equation (4-53) is to compute the annual volume reduction from inflow and outflow data.

4.3 Results and Discussion

4.3.1 Sensitivity analysis

The results of sensitivity analysis on inflow volume, outflow volume, TN concentration, and TP concentrations were displayed as scatter plots to show the impacts of some input parameters on the simulated results.

It can be seen that for inflow volume (Figure 4.5), watershed width and slope both have a positive and proportional relationship with inflow volume. Watershed width can influence inflow more than slope. Watershed length and roughness (expressed as Manning's n) affect inflow with negatively proportional relationship. Decreasing watershed length and roughness can change inflow with more magnitude. Among these 4 parameters, inflow simulation is more sensitive to watershed roughness than the other parameters. Pipe parameters were investigated to evaluate their impacts on outflow (Figure 4.6). Pipe slope and constant demonstrate small positive effects on outflow, while adjustments of pipe head and diameter induce greater changes on outflow. Pipe head is the factor to exert the greatest effect on outflow. Lowering pipe head can definitely collect more pore water to discharge. The variation at 5% decrease of pipe head is due to the pore water initializing collection from pipe holes at this point. The parameter of pipe

diameter is in both denominator and numerator of outflow equations, so there is also a sharp change in its sensitivity scatter plot.

In Figures 4.7 and 4.8, the TN and TP concentrations in outflow were found to be highly sensitive to the inflow concentrations with an almost linear relationship. Increases of temperature, pH, and HRT can affect nutrient concentrations in outflow negatively, but the impacts are not as obvious as inflow concentrations. Thus, source control of pollution and pre-treatment to decease inflow concentration will likely increase performance, at least to a point.

The relative differences from outflow nutrient concentrations with different forms distribution are tabulated as Table 4.1. It can be observed from the results that if inflow TN is composed of organic N or NH_4 totally, the outflow TN will be 47% higher than an average distribution. Contrarily, if inflow TN is only NO_3, outflow TN will decrease 53%. This is because organic N and NH_4 are N forms before NO_3 in the transformation cycle. More organic N and NH_4 will produce more NH_4 and NO_3 at the end of reaction cycle. The reaction rate of NH_4 is slower than other forms. This bottleneck restraints the treatment of N significantly. If NO_3, or the form of the last step is the predominant component in inflow, then N is easier to be treated and release as N_2 from the system.

A similar analysis can be applied on distribution of P forms. If, in the first step, organic P dominates in inflow, then outflow TP increases. If particulate P is the major component, then almost all P forms are adsorbed and TP in outflow is low. If the inflow contains mainly PO_4 as P, a moderate impact on outflow TP can be expected.

4.3.2 Calibration and application

The sensitivity analysis indicates the parameters that are mostly influential to the modeling outputs, and helps direct calibration. To calibrate inflow volumes, Manning's n and watershed width are adjusted to reach desired value of outputs. Although pipe head and diameter are the most influential factors to control outflow, they cannot be changed in the calibration process as they are both given data of the field-scale bioretention. In this case, pipe slope was altered to make modeling outflow closer to measured data. For nutrients, the inflow concentrations are also given, therefore calibrating temperature, pH, and HRT are options to select. The change of N / P forms distribution can also adjust the computational results.

The observed and simulated inflow volumes were plotted as a least-squared line to show the goodness of fit (Figure 4.9) to demonstrate calibration of inflow hydrology. The outflow volumes and TN / TP concentrations from observation and simulation of the 2 events with outflow are compared in Table 4.2.

The least-squared line of inflow has a coefficient of determination over 0.8, and most simulated inflow volumes are close to the observed data. As shown in Table 4.2, the absolute relative differences are mostly less than 10%. A peak of difference is 38.3% for the outflow volume of the last recorded event. This discrepancy is due to the observed outflow volume was extremely low (0.00081 m^3); a focus was maintained on the larger mass flux event. The comparison between the observed and simulated results of outflow / TN / TP demonstrates the robustness of BEAM to accurately estimate the outflow volumes and nutrient concentrations after calibration.

The calibrated BEAM was run with the 2-month climatological data, inflow concentrations and other given parameters to generate the estimated hydraulic outputs and nutrient concentrations. Four graphs of ET (Figure 4.10), inflow (Figure 4.11), infiltration (Figure 4.12), and outflow (Figure 4.13), with precipitation on top, were plotted to show the hydraulic fluctuation during this investigated period of 2 months. During this period, no event with overflow was observed. Inflow and infiltration plots correlated with precipitation, and outflow plot shows the observed pattern with rare events. Figure 4.14 and Figure 4.15 show the TN and TP concentrations in pore water after treatment. Among these nutrient outputs, the results of the 1st and 48th days are also outflow concentrations. Adequate pore water was discharged as outflow on these days.

The long-term simulation results of the Blacksburg bioretention in 2008 were tabulated as nutrient removal (Table 4.3). Due to the fact that outflow volume is much less than inflow volume, the removal calculated with outflow volume results in misleading conclusion that almost all nutrients are treated by the bioretention; in actuality, they are transferred from surface water to pore water. Comparably, the load removals between inflow and pore water demonstrate results with more credibility. Considering the exfiltrated pore water and outflow as a whole, the annual N load removal is less than 7%, and the annual P load removal is over 87%. Although these results are obtained with many simplifications, i.e. unchanged inflow concentrations and assumed outflow parameters, they provide a very possible scenario that most of the nutrients in inflow runoff may exfiltrate to surrounding soil and infiltrate to groundwater or water bodies. This may introduce negative and unexpected impacts to the environment and warrants further study.

4.4 Conclusions

The development of BEAM is based upon physical and mathematical concepts. With the main function and its subroutines, BEAM can compute ET, inflow, infiltration, outflow, biomass, N, and P dynamically within a bioretention system through numerical simulation of its hydraulics and chemistry.

Sensitivity analyses show that higher watershed roughness can greatly reduce the inflow volume, and the head of underdrain pipes is important to regulate outflow. Watershed remediation and pipe placement are key steps to be considered for flow control in the maintenance of bioretention systems. Inflow concentrations can impact the nutrient concentrations in outflow, thus source controls that decrease nutrient accumulation on watersheds is a key process in reducing pollutant loads to bioretention.

The calibration process is necessary prior to the application of BEAM for a specific bioretention cell. The given or settled parameters are input into parameter spreadsheet and cannot be changed. Other parameters can be altered in their reasonable ranges to make the model as calibrated as to predict the performance of the investigated bioretention system. More study will be necessary to develop specific parameters so that the model can be used more generally, i.e., in design.

After calibration on controlling parameters, BEAM performed well to reflect the conditions of a field-scale bioretention site in Blacksburg, VA, and the modeling results were close to the observed data. The validation of BEAM is preliminarily confirmed.

Since most bioretention facilities are not separated from the environment, the influent coming into bioretention is mostly redistributed to the surrounding soil through exfiltration processes. BEAM is capable of estimating the nutrient concentrations in pore

water and outlet to evaluate the potential environmental impact of bioretention flow to the surrounding ecosystem.

The simulation examples indicate BEAM can be used to guide the design work of bioretention facilities prior to construction. With surveyed watershed data and assumed bioretention parameters, the BEAM program is capable to generate simulated hydraulic and nutrient results. The bioretention size, pipe setting, and media composition as input parameters can be adjusted to approach an optimal design for adequate runoff reduction and satisfactory nutrient removal.

Acknowledgments

The authors would like to give their gratitude to Dr. Tess Thompson, Biological Systems Engineering of Virginia Tech, and Dr. Kathy DeBusk, Environmental Science of Longwood University for providing the observed data used for model calibration from their study on a bioretention site in Blacksburg, VA.

TABLES AND FIGURES

Table 4.1 Relative differences of outflow concentrations between the nutrient forms with average and extreme distributions in inflow.

	Org-N as 100%	NO_3 as 100%	NH_4 as 100%	Org-P as 100%	PO_4 as 100%	Par-P as 100%
TN difference	46.6%	-53.0%*	46.6%	-	-	-
TP difference	-	-	-	148%	111%	-99.9%

*: e.g.: -53.0% is calculated from the outflow concentrations of 2 cases: 100% NO_3, 0% org-N, 0% NH_4 in inflow; and 33% org-N, 33% NO_3, 33% NH_4 in inflow

Table 4.2 Observed outflow volumes and TN / TP concentrations of Blacksburg bioretention and corresponding values from BEAM simulation.

Event	Outflow volume observed (m^3/event)	Outflow volume simulated (m^3/event)	TN concentration observed (mg L^{-1}/event)	TN concentration simulated (mg L^{-1}/event)	TP concentration observed (mg L^{-1}/event)	TP concentration simulated (mg L^{-1}/event)
02/01/2008	0.0228	0.0252	5.8	5.90	0.132	0.141
02/04/2008	0	0	NA	NA	NA	NA
02/06/2008	0	0	NA	NA	NA	NA
02/07/2008	0	0	NA	NA	NA	NA
02/13/2008	0	0	NA	NA	NA	NA
02/23/2008	0	0	NA	NA	NA	NA
03/07/2008	0	0	NA	NA	NA	NA
03/14/2008	0	0.0002	NA	NA	NA	NA
03/15/2008	0	0	NA	NA	NA	NA
03/19/2008	0.00081	0.0005	5.3	5.06	2.25	2.27

Table 4.3 Annual estimates of TN / TP removals and volume reduction of 2008 taking outflow and pore water as load outputs from Blacksburg bioretention.

	TN removal	TP removal	Volume reduction
Output as outflow	>99.9%	>99.9%	>99.9%
Output as pore water	6.31%	87.2%	0%

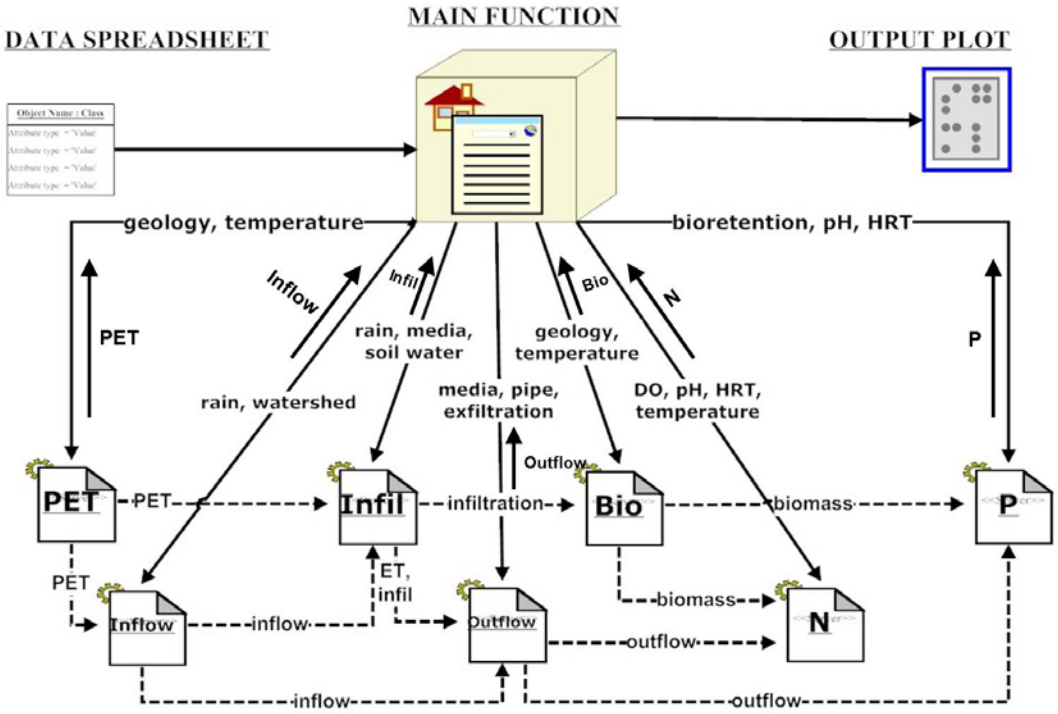

Figure 4.1 Structural diagram of BEAM with main function and subroutines.

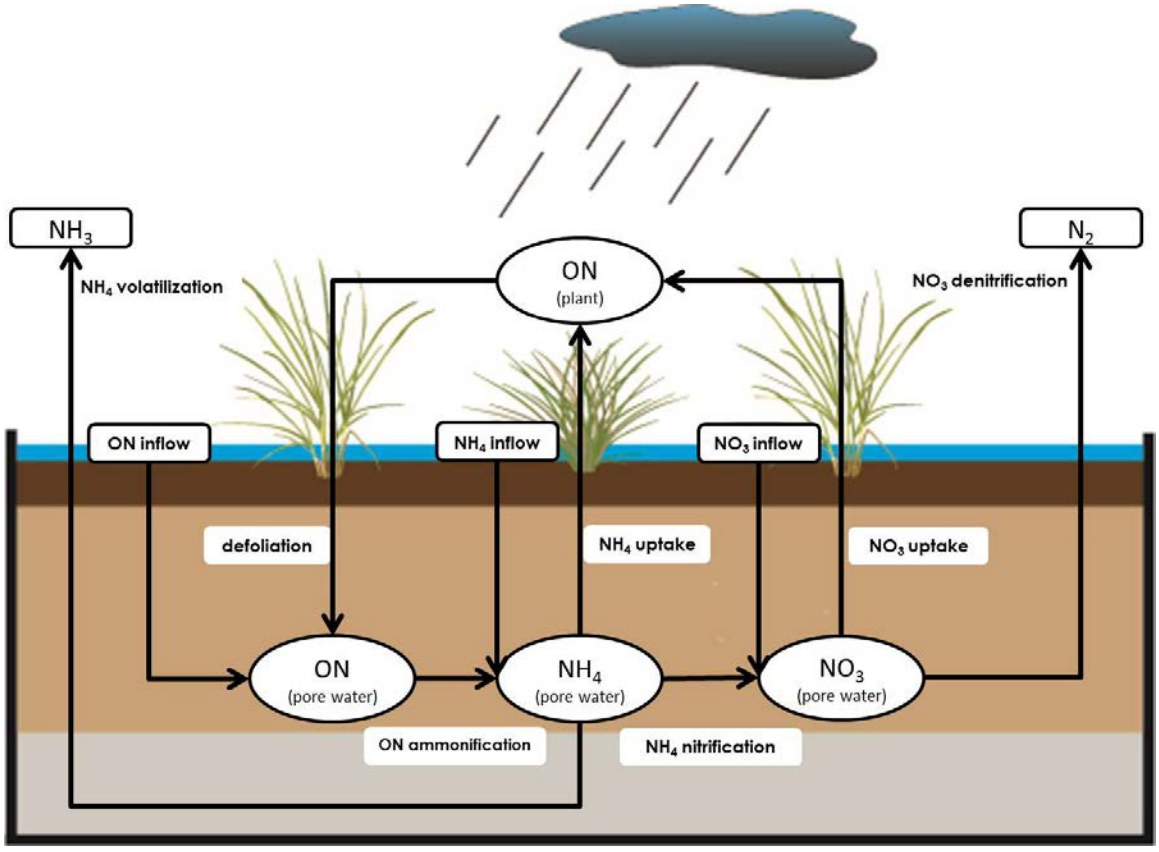

Figure 4.2 Nitrogen transformation and mass flow in bioretention.

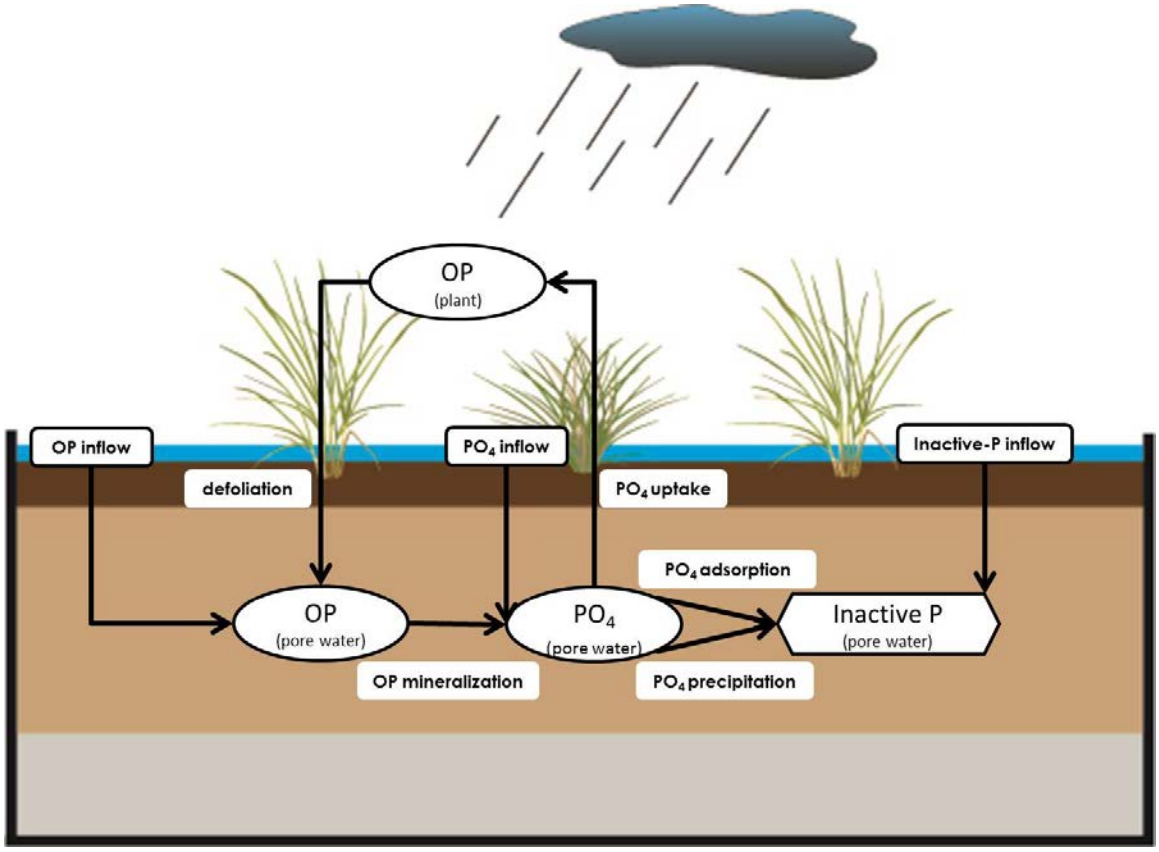

Figure 4.3 Phosphorus transformation and mass flow in bioretention.

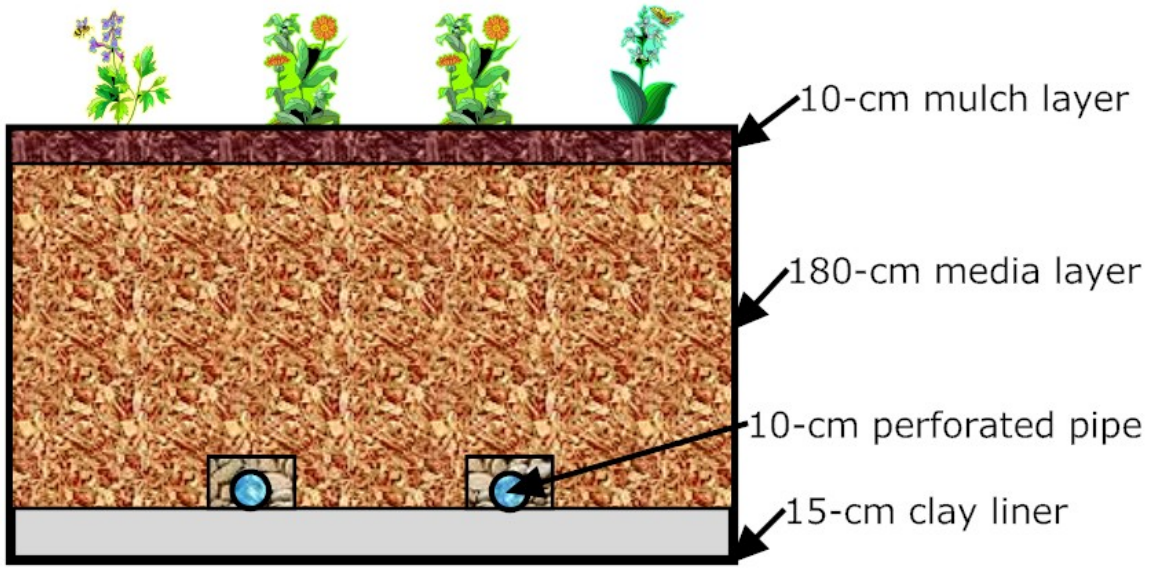

Figure 4.4 Cross-section of the monitored bioretention facility in Blacksburg, VA.

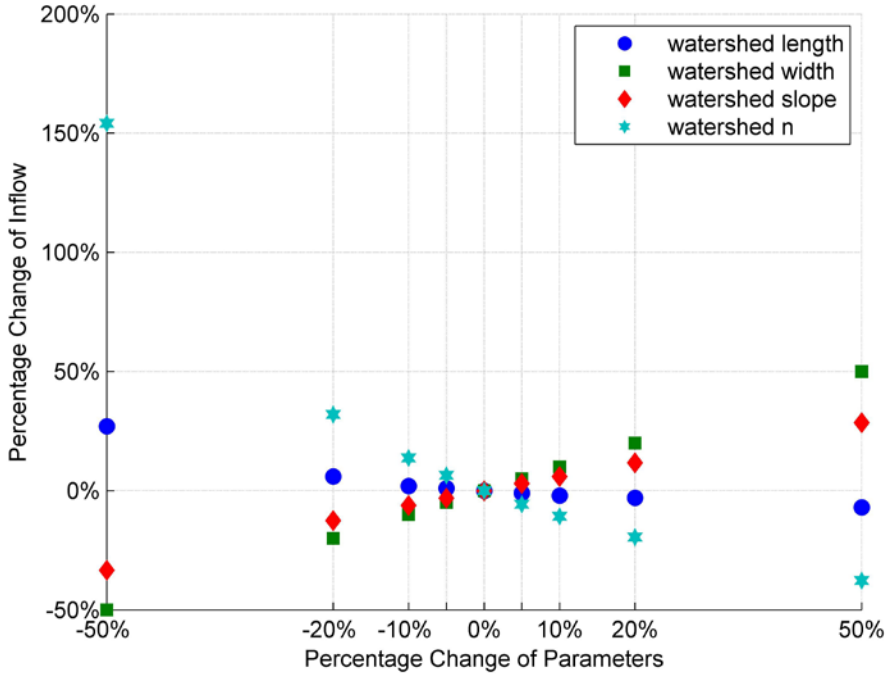

Figure 4.5 Sensitivity analyses of selected watershed coefficients as input parameters on simulated inflow volumes.

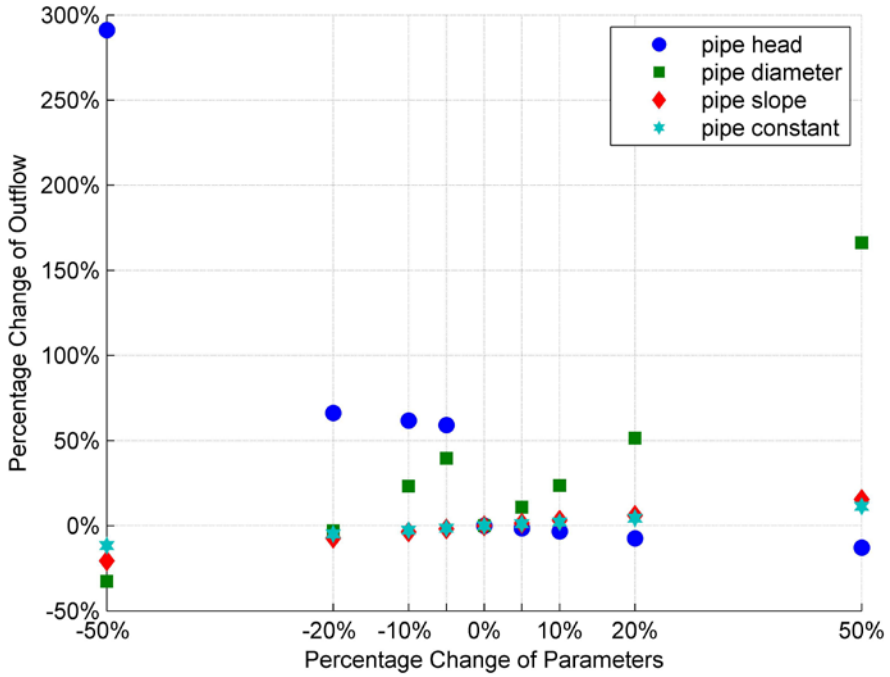

Figure 4.6 Sensitivity analyses of selected pipe coefficients as input parameters on simulated outflow volumes.

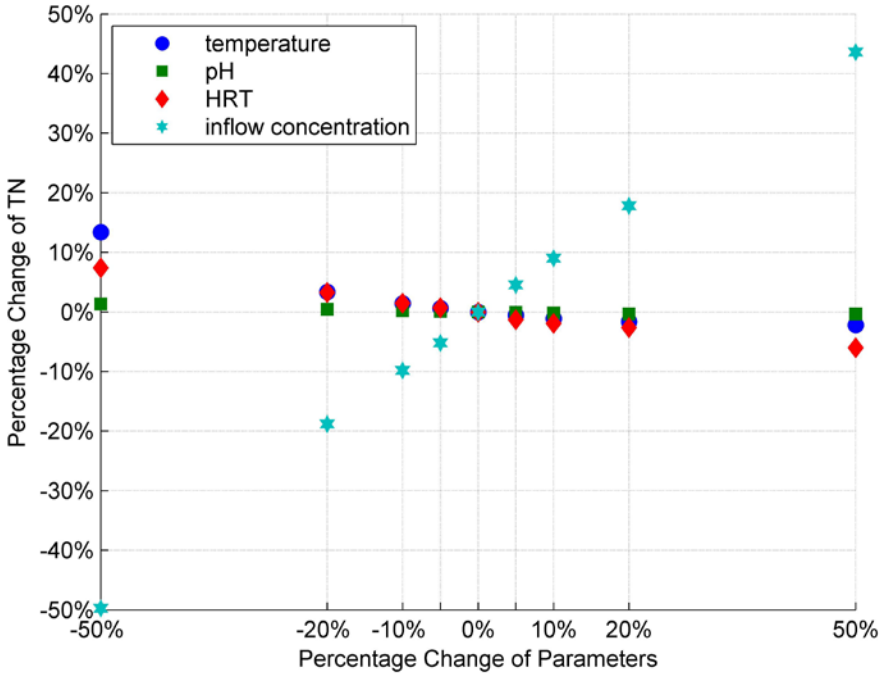

Figure 4.7 Sensitivity analyses of selected coefficients as input parameters on simulated TN concentration in outflow.

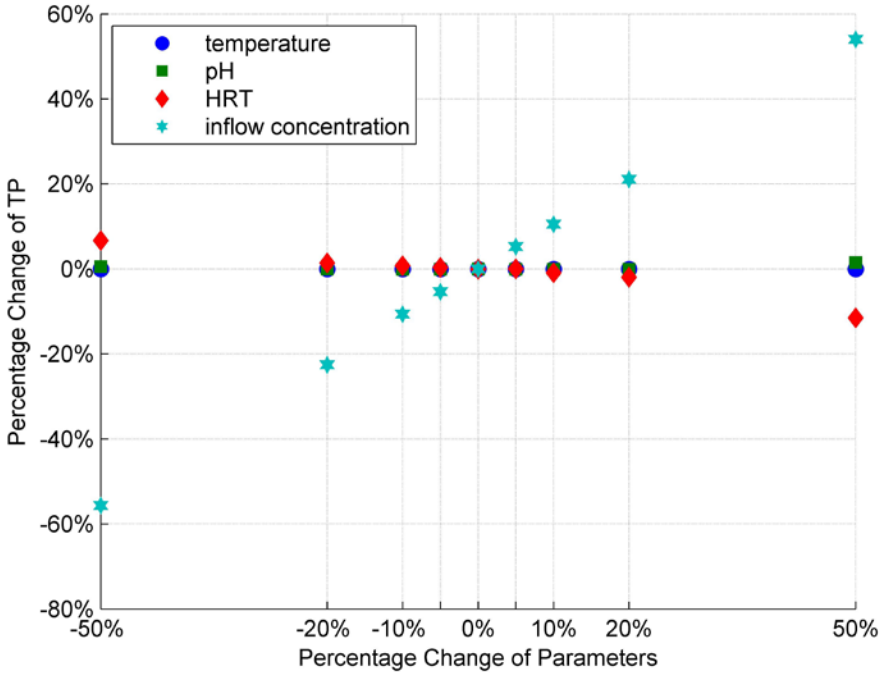

Figure 4.8 Sensitivity analyses of selected coefficients as input parameters on simulated TP concentration in outflow.

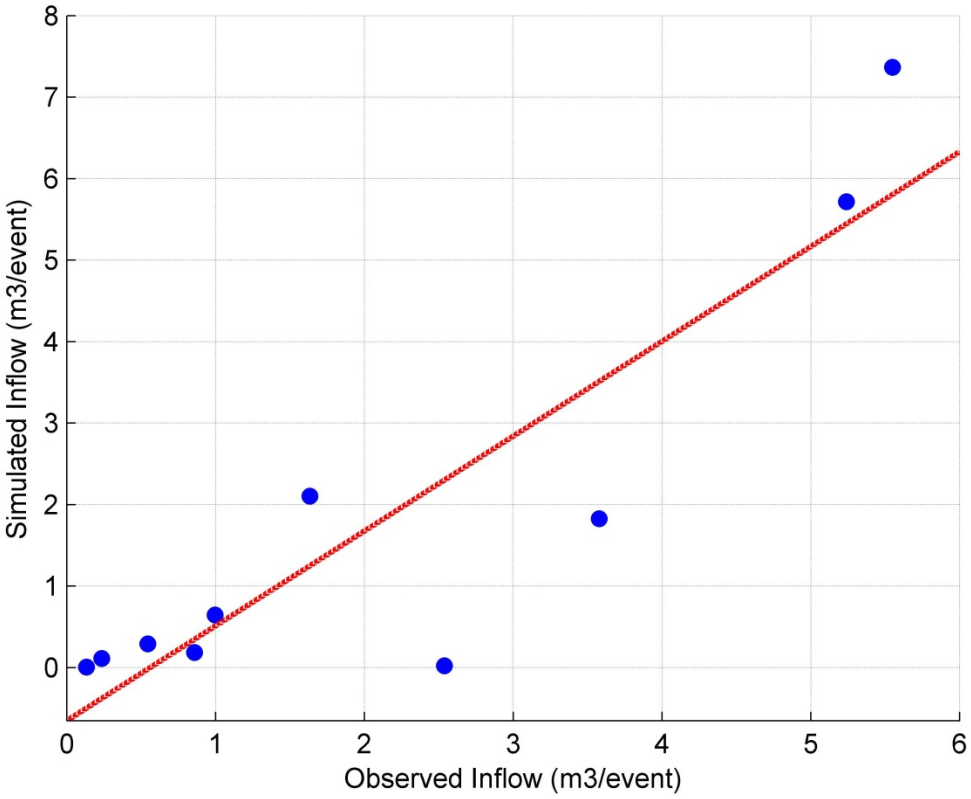

Figure 4.9 Least-squared line generated from calibration process between observed inflow of Blacksburg bioretention and simulated inflow from BEAM.

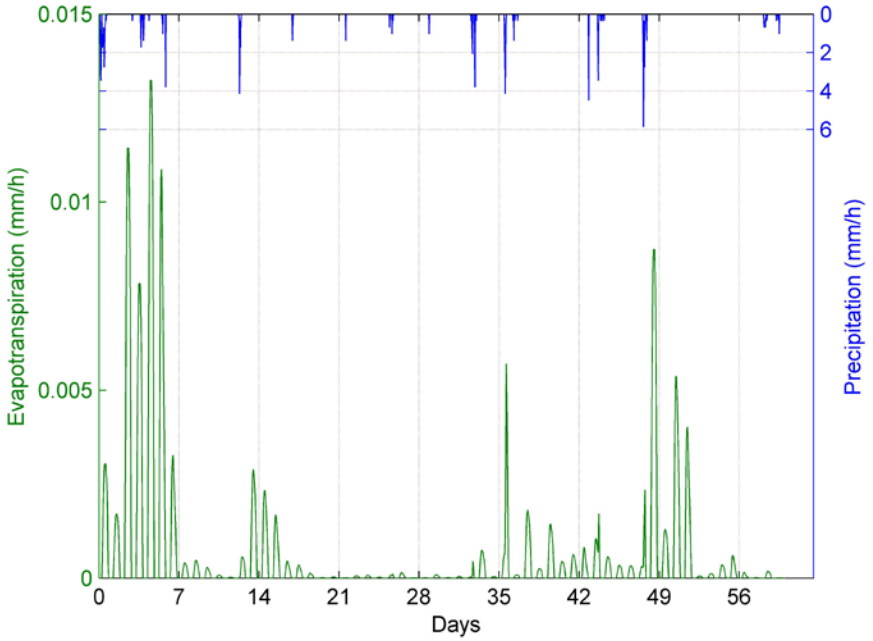

Figure 4.10 Simulated ET rates of Blacksburg bioretention in Feb and Mar 2008 by BEAM after calibration.

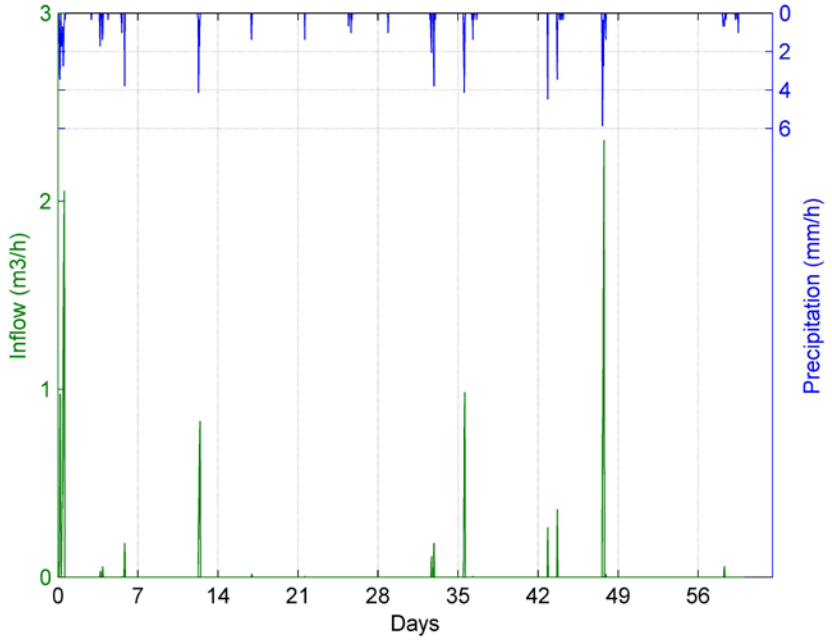

Figure 4.11 Simulated inflow rates of Blacksburg bioretention in Feb and Mar 2008 by BEAM after calibration.

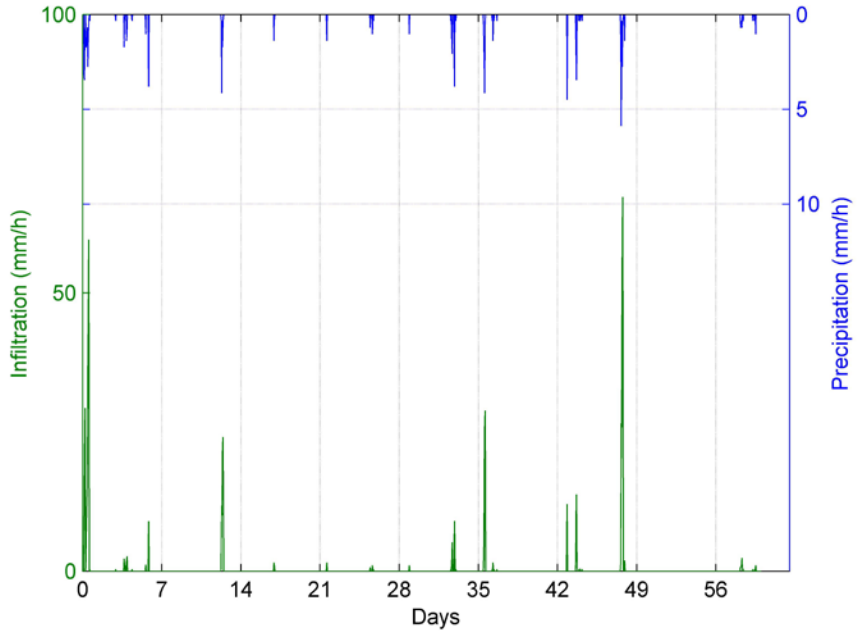

Figure 4.12 Simulated infiltration rates of Blacksburg bioretention in Feb and Mar 2008 by BEAM after calibration.

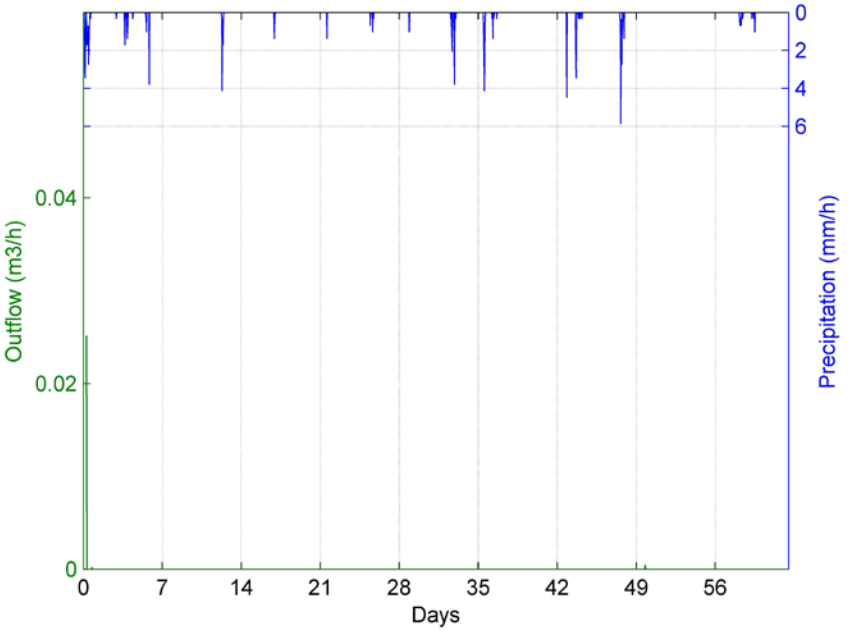

Figure 4.13 Simulated outflow rates of Blacksburg bioretention in Feb and Mar 2008 by BEAM after calibration.

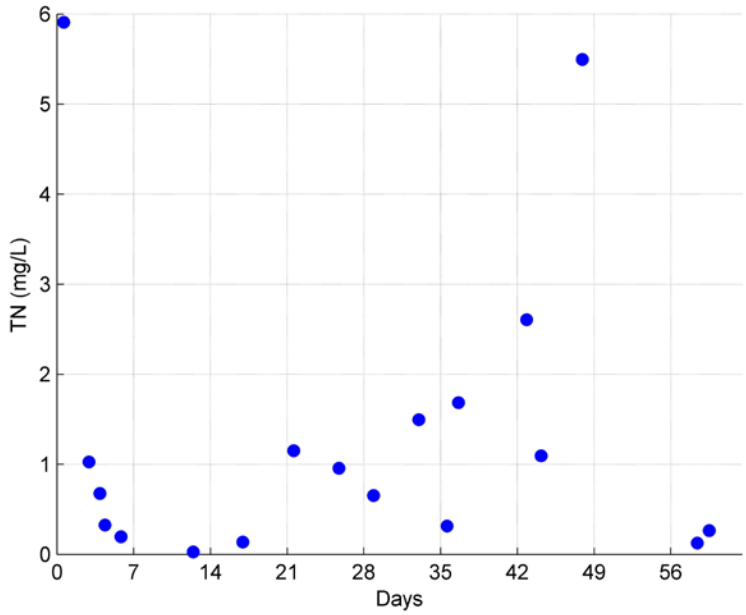

Figure 4.14 Simulated TN concentrations in pore water of Blacksburg bioretention in Feb and Mar 2008 by BEAM after calibration.

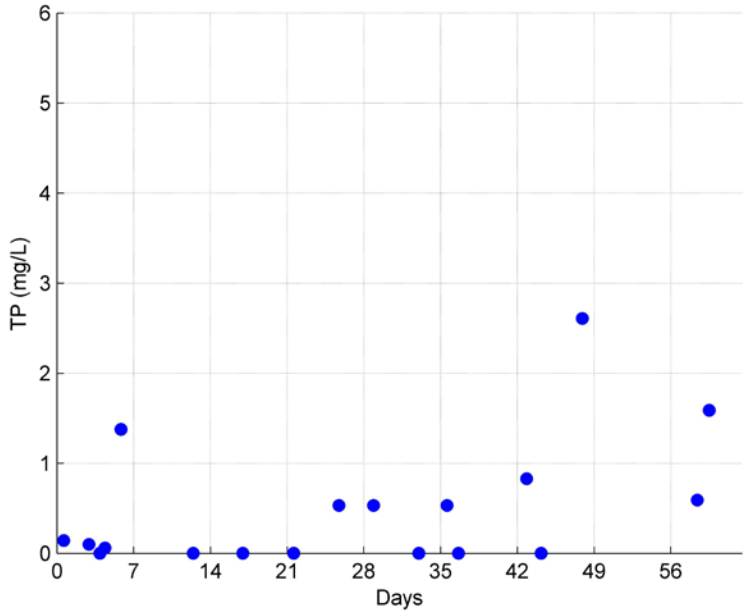

Figure 4.15 Simulated TP concentrations in pore water of Blacksburg bioretention in Feb and Mar 2008 by BEAM after calibration.

References

1. Traver, R., et al., Special issue on urban storm-water management in the 21st century. *Journal of Irrigation and Drainage Engineering*, 2011. **137**(3): p. 113-113.
2. Prince George's County, *Bioretention manual*, 2007, Department of Environmental Resources,: Upper Marlboro, MD.
3. US Department of Housing and Urban Development, *The practice of low impact development*, U. Development, Editor 2003, Office of Policy Development and Research: Washington, D.C.
4. US Environmental Protection Agency, *Storm water technology fact sheet - Bioretention*, 1999, Office of Water: Washington D.C.
5. Holzbecher, E., *Environmental modeling*. 2007, New York, NY: Springer.
6. Beyerlein, D.C. *Why single-event modeling doesn't work for LIDs*. in International Low Impact Development Conference - Redefining Water in the City 2010. San Francisco, CA.
7. ASCE Standardization of Reference Evapotranspiration Task Committee, *ASCE's standardized reference evapotranspiration equation*, in National Irrigation Symposium 2000: Phoenix, AZ.
8. Allen, R., et al., FAO-56 dual crop coefficient method for estimating evaporation from soil and application extensions. *Journal of Irrigation and Drainage Engineering*, 2005. **131**(1): p. 2-13.
9. Allen, R.G. and Food and Agriculture Organization of the United Nations, *Crop evapotranspiration : guidelines for computing crop water requirements*. 1998, Rome, Italy: Food and Agriculture Organization of the United Nations.
10. Allen, R.G. *REF-ET: reference evapotranspiration calculation software for FAO and ASCE standardized equations*. 2011; Available from: http://www.kimberly.uidaho.edu/ref-et/index.old.htm.
11. Thornthwaite, C.W., *An approach toward a rational classification of climate*. 1948: American Geographical Society.
12. Pereira, A.R. and W.O. Pruitt, Adaptation of the Thornthwaite scheme for estimating daily reference evapotranspiration. *Agricultural Water Management*, 2004. **66**(3): p. 251-257.
13. Murphy, E.A., *Comparison of potential evapotranspiration calculated by the LXPET (Lamoreux Potential Evapotranspiration) program and by the WDMUtil (Watershed Data Management Utility) program*, 2005: Reston, VA.
14. Huber, W.C. and R.E. Dickinson, *Storm Water Management Model, version 4*, 1992, US Environmental Protection Agency, Office of Research and Development: Athens, GA.
15. Hirschman, D., K. Collins, and T. Schueler, *The runoff reduction method*, 2008, Center for Watershed Protection and Chesapeake Stormwater Network: Ellicott City, MD.
16. Maidment, D.R., *Handbook of hydrology*. 1993, New York: McGraw-Hill.
17. Aravena, J. and A. Dussaillant, Storm-water infiltration and focused recharge modeling with finite-volume two-dimensional Richards Equation: application to an experimental rain garden. *Journal of Hydraulic Engineering*, 2009. **135**(12): p. 1073-1080.

18. Novak, V., J. Simaunek, and M.T.v. Genuchten, Infiltration of water into soil with cracks. *Journal of Irrigation and Drainage Engineering*, 2000. **126**(1): p. 41-47.
19. Lee, R.S., *Modeling infiltration in a stormwater control measure using modified Green and Ampt*, in Department of Civil and Environmental Engineering 2011, Villanova University: Villanova, PA.
20. Osman, A., *Urban stormwater hydrology: a guide to engineering calculations*. 1993, Lancaster, PA: Technomic Pub. Co.
21. Sample, D. and J. Heaney, Integrated management of irrigation and urban storm-water infiltration. *Journal of Water Resources Planning and Management*, 2006. **132**(5): p. 362-373.
22. Dingman, S.L., *Physical hydrology*. 2002, Upper Saddle River, N.J.: Prentice Hall.
23. Atchison, D. and L. Severson, *Recarga user's manual, version 2.3*, 2004, University of Wisconsin - Madison: Madison, WI.
24. Finnemore, E.J. and J.B. Franzini, *Fluid mechanics with engineering applications*. 2002, Boston, MA: McGraw-Hill.
25. Sample, D.J. and D.B. Powers, Technical note: an analytical method for evaluating pumps for a storage-pump system. *Applied Engineering in Agriculture*, 2012. **28**(4): p. 559-565.
26. Swaffield, J.A. and S. Bridge, Applicability of the Colebrook-White formula to represent frictional losses in partially filled unsteady pipeflow. *Journal of Research of the National Bureau of Standards*, 1983. **88**(6): p. 389-393.
27. Clamond, D., Efficient resolution of the Colebrook equation. *Industrial & Engineering Chemistry Research*, 2009. **48**(7): p. 3665-3671.
28. Chadwick, A.J., J.C. Morfett, and M. Borthwick, *Hydraulics in civil and environmental engineering*. 2004, London, United Kingdom: Spon Press.
29. Steudle, E., Water uptake by plant roots: an integration of views. *Plant and Soil*, 2000. **226**(1): p. 45-56.
30. Greene, A., et al., *Impacts of biota on bioretention cell performance during establishment in the Midwest*, in World Environmental and Water Resources Congress 2009: Kansas City, MO. p. 1-13.
31. Debusk, W.F. and K.R. Reddy, Litter decomposition and nutrient dynamics in a phosphorus enriched Everglades marsh. *Biogeochemistry*, 2005. **75**(2): p. 217-240.
32. Lucas, W.C. and M. Greenway, Nutrient retention in vegetated and nonvegetated bioretention mesocosms. *Journal of Irrigation and Drainage Engineering*, 2008. **134**(5): p. 613-623.
33. Ramos e Silva, C.A., et al., Dynamics of phosphorus and nitrogen through litter fall and decomposition in a tropical mangrove forest. *Marine Environmental Research*, 2007. **64**(4): p. 524-534.
34. Stockle, C.O., et al., A method for estimating the direct and climatic effects of rising atmospheric carbon dioxide on growth and yield of crops. Part I: modification of the EPIC model for climate change analysis. *Agricultural Systems*, 1992. **38**(3): p. 225-238.

35. Williams, J.R., C.A. Jones, and P.T. Dyke, A modelling approach to determining the relationship between erosion and soil productivity. *Transactions of the ASABE*, 1984. **27**(1): p. 129-144.
36. Jonckheere, I., et al. *Methods for leaf area index determination. Part I: theories, techniques and instruments*. 2003; Available from: http://w3.avignon.inra.fr/valeri/documents/JonckheereAFM2003Accepted.pdf.
37. Barr, A.G., et al., Inter-annual variability in the leaf area index of a boreal aspen-hazelnut forest in relation to net ecosystem production. *Agricultural and Forest Meteorology*, 2004. **126**(3–4): p. 237-255.
38. Sumner, D.M. and J.M. Jacobs, Utility of Penman–Monteith, Priestley–Taylor, reference evapotranspiration, and pan evaporation methods to estimate pasture evapotranspiration. *Journal of Hydrology*, 2005. **308**(1–4): p. 81-104.
39. Irmak, S., et al., Predicting daily net radiation using minimum climatological data. *Journal of Irrigation and Drainage Engineering*, 2003. **129**(4): p. 256-269.
40. Purcell, L.C., et al., Radiation use efficiency and biomass production in soybean at different plant population densities. *Crop Science*, 2002. **42**(1): p. 172-177.
41. Monsil, M. and T. Saeki, On the factor light in plant communities and its importance for matter production. *Annals of Botany*, 2005. **95**(3): p. 549-567.
42. Monteith, J.L. and C.J. Moss, Climate and the efficiency of crop production in Britain. *Philosophical Transactions of the Royal Society of London. Series B, Biological Sciences*, 1977. **281**(980): p. 277-294.
43. Dewar, R.C., The correlation between plant growth and intercepted radiation: an interpretation in terms of optimal plant nitrogen content. *Annals of Botany*, 1996. **78**(1): p. 125-136.
44. Narayanan, S., et al., Water and radiation use efficiencies in sorghum. *Agronomy Journal*, 2013. **105**(3): p. 649-656.
45. Hoffmann, W.A. and H. Poorter, Avoiding bias in calculations of relative growth rate. *Annals of Botany*, 2002. **90**(1): p. 37-42.
46. Olson, J.S., Energy storage and the balance of producers and decomposers in ecological systems. *Ecology*, 1963. **44**(2): p. 322-331.
47. Vitousek, P.M., et al., Human alteration of the global nitrogen cycle: sources and consequences. *Ecological Applications*, 1997. **7**(3): p. 737-750.
48. Robertson, G.P. and P.M. Groffman, *Nitrogen transformation*, in *Soil microbiology, ecology, and biochemistry*. 2007, Springer: New York, NY. p. 341-364.
49. Mayo, A.W. and T. Bigambo, Nitrogen transformation in horizontal subsurface flow constructed wetlands I: model development. *Physics and Chemistry of the Earth, Parts A/B/C*, 2005. **30**(11-16): p. 658-667.
50. Lee, P.G., et al., Denitrification in aquaculture systems: an example of a fuzzy logic control problem. *Aquacultural Engineering*, 2000. **23**(1–3): p. 37-59.
51. Golterman, H.L., *The chemistry of phosphate and nitrogen compounds in sediments*. 2004, Dordrecht, the Netherlands: Kluwer Academic Publishers.
52. Wang, Y., et al., A simulation model of nitrogen transformation in reed constructed wetlands. *Desalination*, 2009. **235**(1-3): p. 93-101.
53. US Environmental Protection Agency, *Nitrification*, 2002, Office of Ground Water and Drinking Water: Washington, D.C.

54. Bernet, N., et al., Nitrification at low oxygen concentration in biofilm reactor. *Journal of Environmental Engineering*, 2001. **127**(3): p. 266-271.
55. Senzia, M.A., et al., Modelling nitrogen transformation and removal in primary facultative ponds. *Ecological Modelling*, 2002. **154**(3): p. 207-215.
56. Strous, M., J.G. Kuenen, and M.S.M. Jetten, Key physiology of anaerobic ammonium oxidation. *Applied and Environmental Microbiology*, 1999. **65**(7): p. 3248-3250.
57. Hamlin, H.J., et al., Comparing denitrification rates and carbon sources in commercial scale upflow denitrification biological filters in aquaculture. *Aquacultural Engineering*, 2008. **38**(2): p. 79-92.
58. Wang, Y.P., B.Z. Houlton, and C.B. Field, A model of biogeochemical cycles of carbon, nitrogen, and phosphorus including symbiotic nitrogen fixation and phosphatase production. *Global Biogeochemical Cycles*, 2007. **21**(1): p. GB1018.
59. Roy-Poirier, A., P. Champagne, and Y. Filion, Bioretention processes for phosphorus pollution control. *Environmental Reviews*, 2010. **18**: p. 159-173.
60. McGechan, M.B. and D.R. Lewis, Soil and water: sorption of phosphorus by soil. Part 1: principles, equations and models. *Biosystems Engineering*, 2002. **82**(1): p. 1-24.
61. Schachtman, D.P., R.J. Reid, and S.M. Ayling, Phosphorus uptake by plants: from soil to cell. *Plant Physiology*, 1998. **116**(2): p. 447-453.
62. Noe, G.B., Measurement of net nitrogen and phosphorus mineralization in wetland soils using a modification of the resin-core technique. *Soil Science Society of America Journal*, 2011. **75**(2): p. 760-770.
63. Ouyang, X., et al., Effect of N and P addition on soil organic C potential mineralization in forest soils in South China. *Journal of Environmental Sciences*, 2008. **20**(9): p. 1082-1089.
64. Haas, D.d., M. Wentzel, and G. Ekama, The use of simultaneous chemical precipitation in modified activated sludge systems exhibiting biological excess phosphate removal. Part 6: modelling of simultaneous chemical-biological P removal - review of existing models. *Water SA*, 2001. **27**(2): p. 135-150.
65. Patnaik, P. and J.A. Dean, *Dean's analytical chemistry handbook*. 2004, New York, NY: McGraw-Hill.
66. Jiao, Y., W.H. Hendershot, and J.K. Whalen, Modeling phosphate adsorption by agricultural and natural soils. *Soil Science Society of America Journal*, 2008. **72**(4): p. 1078-1084.
67. Roy-Poirier, A., *Bioretention for phosphorus removal: modelling stormwater quality improvements*, in Department of Civil Engineering 2009, Queen's University: Kingston, Canada.
68. Azizian, S., Kinetic models of sorption: a theoretical analysis. *Journal of Colloid and Interface Science*, 2004. **276**(1): p. 47-52.
69. Xiao, Y., et al., Characteristics of phosphorus adsorption by sediment mineral matrices with different particle sizes. *Water Science and Engineering*, 2013. **6**(3): p. 262-271.
70. Roose, T., *Mathematical model of plant nutrient uptake*, in Linacre College 2000, University of Oxford: Oxford, United Kingdom.

71. Barber, S.A., *Soil nutrient bioavailability: a mechanistic approach*. 1984, New York, NY: Wiley.
72. Saltelli, A., et al., *Global sensitivity analysis: the primer*. 2008, Hoboken, NJ: John Wiley & Sons.
73. Brown, R.A., R.W. Skaggs, and W.F. Hunt, Calibration and validation of DRAINMOD to model bioretention hydrology. *Journal of Hydrology*, 2013. **486**(0): p. 430-442.
74. DeBusk, K.M., *Stormwater treatment by two retrofit infiltration practices*, in Biological Systems Engineering 2008, Virginia Polytechnic Institute and State University: Blacksburg, VA.
75. DeBusk, K. and T. Wynn, Storm-water bioretention for runoff quality and quantity mitigation. *Journal of Environmental Engineering*, 2011. **137**(9): p. 800-808.

5 Conclusion

5.1 Summary of Results

This dissertation composes 3 major components as frequency analyses of precipitation events and dry durations of Virginia; mesocosm experiment for assessment of selected bioretention blends on nutrient retention; and development of a computation model to simulate the hydraulics and treatment of bioretention systems. Through these studies, an overall investigation on the representative LID of bioretention was conducted through the means of theoretical analyses, laboratory experiment, and model development.

The main findings of frequency analysis are plotted as frequency curves to show the exceedance probabilities of precipitation depth and dry duration in different regions across Virginia. The rainfall depth and dry duration with 90% exceedance probability or 10-year return period is between 22.9 to 35.6 mm and 15.3 to 25.8 days respectively. With the curves, a precipitation-drought pattern can be established with the corresponding exceedance probability. The mesocosm experiment simulated the conditions of field-scale bioretention systems to evaluate 3 different blends on nutrient retention. Results show that the blend with WTR had the highest P removal capabilities; while another blend with mulch-free compost performed well to treat N. The experimental data also indicated that increasing retention time to 6 h or longer positively promoted effluent water quality, and plant health should also be considered to improve treatment efficacies. The computational model, BEAM, was developed with previous findings and physical concepts to simulate the hydraulics and treatment of bioretention systems. Interrelated subroutines are called by the main function to compute ET, inflow, infiltration, outflow, biomass, and N / P treatment. The major contribution of BEAM is

that it considers the fluctuation of biomass, and takes this factor into account as part of the nutrient cycles. The model generated results close to the observed data of inflow, outflow, TN and TP from a field-scale bioretention after calibration, and it can estimate the environmental impact from storm runoff through bioretention.

5.2 Research Implications

This dissertation introduces potential research implications through several aspects of the studies.

The frequency analysis with precipitation-drought curves can be a useful guidance for the design of bioretention or other SCMs. Considerations on the exceedance probabilities of precipitation depth and dry duration are necessary steps to estimate the inflow rate and drought possibility, and thus determine the size of SCMs and the type of vegetation.

Assessment on the nutrient retention of bioretention blends identified important components affecting treatment of N and P. These identified components can be mixed into bioretention blends to enhance treatment effectiveness. The influences of HRT and plants on removal effectiveness are instructive for the operational practices of bioretention, and it’s important to promote the regulations to be updated with a recommended HRT for SCMs.

BEAM is applicable to bioretention evaluation and estimation of treatment effectiveness. The program provides the possibility for the designers to estimate expected treatment from a bioretention facility with limited data prior to its implementation. The predicted results can guide the design in order to optimize its performance. The merit of BEAM also includes its capability to estimate the potential impact of runoff inflow on

groundwater and water bodies. This function remedies the incomplete estimate of nutrient removal with inflow and outflow volumes by taking the pore water into account. The simulated results of BEAM can be used as informative guidance for designers to develop bioretention systems with adequate runoff reduction and satisfactory nutrient removal. BEAM can be enhanced and expanded as it is applied to different projects to improve design criteria and regulation of bioretention practices.

5.3 Future Studies

There are some potential research needs to advance the existing studies in this dissertation.

The frequency analysis for precipitation and dry duration can be extended to a larger region with comparable examination of historical data. This comparison, with necessary statistical analysis, could provide a means of evaluating climate change impacts on the pattern of precipitation and drought.

Preliminary results were collected from the mesocosm experiment for assessment of bioretention blends. With the conclusion that WTR and compost are positive for P and N removals respectively, a new blend with both components should be tested. The next phase of mesocosm experiment can also consider the plant uptake effect by analyzing nutrient contents in vegetation tissues before and after experiments. Long-term observation is necessary to enhance the plant uptake of N and P. If conditions permit, the newly mixed blend can be experimented in a field scale bioretention to measure its performance in natural environment, and improve its retention for nutrients with amended component ratios.

There remain some spaces to improve the programming codes of BEAM, making it run faster with more accurate outcomes. The performance of BEAM can be thoroughly examined through application to more field-scale bioretention designs with monitoring data. The application process can direct upgrading needs with actual requirements from end users. The upgraded BEAM can include more subroutines to expand its scope on bioretention simulation. For the user-friendly purpose, the program should be converted to an installable executable file with a graphical interface for convenient installation and adjustment. Moreover, the data from BEAM can be combined with analysis of uncertainty to reveal the internal pattern of bioretention and improve the understanding of the mechanisms of this complex and dynamic ecosystem.